Improvement of the efficiency of an electric car by the use of electronics (within the E³-Car Project)

Diploma thesis

carried out by

Christian Schuß

Institute of Electronics
Graz – University of Technology

Director: Univ.-Prof. Dipl.-Ing. Dr. techn Wolfgang Pribyl

Advisors: Ass. Prof. Dipl.-Ing. Dr. Bernd Eichberger
Dipl.-Ing. (FH) Harald Gall

Graz, August 2010

STATUTORY DECLARATION

I declare that I have authored this thesis independently, that I have not used other than the declared sources / resources and that I have explicitly marked all material which has been quoted either literally or by content from the used sources.

…… ……..
date (signature)

Foreword

I would like to thank a lot of people for helping and supporting me during my work on this diploma thesis. First of all I would like to mention my dear, beloved father (†2009) who introduced me to electronics many years ago. He always tried to help me and let me learn from his wide experience and knowledge about electronic devices. He is the reason why I came to this field and also why I wanted to study it. I feel deeply sad that he cannot be here when I will complete my diploma studies. I really miss him.
I also would like to thank my university, the Graz University of Technology, for giving me the opportunity to study electrical engineering and information technology. Specially I would like to mention my diploma thesis instructor Bernd Eichberger who has brought me to the interesting field on automotive electronics. He is working for the institute for electronics and I would like to thank him for guiding me through my work.
Furthermore I would like to thank my company austriamicrosystems AG for offering me the opportunity to perform research on that topic. I would like to mention Harald Gall who always gave me a helping hand with the work on this thesis and also the many years before that, since I have started to work for austriamicrosystems AG. It has been always a pleasure to work there and it also led me to the idea of getting interested in alternative energies and reducing energy consumption by the help of electronics. Thanks also for the good cooperation on the E^3Car-Project to the University of Applied Science Joanneum.
Finally I would like to thank and mention my family, my girlfriend Maija and my friends for their love, support and help throughout this thesis.

Graz, August 2010

Christian Schuß

Content

1. Abstract

The energy demand of today's society is growing, and the energy amount which is used daily will continue to rise in the future. To meet the strong demands, on the one hand new technologies have to be developed, and on the other hand current technologies have to be improved by lowering the energy consumption itself and increasing the degree of efficiency. Furthermore it is necessary on environmental grounds, alongside energy reduction, to avoid and reduce emissions and pollution. Actions need to be established today to meet the requirements of the future. The degree of efficiency of individual transportation can be improved by the use of electronics and alternative energies, for example in hybrid and electrical cars. This supports a sought-after reduction of energy in the transportation sector. By extending the driving distance which can be taken electrically a possibility is established to reduce fuel consumption, thus providing a transition away from fossil energy to alternative, renewable energy. This work concentrates on the opportunity to use solar energy in hybrid cars.

2. Introduction to the topic

2.1. Costs of the battery

Efforts to increase the efficiency of the electronics in electric cars are centred on the battery. The battery restricts the possible driving range of the car, and to achieve a better performance the energy consumption has to be reduced as much as possible. Also, new sources have to be found which offer the driver more freedom. A greater range which can be driven electrically leads to more flexibility timewise, because of the longer interval between connections to the energy grid for recharging the vehicle itself. By the use of electricity, emissions emitted by fossil fuels can be reduced. It has, however, to be taken into account that electricity also causes pollution.
Battery capacity is expensive. Depending on the used technology, at the moment an average price of between €700 to €1000 can be estimated for 1kWh capacity. Current electrical vehicles can run a distance of about 120km to 200km. According to this, an average distance can be calculated to be around 140km. Furthermore, average energy consumption can be estimated at 15 to 20kWh/100km. With these values, a price range for the distance of 140km is calculated to be between €10,500 and €20,500 (Schöllmann M., Hoff C., Schriek J., 2010; Kleine Zeitung, 2010; Think, 2010; Helmers, 2009; VIS!ON, 2010, Citroën, 2010, Peugout, 2010)

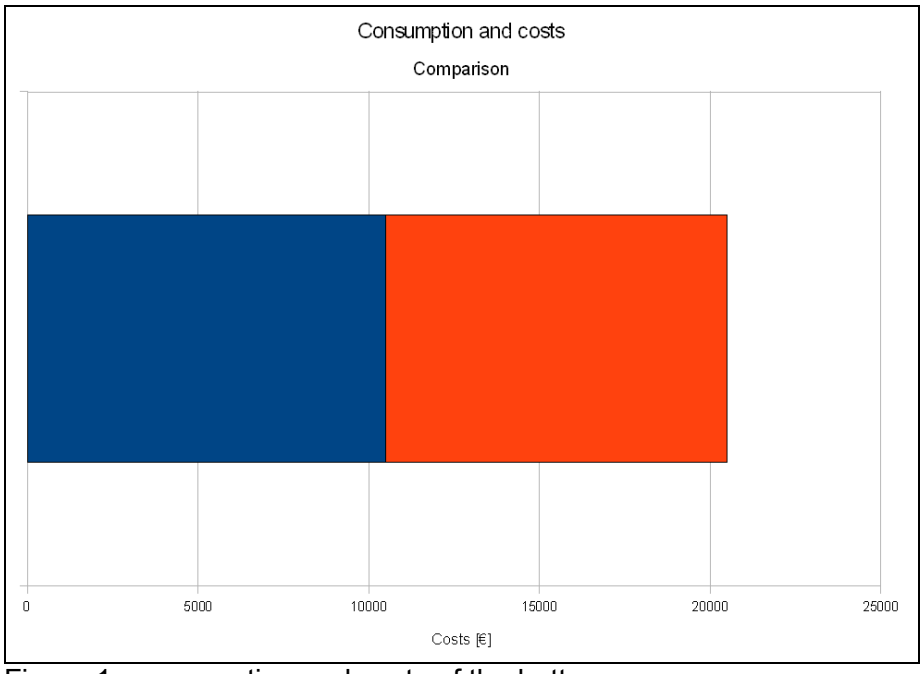

Figure 1: consumption and costs of the battery

The figure above illustrates clearly that the battery price varies and can lead to an enormous cost factor for the production of an electric car.

Factors in primary focus for an electric car are weight, driving range and costs for the vehicle. There is a strong connection between those different factors. If more driving range is expected, the battery capacity has to be increased, which leads to a heavier and more battery. With more weight the average consumption increases, which shortens the expected driving range. To avoid this counter-effect the only correct option available is to reduce energy consumption, as well as battery capacity, which ends then in a lower energy consumption demand, which also has a positive impact back on the possible driving distance. Solar energy offers a couple of possibilities as an alternative energy resource in that situation. It has to be evaluated whether the energy output is suitable to power an electrical vehicle or a hybrid vehicle (Helmers, 2009; Schöllmann M., Hoff C., Schriek J., 2010).

Moreover, the overall price for an electric car can be reduced. The current situation can be demonstrated in the following figure.

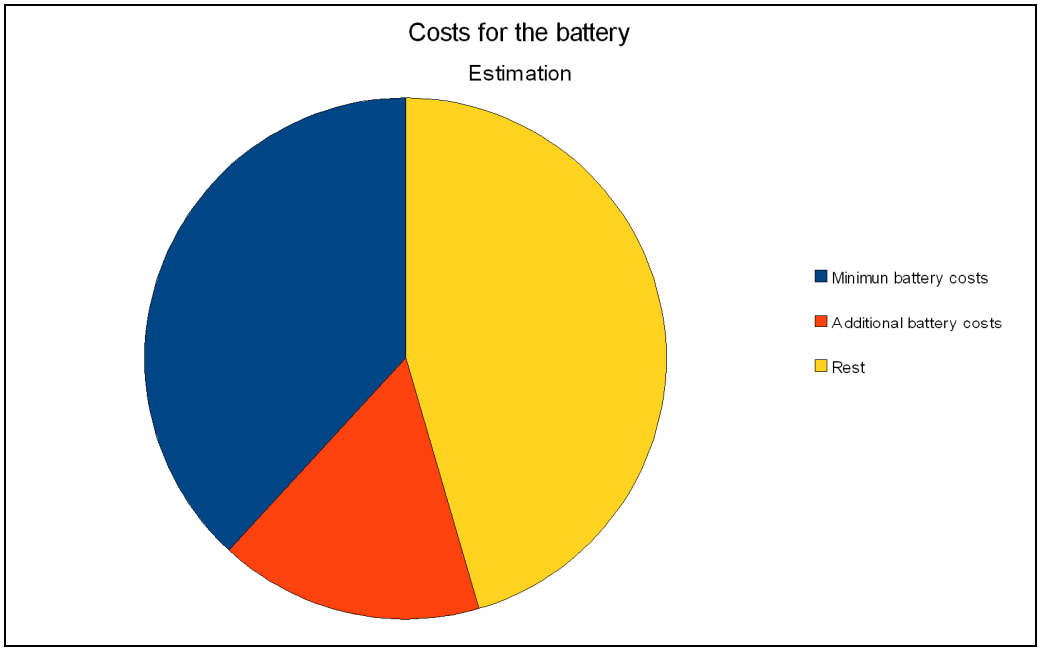

Figure 2: costs of the battery in comparison to the total price of the vehicle

The price of the battery can extend in certain cases to half of the total price of the electric car. The reason why a fast introduction of the electric car is not possible is this fact of the high purchase costs of the vehicle. There is a discussion about the possibility of batteries not being sold with the car; in this scenario the batteries could only be rented. This would cut the costs of the electric car itself by half, as already indicated in the figure above.
The solution in the case of electric cars without batteries would be that batteries are just recharged at recharging stations, which are comparable to conventional gas stations. With a common battery mechanism which could be introduced to basically similar vehicles (Mitsubishi MiEV, Peugeot iOn, Citroën C-Zero), batteries could also be just changed instead of recharged. To operate a supply chain of this sort, about 2.5 batteries for each vehicle would be needed. Furthermore it is uncertain who would bear the costs of the batteries. This could be an energy supplying company or a city.

Figure 3: Citroën Z-Zero and Mitsubishi i-MiEV (Source: Citroën and Mitsubishi)

In any case, it will be the situation that the costs will be redirected to the customer who is the driver of the electric car. This means that although the electric car itself is cheaper, the price for each kilometer driven gets higher. At the moment the lithium-ion battery is the battery most commonly built into electric vehicles. With future technologies, in combination with alternative materials and mass production of batteries, there is the chance of price reduction. The primary goal has to be to reduce the size of the required battery itself, which means less weight and less energy consumption (Citroën, 2010; Peugout, 2010; Helmers, 2009; Schöllmann M., Hoff C., Schriek J., 2010).

Figure 4: Peugeot iOn (Source: Peugeot)

2.2. Solar energy in combination with vehicles

2.2.1. Motivation and background

Solar energy will become an important renewable energy source in future. Growth in the solar energy sector is exponential. More and more roofs of houses are being covered with solar panels to make households independent of electricity companies by producing their own electricity. Some households produce more energy than they able to use. Transportation requires a big part of society's total energy demand every day. The question comes up why renewable energy cannot be used in transportation systems as well. In the case of public transport, for example railways, such a shift is not difficult to implement. Renewable energy can be introduced into the power grid, which provides railways with energy. But in the same way as for the roof of a house, also the roof of a car can be used for renewable energy (Nijs, 2009; Photon, 2010).

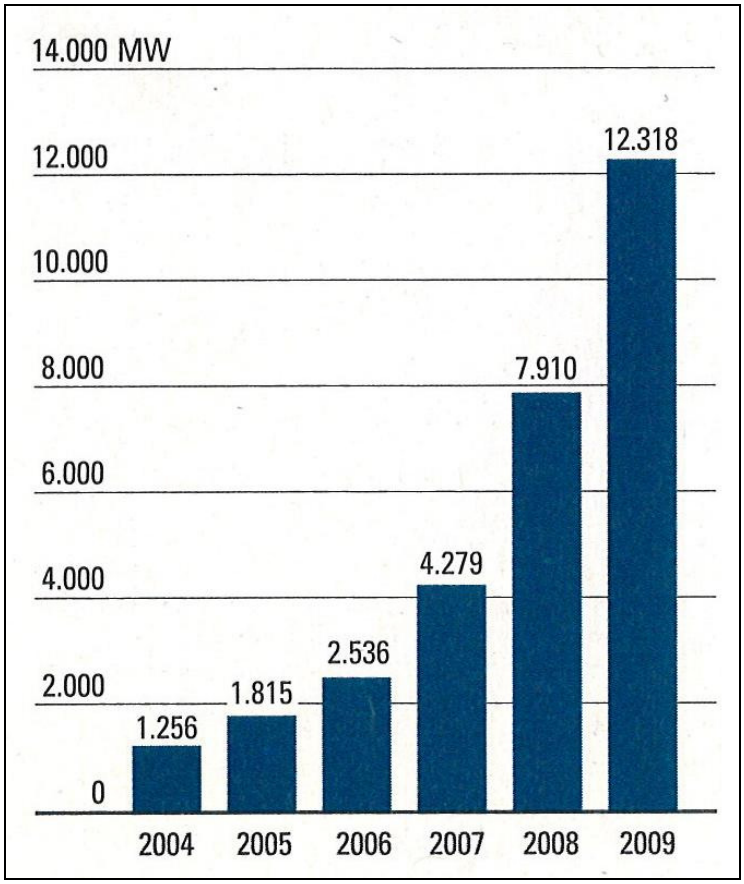

Figure 5: trend of solar cell production worldwide (Source: Photon)

Figure 6: car with sail

Wind energy is not the most efficient way to use the area on the roof of a car. On average the roof of a conventional car is approximately one to two square meters in size. Germany is one of the world's most popular car manufacturers. In Germany it is possible to produce from 975 up to 1,275kWh solar energy out of an area of one square meter a year. Calculations can be based on an average value of 1,125kWh for Germany yearly. Even in the cities with the least illumination, 90% of the average solar energy amount can be gained. This offers the possibility to produce solar energy in a good way in the whole of Germany. This solar energy which can be gained is equal to the energy level of 230-310kg of firewood, 180-235kg of brown coal briquettes, 95-120m³ of natural gas or 95-120l of fuel oil. The energy which lies in fuel oil is equal to the possible energy out of benzene or diesel. This leads to the opportunity to save the fuel amount used in a car by the use of solar energy. If the energy is produced at a fixed location, for different kinds of renewable energy resources and an area of one square meter, the following values can be given for the possible driving distance of an average conventional car (Nijs, 2009; Photon, 2010; DFS, 2002; Benkler, 2010).

renewable energy	possible driving distance
oil seed	1.5km
cooled photovoltaics	979km
wind energy	1,529km

Table 1: possible driving distance (Source: Nijs, 2009; DFS, 2002; Benkler, 2010)

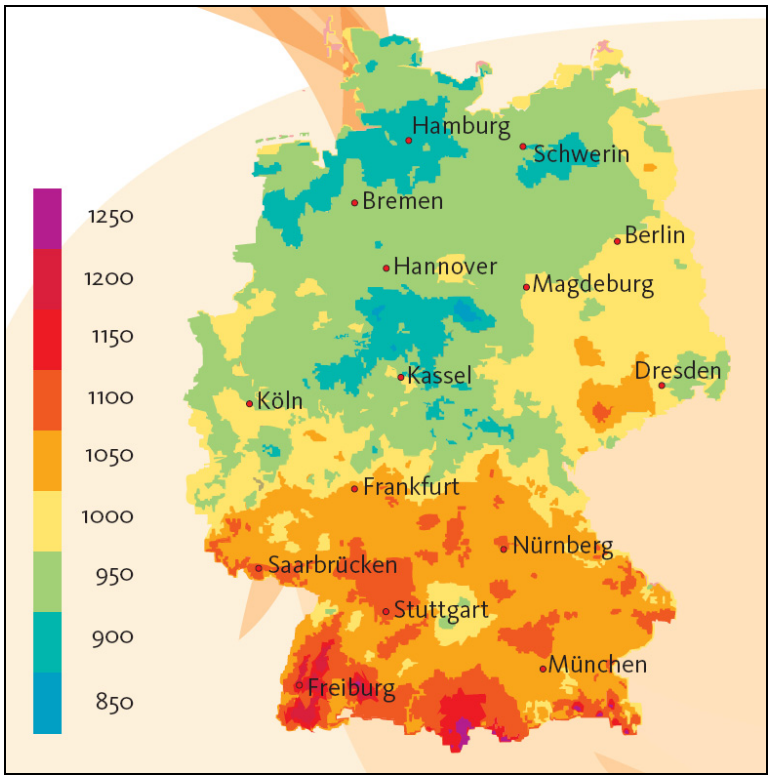

Figure 7: possible amount of solar energy in Germany (Source: DFS)

2.2.2. Availability of solar modules and prices

For the experimental vehicle, which is a Toyota Prius, mono crystalline solar cells are used. The price for the solar panel actually integrated into the roof of the Toyota Prius cannot be used for a comparison based on prices which can be estimated for a series production. This is the case because the solar panel is a prototype, which is designed to offer the opportunity to connect and evaluate electronics described in later chapters. To estimate a realistic price for a solar panel, prices for modules can be used. At first a calculation needs to be made regarding how much solar energy can be installed on the experimental vehicle. Afterwards an estimation can be made of how expensive this solar energy will be and which usage it has over an average expected driving capability of a conventional car.
There is a degree of uncertainty in that prices of energy cannot predicted over several years. It is the case that the efficiency of solar energy is increasing. As an absolute percentage this will be about 25% from the year 2010 to the year 2020. For a clear statement, criteria need to be found which restrict uncertainty. The final result will give a bandwidth for the approximate costs and usage over a vehicle's lifetime. The lifetime is estimated at 15 years with an annual driving distance of 12,000km (Nijs, 2009; Photon, 2010; DFS, 2002; Benkler, 2010; Format, 2010).

2.2.2.1. Used solar cell for the prototype vehicle

For the experimental vehicle, solar cells from the company Blue Chip Energy are used. These solar cells have a dimension of 156mm by 156mm, and a thickness of 180µm (Blue Chip Energy, 2010).

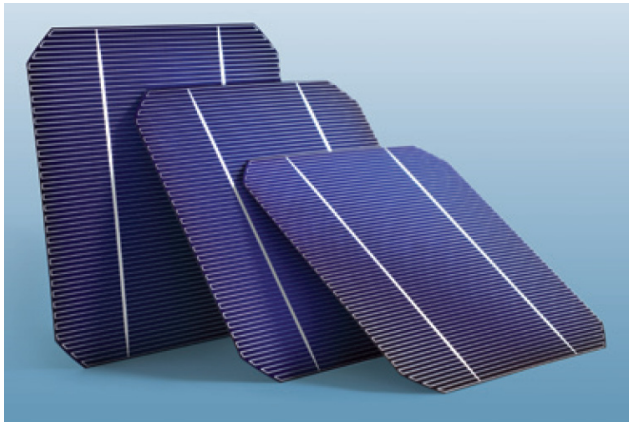

Figure 8: Blue Chip Energy solar cell (Source: Blue Chip Energy)

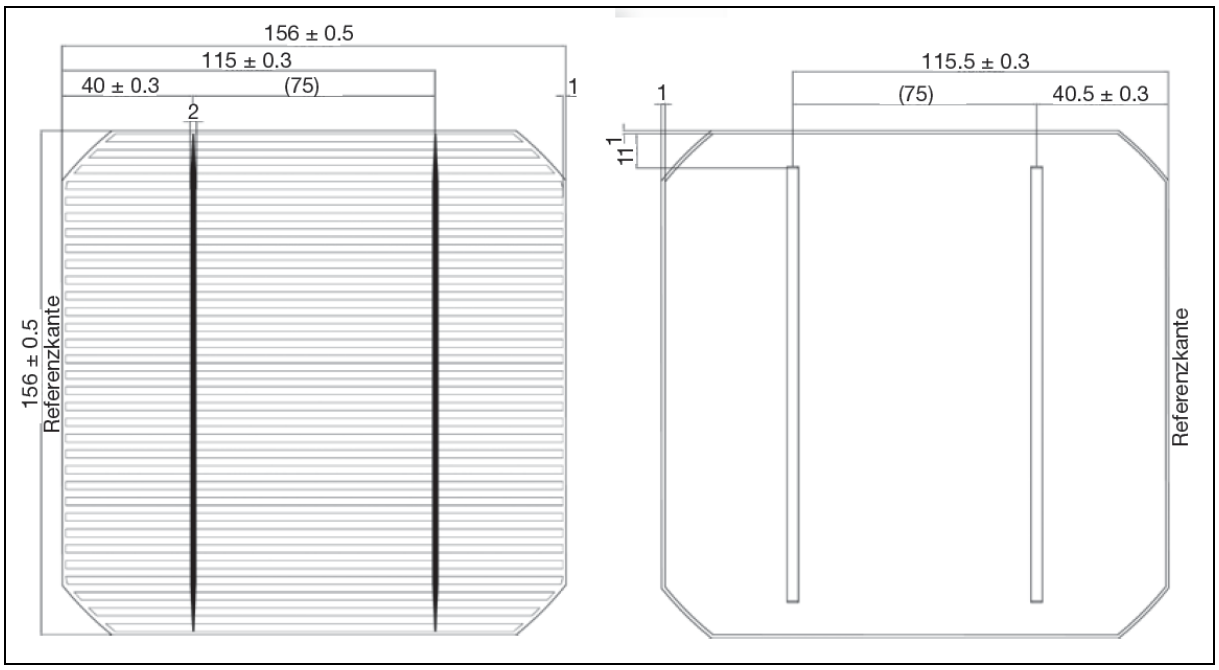

Figure 9: Blue Chip Energy solar cell dimensions (Source: Blue Chip Energy)

The cells themselves can be sorted into different power classes concerning their degree of efficiency, output voltage or output current. More information about these parameters is given in the later chapters.

power class P_{mp} [W]	efficiency min [%] to max [%]	V_{mp} [V]	I_{mp} [A]	V_0 [V]	I_{SC} [A]
4.320	17.95% to 18.20%	0.522	8.276	0.621	8.710
4.260	17.70% to 17.95%	0.520	8.193	0.618	8.679
4.200	17.44 %to 17.70%	0.519	8.093	0.615	8.634
4.140	17.20% to 17.44%	0.515	8.039	0.613	8.602
4.080	16.95% to 17.20%	0.510	8.001	0.610	8.569
4.020	16.69% to 16.95%	0.506	7.945	0.609	8.532
3.961	16.45% to 16.69%	0.505	7.844	0.608	8.508
3.931	16.20% to 16.69%	0.503	7.816	0.607	8.493
3.901	16.20% to 16.45%	0.501	7.787	0.605	8.478

Table 2: different power classes and output parameters (Source: Blue Chip Energy)

The plan is to install 45 solar cells on the roof of the experimental vehicle. With a possible output power of each cell of about 4W, the installed solar power is 180W.

2.2.2.2. Prices for modules made with different materials

For a price calculation, prices from January 2010 to July 2010 are taken. For January to June for each month four prices are given, and one price is given for July. There are different price ranges for the different categories of solar modules. Actual prices show a rising in costs of about 1.7% up to 5.5%, depending on the solar module category, from the beginning of June to the beginning of July. Furthermore the difference in prices between solar modules from Asia with the exception of Japan to Europe and USA declined from 25% to 6.8%. Solar modules from Japan are at the moment the most expensive ones on the entire market. To avoid influences from current and short term price instabilities, an average value is calculated over the prices since the beginning of the year without special consideration of prices.
For a comparison, especially modules made of mono crystalline silicon are interesting. The average price range calculated from prices from different manufacturers is from €1.42 per Watt at the beginning of April up to €1.74 per Watt at the end of May. A further average value can be calculated for that category of solar modules at €1.52 per Watt. For example the average prices for solar modules made out of multi crystalline silicon are from €1.41 per Watt at the beginning of April to €1.85 per Watt at the middle of June with an average price for this category of €1.66 per Watt. For 180W installed solar power on the experimental vehicle a price of €255.6 can be calculated. In comparison with latest prices the solar module costs €293.4 but this price value is not suitable for the price estimation. The Toyota Prius roof is a curved surface, which means that conventional module prices can not be used directly. The flexible Enecom solar panel mentioned in later chapters which can be used for a possible implementation already costs €530, which leads to a price of €6.63 per Watt or a price of €1,192.5 for the solar panel for the Toyota Prius (Photon, 2010; Wöhe, 2008; Enecom, 2009).

2.2.2.3. Impacts of solar panels on vehicles

In light of the above facts, the solar panel for the car will be more expensive than a conventional one. Furthermore an impact is given by the alignment to the sun of the solar panel on the roof. Approximately 95% of the nominal maximum output power can be gained. This value is taken from the mounting of solar panels on flat house roofs. This is the situation because with the flat mounted roof a perfect taken illumination will not be achieved as it would be the case if the roof were mounted in an alignment of an angle of 30° facing to the south. In that case 99% of the nominal maximum output power is possible. If 180W of solar power are installed on the roof of the vehicle 95% or 171W are used. This value can drop because of the curved surface of new cars' roofs. With an alignment to the west or the east and an angle of 30°, about 87% (156.6W)are possible . If the angle is lowered to 45°, for example, 83% are possible. The driver of the vehicle has to deal with the fact that different energy outputs of the solar panel will occur over the whole year with a possible maximum in August (Nijs, 2009; Photon, 2010).

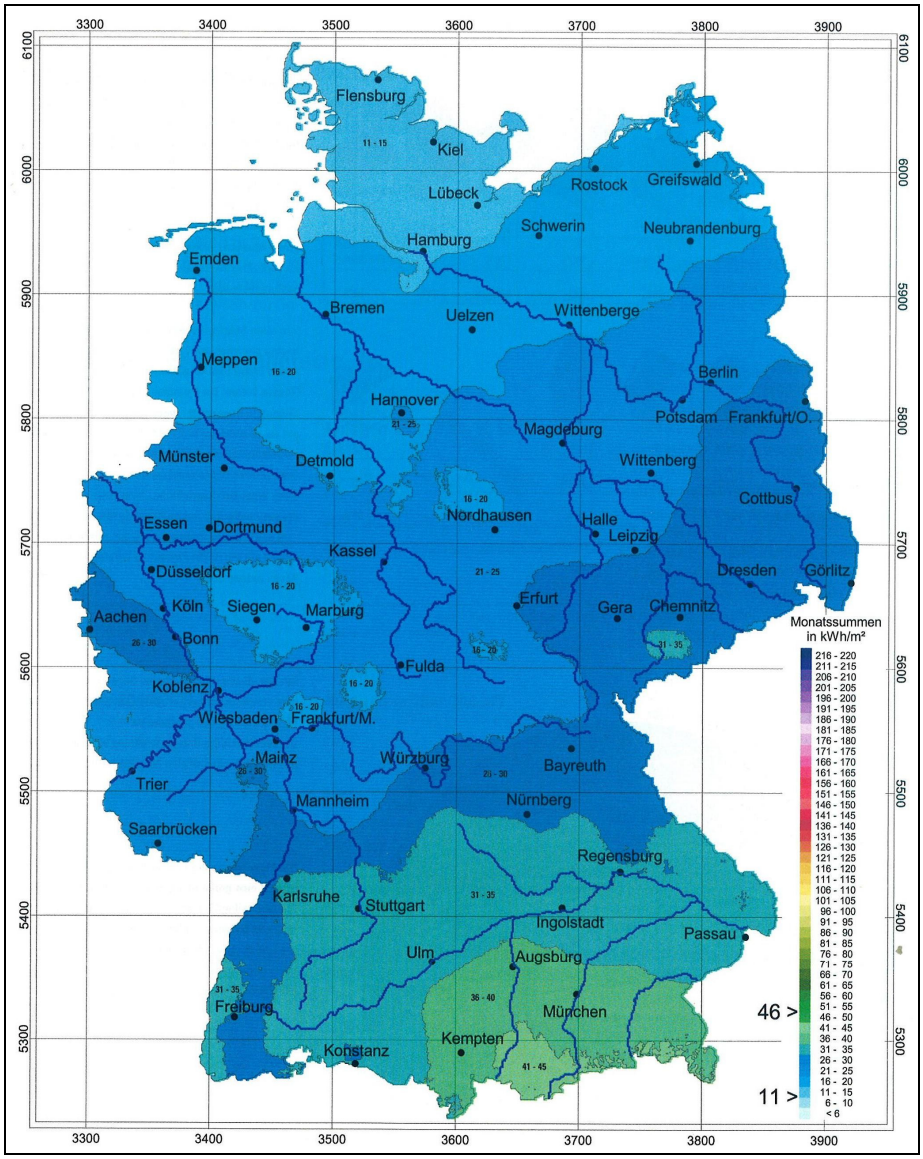

Figure 10: sun intensity and possible power, Germany November 2009 (Source: Photon)

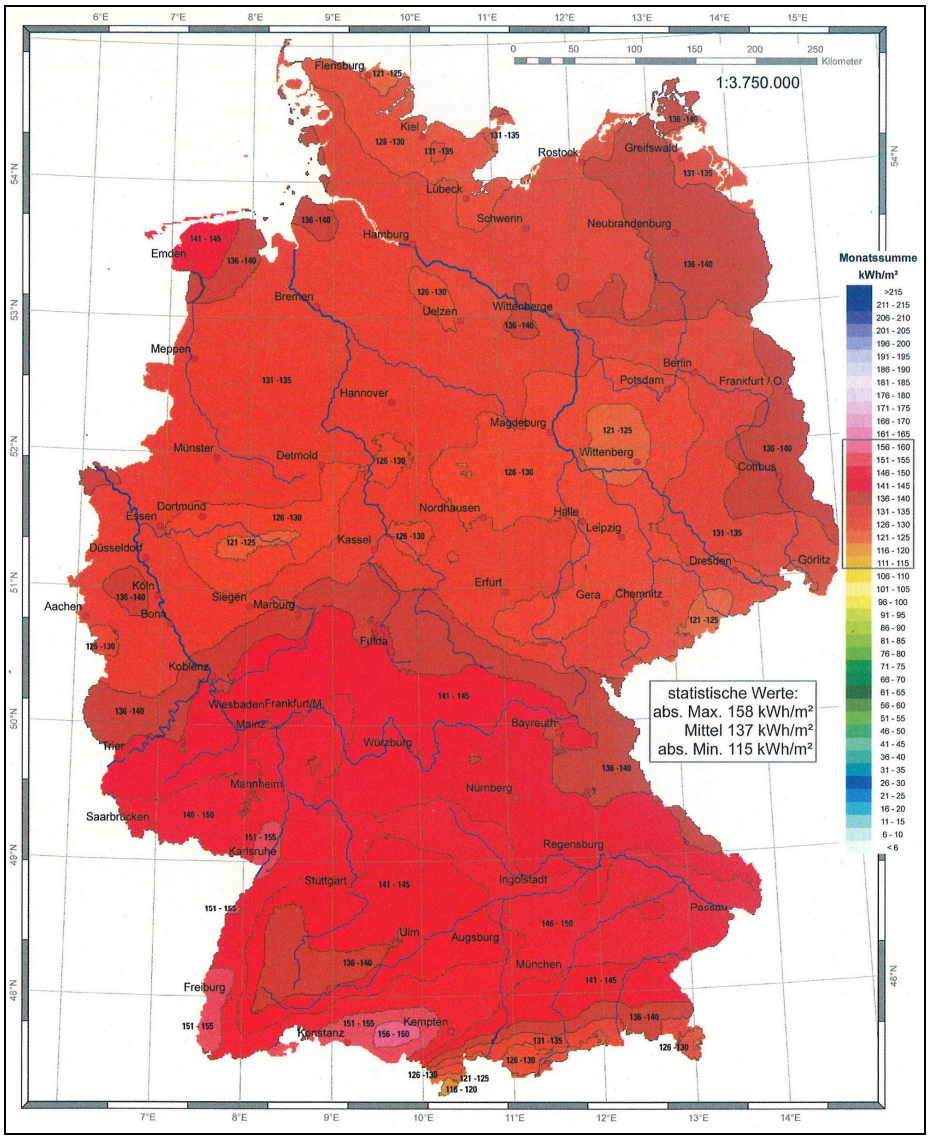

Figure 11: sun intensity and possible power, Germany April 2010 (Source: Photon)

2.3. Smart Grid

The 'Smart Grid' provides the possibility to use the electric cars connected to the power supply grid as a capacity to establish short term needed energy for the complete power supply network. Under normal conditions the electric vehicles can be an additional problem for the current energy amount. With the additional load and requirement a solution needs to be developed such that the complete power supply network will not be destabilized. To support the power net a good exchange of energy is needed. Therefore a normal power supply plug is not suitable. With a voltage of 230V and 16 Ampere only an amount of about 3.7kW can be exchanged between an electrical vehicle and the power grid. This is less in comparison with what is possible with the 400V and 32 Ampere plug. With this plug 22kW can be exchanged (Helmers, 2009; Schöllmann M., Hoff C., Schriek J., 2010; European Commission – Community Research, 2006; U.S. Department of Energy, 2008).

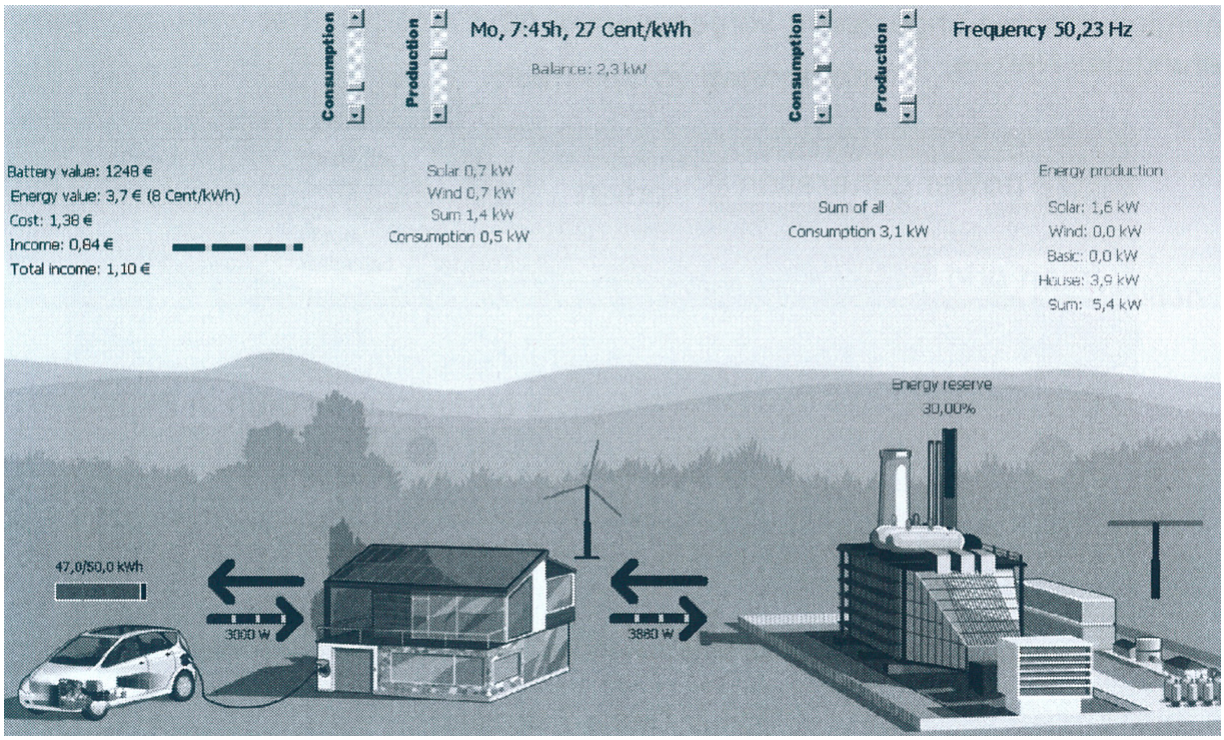

Figure 12: energy transfer along the smart grid (Source: Schöllmann M., Hoff C., Schriek J.)

Some of the smaller electrical vehicles with a battery capacity for a driving distance of about 100 to 130km with a full battery charge only offer the possibility to charge with the 230V power plug. This leads to the situation that the less expensive and smaller cars cannot help with the stabilization of the power net. It is obvious that more electrical vehicles on the road mean an additional energy demand. Therefore even renewable energy is required. Nevertheless it is also a good idea to load the electric cars with fossil energy because with this solution the pollution of urban areas can be reduced. Emissions will be released in areas away from family houses. Furthermore it makes sense to spread out energy in the sense that instead of big power plants, smaller and distributed power plants are used (Helmers, 2009; Schöllmann M., Hoff C., Schriek J., 2010; European Commission – Community Research, 2006; U.S. Department of Energy, 2008).

On average a car is only driven for about 10% of its life; the rest of the time it is parked for example on the parking area close to a house. This means that there is a lot of time available on the one hand to load the vehicle and also use it as an additional capacity for the entire power net. The system works in the same way as a storage power plant which has the opportunity either to take energy by pumping water to a higher point or in the other way to produce energy. To establish an opportunity for such a system to really work, the basic thing has to be that an input and an output of energy of the battery is as efficient as possible. It does not make sense when the stored energy in the battery is in a kind of way expensive because the loss of energy is too high.
Furthermore the whole chain in which the electrical vehicle supports the energy production by supplying energy to the power net has to be intelligent;a system of measurement has to be installed to monitor how much energy is taken and given to the car. There has to be a built-in price benefit to convince the owner of the the importance of the electric vehicle being connected to the power net to support the net itself. With a Lithium Ion battery it can be stated that there is no memory effect and that the lifetime of the battery is not reduced due to the procedure of loading and unloading. The first benefit will be that the power supply net can be stabilized. This stabilization is dependent on the available cars connected to the power supply, and the cars themselves have to work as a bidirectional energy storage possibility and therefore a higher exchange amount of energy is required. With a 400V power supply and 63 Ampere, already up to 43kW can be transferred.
The next step will be to enhance the capabilities of the electric car itself in such a way that it will be a kind of electrical power plant. With a photo voltaic system placed on the roof of the vehicle, energy can be gained to reload the battery for electrical driving. Additionally this energy can also be taken by the power net to support short term high demand of energy. It also makes sense to see this relationship of the electric car and the power supply net for the case where the electric car is fully recharged with the photo voltaic system and there is no additional energy needed anymore. Nevertheless energy can still be taken from the sun to reload the battery. If energy is given to the power supply net at such times, the photo voltaic system can be used continuously. One additional advantage will be in this case that the energy is renewable. So it also requires the option to have this exchange with the power supply net in constant use, and not only when energy is needed by the power supply net.
To compensate the need of energy the electric car has an example the possibility of recuperative braking. This technology is also implemented in a hybrid car. Along this type of car a difference is given. The amount of energy which can be stored in the battery is limited in comparison to an electric car without a compulsion engine. In the case of the hybrid car the idea can be to deliver the energy directly to the power grid, instead of the usage of an additional battery. In general this can be a suitable solution to avoid converter losses and enhance the degree of efficiency (Helmers, 2009; Schöllmann M., Hoff C., Schriek J., 2010; European Commission – Community Research, 2006; U.S. Department of Energy, 2008).

2.4. Hybrid Technology in cars

2.4.1. Overview

In order to fulfil the criteria for emissions and noise reduction, car manufacturers place an emphasis on alternative propulsion systems. Additionally new ideas can also increase the fun-to-drive factor and the comfort level of the car. A combination of an electrical engine with a combustion engine offers the opportunity to downsize the combustion engine. The most noteworthy benefits of a hybrid car are the start-stop technology, the use of the combustion engine with the best degree of effectiveness and the recuperative braking. The weaknesses of the normal conventional system are largely eliminated. Hybrid technology is a possibility to arrange a transition from the combustion to the electric vehicle (Bosch, 2007; Helmers, 2009).

2.4.2. Propulsion concepts

The meaning of hybrid is that the propulsion is offered by more than one engine. It is a combination of a combustion engine, one or two electrical engines and an energy storage component. In general the whole system can be divided into basic structures. On the one hand the serial drive and on the other hand the parallel drive. Furthermore also a combination of these two structures is possible (Bosch, 2007).

2.4.2.1. Serial hybrid

The engines are mounted in a serial combination together. This solution requires two electrical engines and one combustion engine. One of the electrical engines is used as a generator to produce the electrical energy while the other one is used as a motor and takes care of the propulsion. The combustion engine is used to run the generator and not used for the propulsion. The generator can either provide electricity to recharge the batteries or supply the motor directly with energy so that the electrical motor is the only one which handles the propulsion.
The advantage lies in the possibility to run the combustion engine at its best degree of effectiveness and it can be built in separately into the vehicle. The disadvantage lies in the need to convert the energy several times which can lead to a loss up to 30% on average.
The serial concept is used in diesel locomotives and furthermore for buses. In a conventional vehicle the serial concept is not used (Bosch, 2007).

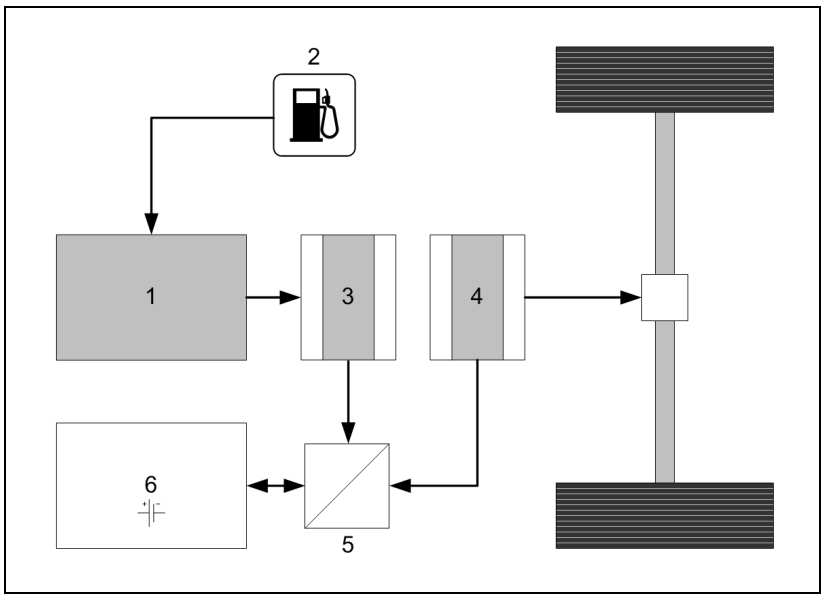

Figure 13: serial hybrid scheme (Source: Bosch)

number	description
1	combustion engine
2	tank
3	generator
4	motor
5	converter
6	battery

Table 3: description of the parts from the serial hybrid scheme (Source: Bosch)

2.4.2.2. Parallel hybrid

This case offers the possibility for the combustion engine and for the electrical engine to provide the propulsion. By the use of the clutch the power of both engines can be combined. This addition offers a downsizing of both engines without an impact on the driving capabilities of the vehicle. The system includes only one electrical engine which means that the vehicle cannot be driven electrically and recharge the battery at the same time. If a clutch is installed between the two engines the combustion engine need not be integrated in the vehicle and can be used for example as an additional range extender (Bosch, 2007).

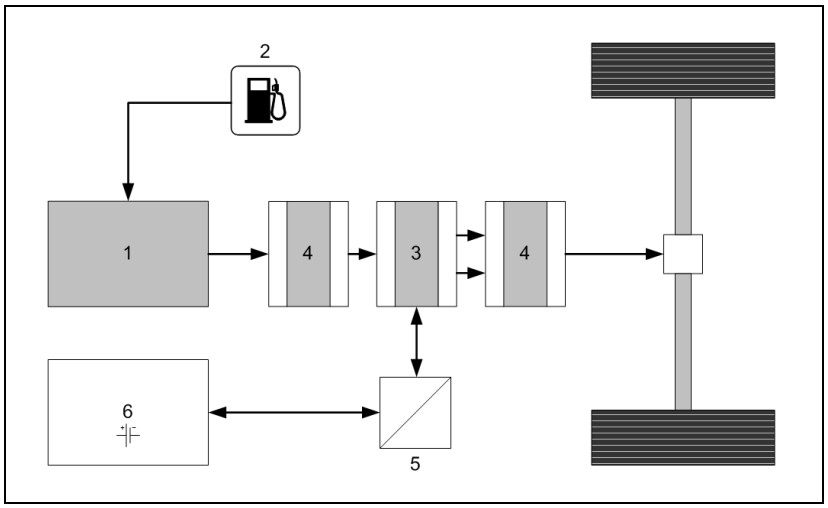

Figure 14: parallel hybrid scheme (Source: Bosch)

number	description
1	combustion engine
2	tank
3	electrical engine (generator and motor)
4	clutch
5	converter
6	battery

Table 4: description of the parts from the parallel hybrid scheme (Source: Bosch)

2.4.2.3. Serial-Parallel hybrid

By the help of a special gear system, the planetary device, it is possible to split the power provided from the combustion engine. While one part of the power is used for propulsion, the other part is used to run the generator. The energy produced by the generator can either be taken to recharge the battery or supply the electrical motor. As a parallel hybrid system, both engines (the combustion engine and electrical motor) can be used for propulsion.
The target for this model is to run at the most efficient operating point. The planetary device is the only required gear system. The experimental vehicle, the Toyota Prius, uses this kind of system for the propulsion, and the vehicle itself is a strong hybrid. The strong hybrid differs from the micro hybrid and mild hybrid in that it offers to drive only electrically with energy from the high voltage battery. Therefore a higher effort needs to be made to realize this possibility (Helmers, 2009; Schöllmann M., Hoff C., Schriek, J., 2010; Bosch, 2007)).

2.5. Toyota Prius

2.5.1. Solar panel on the 3rd generation of the Toyota Prius

The Toyota Prius offers the opportunity for implementation of a solar roof. A primary question which needs to be solved is for which source the gathered energy should be used. Basically the idea is not new to integrate a solar roof in a car. Toyota offers to the customer a solar roof as an optional feature in the 3rd generation of the Prius.

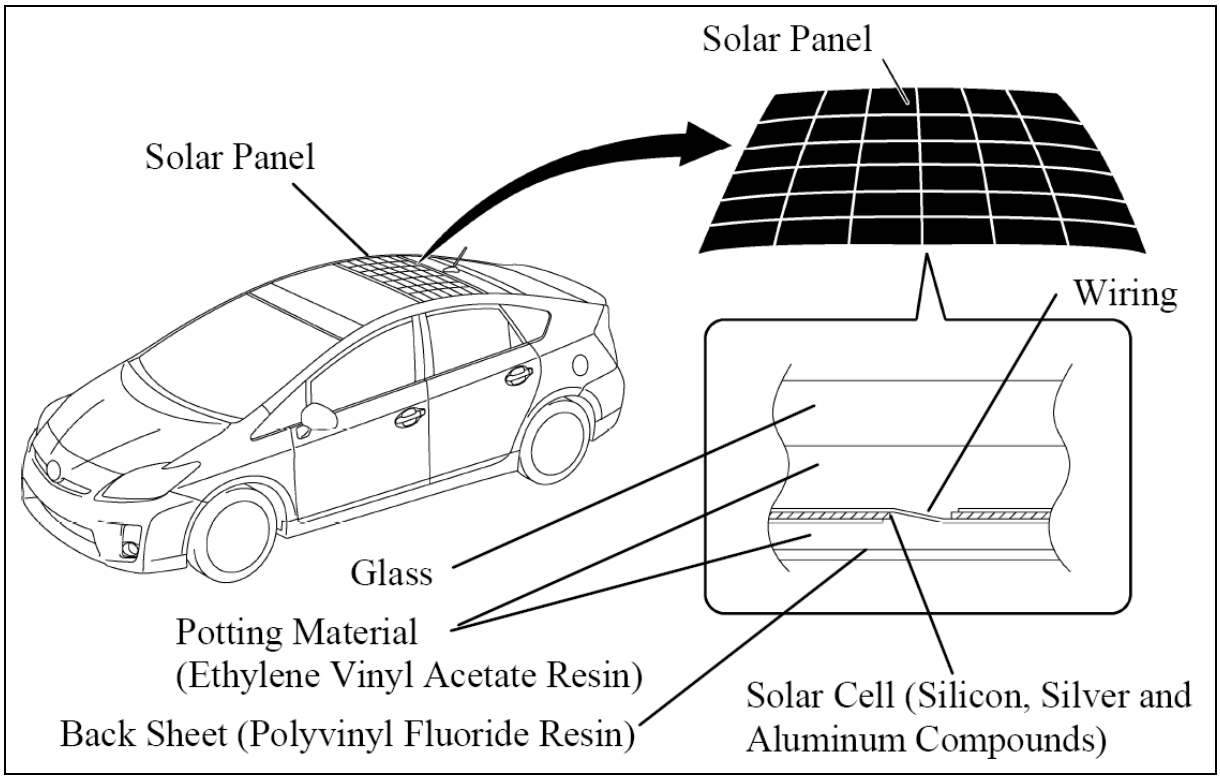

Figure 15: solar panel on Toyota Prius – schematic (Source: Toyota)

The purpose of the solar roof in the currently latest option from 2010 is to supply a ventilation system which is used when the vehicle is shut off and parked, to control the temperature in the driver's cabin to enhance the comfort. The gathered energy from the supply powers a blower fan to work alongside the air conditioning system, which is useful if the vehicle is parked in the sunlight.
The solar panel is mounted on the rear side of roof and consists of 36 poly crystalline silicon solar cells which are connected in series. The roof components are glass, potting material, silicon, silver and aluminium compounds and a back sheet. The solar panel is available as an additional package in combination with a sun roof for €1,150. For the solar roof also the additional comfort package needs to be chosen which includes for example a rain sensor and the smart-key-system which costs a further €750 (Toyota, 2010).

Figure 16: solar panel on Toyota Prius – figure (Source: Toyota)

The solar panel has the following values:

value	Description
60W	nominal output power
22V	at 25C°,77°F and on an average sunny day
27V	at -30C°,-22°F and on an average sunny day
3.6A	maximum output current

Table 5: Toyota Prius solar panel values (Source: Toyota)

Different parameters have an impact on the output values, such as temperature and sunlight intensity. Basically the solar panel is equal to a conventional solar panel which is mounted on the roof of a building for producing electricity, with the exception that it does not operate on high voltage or charge batteries.
A decision for the energy sink requires analyzing the vehicle and the possibilities. In general the height of the energy output also defines the usage. In the Toyota Prius the solar panel is not connected to the 12V auxiliary battery, the high voltage battery or the SRS airbags. It only supplies a blower fan. During driving and other conditions the solar panel produces energy as well as when it is parked in the sun. The opportunity is available to use this energy to reduce fuel consumption. For example by charging the 12V auxiliary battery or the high voltage battery with the gathered energy from the solar panel, the drive distance which can be taken electrically would be extended. This makes sense because the 3rd generation of the Toyota Prius is a plug-in version. That means that the high voltage battery can be recharged with external power. An evaluation can be made to figure out how much the external recharging time can be reduced by recharging the batteries with the solar panel (Toyota, 2010).

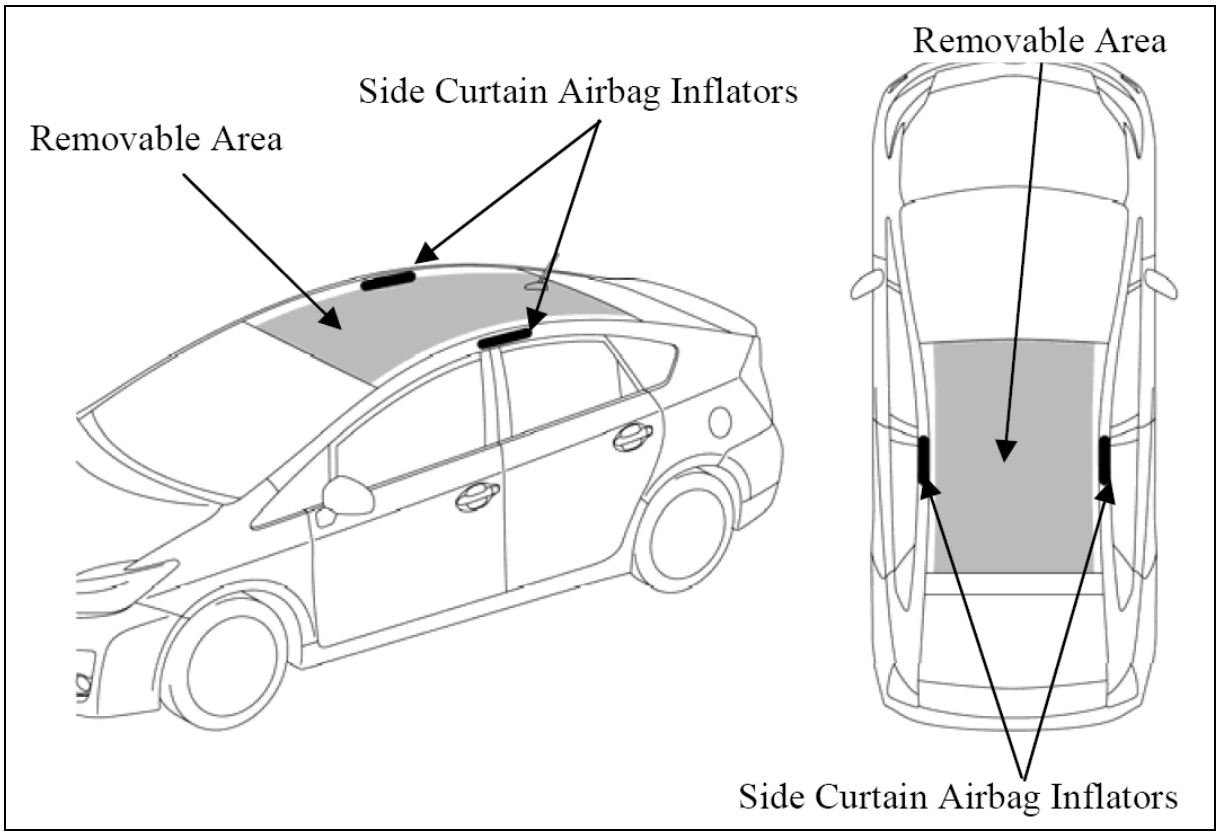

Figure 17: removable roof area of the Toyota Prius (Source: Toyota)

With the implementation of a larger solar panel and a different one from that which is available from Toyota, a larger amount of area can be used. If a full integration is required or holes need to be drilled, the side curtain airbags have to be considered. Normally this area should only be removed in case of an emergency by the firefighters. A negative impact on the stability of the car itself has to be considered. Removing the roof has to be performed carefully to avoid breaching the side curtain airbags, and with a focus to ensure stability (Toyota, 2010).

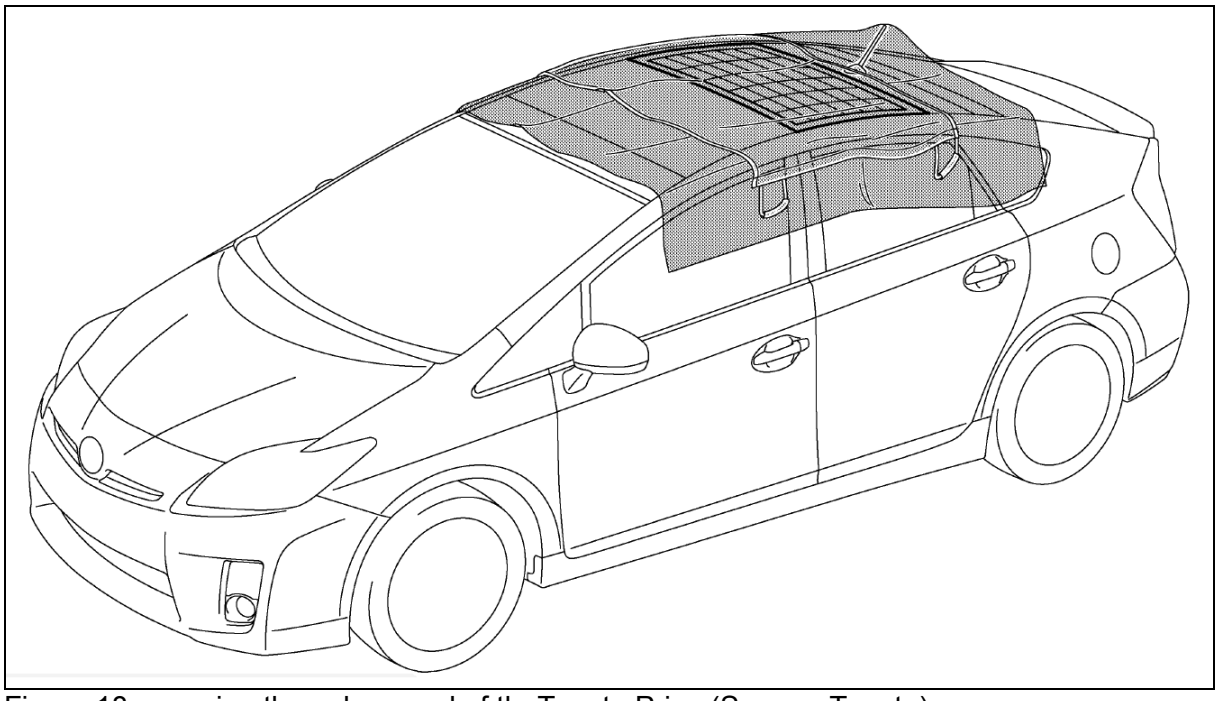

Figure 18: covering the solar panel of theToyota Prius (Source: Toyota)

With the solar panel as an additional power source on the roof, additional scenarios have to be considered. In case of an accident the solar panel still produces energy. To avoid injuries the solar panel has to be disabled. This can be done by covering the roof with a material which blocks the sun light. For example a cover folded in several layers delivers enough protection. After the entire area of the solar panel has been covered the solar panel itself will immediately stop producing power (Toyota, 2010).

2.5.2. Enecom solar panel

The solar panel from Enecom Italia is similar to the optional solar panel from Toyota for the Toyota Prius. It differs in the higher possible output values such as current and power. For a measurement to gather comparable data the HF80 from Enecom was chosen. The HF80 is a flexible module which uses 36 crystalline silicon cells which are connected in serial, as with the solar panel of the Toyota Prius. The cells have a high efficiency and the design of the Enecom solar panel makes it shatterproof, durable, waterproof and lightweight (Enecom, 2009).

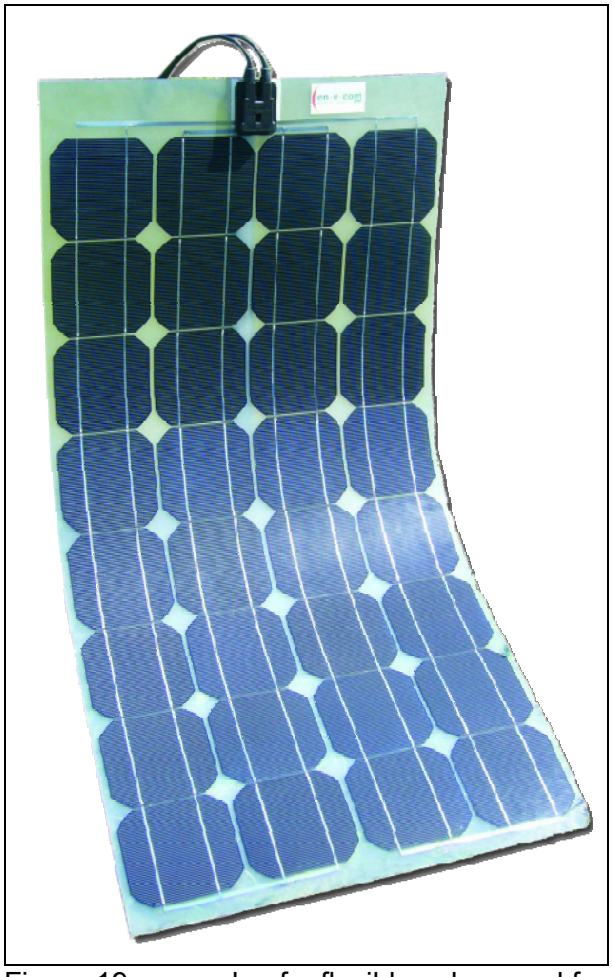

Figure 19: example of a flexible solar panel from Enecom (Source: Enecom)

value	Description
80 ±3%	peak power [W]
21.96	open circuit voltage, V_{OC} [V]
5.1	short circuit current, I_{SC} [A]
18.18	voltage at maximum power, V_{mp} [V]
4.6	maximum power current, I_{mp} [V]

Table 6: Enecom solar panel values (Source: Enecom)

It is developed basically for the use on the decks of boats and for roofs of mobile homes, without the fear of damage caused by vibration, high temperatures or seawater contact. The panel itself, the junction box and the cables are also resistant to seawater and UV light. Furthermore Enecom panels can be curved up to a maximum of 30% of their length (Enecom, 2009).

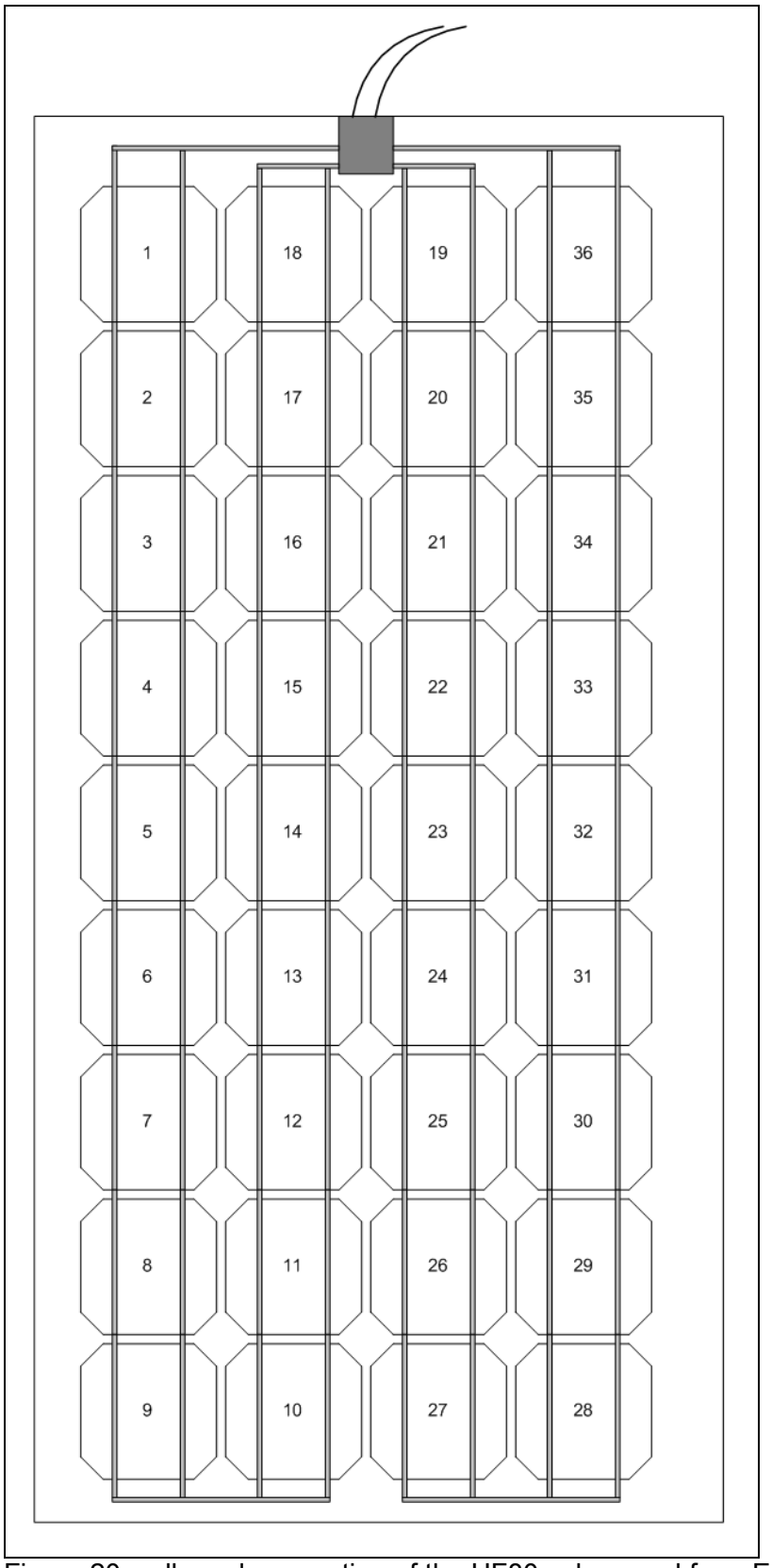

Figure 20: cells and connection of the HF80 solar panel from Enecom

2.5.3. Comparison between the solar panels and possible output power

The nominal output power of the Toyota Prius solar panel is 60W. With a calculation of the parameters of the panel the theoretical maximum output power can be calculated as follows:

$$P_{max} = V_{max} \times I_{max} = 22V \times 3.6A = 79.2W$$

The maximum output power from the solar panel comes close to the given output power of the Enecom solar panel, which is 80W with a tolerance of ±3%. Basically it has to be said that the solar panel of the Toyota Prius is designed to power a blower fan. The question is how shadowing on the solar panel affects the power supply of this fan (Toyota, 2010; Enecom, 2009).

2.5.4. Load for comparison measurement

To take measurements with the Enecom solar panel a load has to be designed. To calculate the current out of the measured voltage and the given resistor, the voltage needs to be below +10V. This is a requirement given by National Instruments (NI), the manufacturer of the multifunction data acquisition (DAQ) module which can be connected via USB to a computer. For the measurement the model 6259 is used, which offers for example 32 analog inputs and 4 analog outputs (National Instruments, 2009).

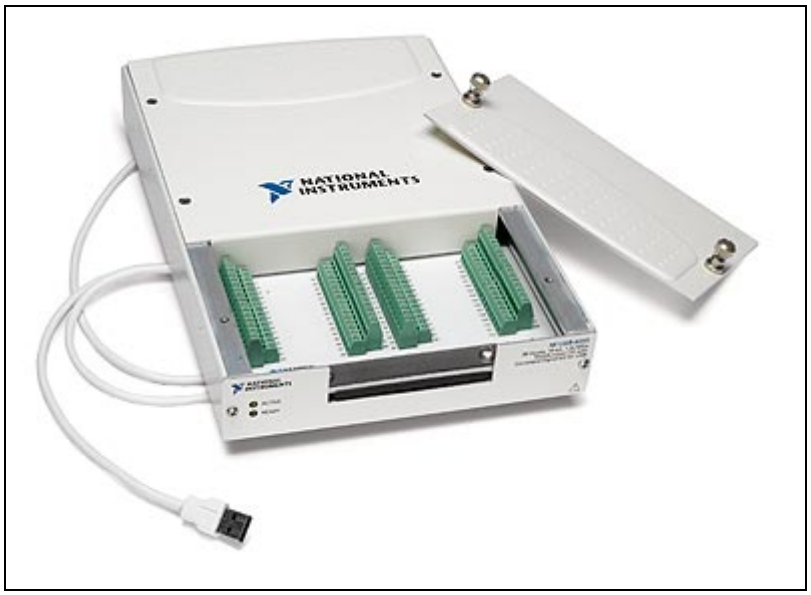

Figure 21: NI USB-6259 (Source: National Instruments)

The maximum voltage restriction has to be considered by the dimensioning of the load. For the measurement load resistances of the type RB50 from ATE are used. Each resistor has a resistance of 10Ω and a nominal power of 50W. For the nominal power a heat sink is required; without a heat sink the maximum power is 20W (ATE, 2007).

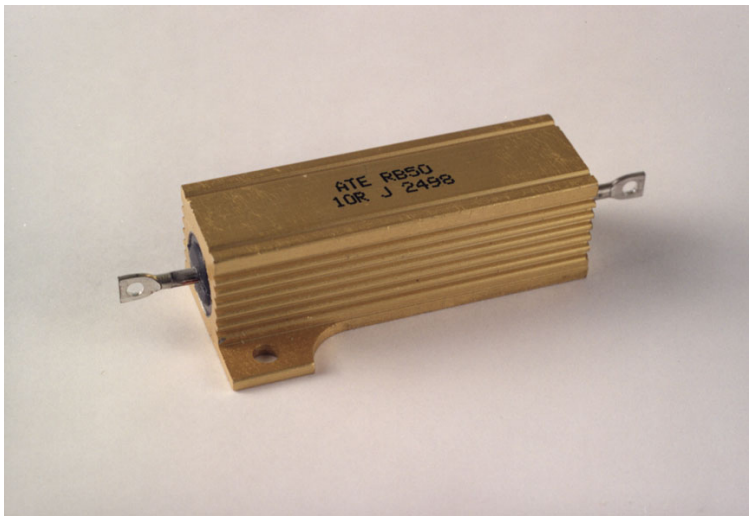

Figure 22: ATE RB50 with 10Ω (Source: ATE)

A maximum output voltage of about 18V and a maximum output power of about 80W can be expected from the Enecom solar panel. For that possible output three resistances have to be taken. The two basic options are to connect them in serial or in parallel.

2.5.4.1. Serial connection of the resistances

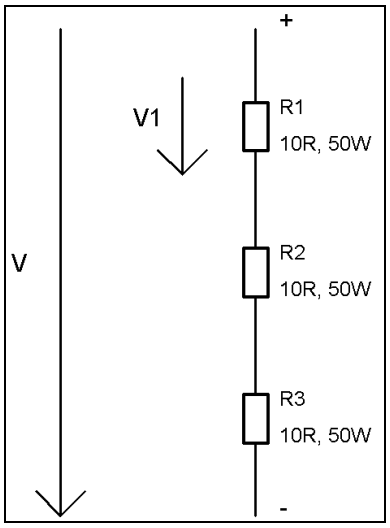

Figure 23: serial connection of the resistances

$$V_1 = \frac{V_{\max}}{3} = \frac{18.18V}{3} = 6.06V$$

$$P_{\max,R1} = V_1 \times I_{\max} = 6.06V \times 4.6A = 27.88W$$

$$R_{tot} = R_1 + R_2 + R_3 = 10\Omega + 10\Omega + 10\Omega = 30\Omega$$

On each resistor a maximum power of about 28W will occur. The maximum voltage V_1 on one resistor of about 6V is suitable for measurements with the NI DAQ module.

2.5.4.2. Parallel connection of the resistances

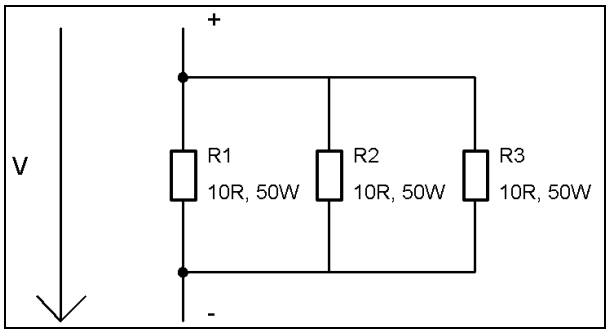

Figure 24: parallel connection of the resistances

$$I_1 = \frac{I_{\max}}{3} = \frac{4.6A}{3} = 1.53V$$

$$P_{\max,R1} = V_{\max} \times I_1 = 18.18V \times 1.53A = 27.82W$$

$$R_{12} = \frac{R_1 R_2}{R_1 + R_2} = \frac{10\Omega \times 10\Omega}{10\Omega + 10\Omega} = 5\Omega$$

$$R_{tot} = \frac{R_{12} R_3}{R_{12} + R_3} = \frac{5\Omega \times 10\Omega}{5\Omega + 10\Omega} = 3.3\Omega$$

On each resistor a maximum power of about 28W will occur. The maximum voltage V on one resistor of a maximum of 18.18V is not suitable for measurements with the NI DAQ module because the voltage is too high.

2.5.4.3. Chosen load for the measurement

For the measurement the serial connection of the load resistances is chosen. The configuration of the measurement is shown in the following figure.

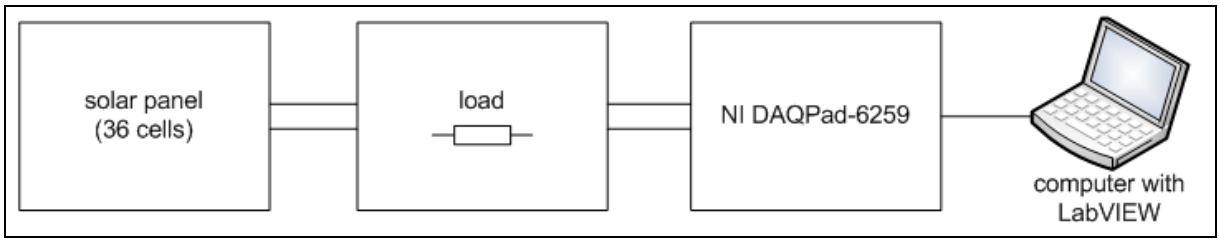

Figure 25: measurement structure with serial load

2.5.5. Shadowing on the solar panel and measurements

To ascertain the negative impact of shadowing the cell at the measurements was completely covered. This was done to avoid the case that the cell could still receive light to produce power and thus to operate with reproducible measurement criteria. The output voltage was measured and the current calculated on the computer. The voltage was measured on R_1 which has a nominal value of 10Ω and a real value of 10.5Ω. For R_2 and R_3 the situation is similar. This yields the following equations:

$$V_{\max} = I_{\max} \times R_{tot} \rightarrow I_{\max} = \frac{V_{\max}}{R_{tot}}$$

$$P_{\max} = V_{\max} x I_{\max} = V_{\max} \frac{V_{\max}}{R_{tot}} = \frac{(18.18V)^2}{30\Omega} = 11.02W$$

$$I_{\max} = \frac{V_{\max}}{R_{tot}} = \frac{18.18V}{30\Omega} = 0.61A$$

$$P_{\max,real} = V_{\max,real} \times I_{\max,real} = V_{\max,real} \frac{V_{\max,real}}{R_{tot,real}} = \frac{(18.09V)^2}{31.5\Omega} = 10.39W$$

$$I_{\max,real} = \frac{V_{\max,real}}{R_{tot,real}} = \frac{18.09V}{31.5\Omega} = 0.57A$$

The first step of the measurement is to cover one cell. In further steps of the measurement two, four or more cells are covered. The cells are arranged with numbers as shown on the figure in chapter 2.4.2. for a better record of the measurement.

Figure 26: Enecom HF80 solar panel in the sun at the time of measurement

2.5.5.1. One cell covered

covered cell	voltage [V]	current [A]	power [W]	loss of power [W]	loss of power [%]
1	14.20	0.45	6.39	4.00	38.50
9	16.80	0.53	8.90	1.47	14.15
28	16.78	0.53	8.89	1.50	14.44
36	14.77	0.47	6.94	3.45	33.21

Table 7: measurement results for one cell covered

2.5.5.2. Two cells covered

covered cell	voltage [V]	current [A]	power [W]	lost of power [W]	lost of power [%]
1,2	13.17	0.42	5.53	4.86	46.78
8,9	10.90	0.35	3.82	6.57	63.23
28,29	13.84	0.44	6.09	4.30	41.39
35,36	10.63	0.34	3.61	6.78	65.26

Table 8: measurement results for two cells covered

2.5.5.3. Four cells covered

covered cell	voltage [V]	current [A]	power [W]	lost of power [W]	lost of power [%]
1,2,3,4	4.40	0.14	0.62	9.77	94.03
6,7,8,9	7.14	0.23	1.64	8.75	84.22
28,29,30,31	6.70	0.21	1.40	8.99	86.53
33,34,35,36	6.63	0.21	1.39	9.00	86.62

Table 9: measurement results for four cells covered

2.5.5.4. Other cell groups covered

covered cell	voltage [V]	current [A]	power [W]	lost of power [W]	lost of power [%]
1,18,19,36	7.45	0.24	1.79	8.60	82.77
9,10,27,28	7.21	0.23	1.66	8.73	84.02
1,18,19,36, 2,17,20,35	3.69	0.12	0.44	9.95	95.77
9,10,27,28, 8,11,26,29	4.5	0.14	0.63	9.76	93.94
1,18,19,36, 2,17,20,35, 3,16,21,34	2.01	0.06	0.12	10.27	98.85

Table 10: measurement results for other cell groups covered

2.5.5.5. Average loss of power

$$P_{loss,1} = \frac{(38.50\% + 14.15\% + 14.44\% + 33.21\%)}{4} = 25.08\%$$

$$P_{loss,2} = \frac{(46.78\% + 63.23\% + 41.39\% + 65.26\%)}{4} = 54.17\%$$

$$P_{loss,4} = \frac{(94.03\% + 84.22\% + 86.53\% + 86.62\% + 82.77\% + 84.02\%)}{6} = 86.37\%$$

$$P_{loss,8} = \frac{(95.77\% + 93.94\%)}{2} = 94.86$$

$$P_{loss,12} = 98.85\%$$

amount of covered cells	average loss on power [%]
1	25.08
2	54.17
4	86.37
8	94.86
12	98.85

Table 11: measurement results for other cell groups covered

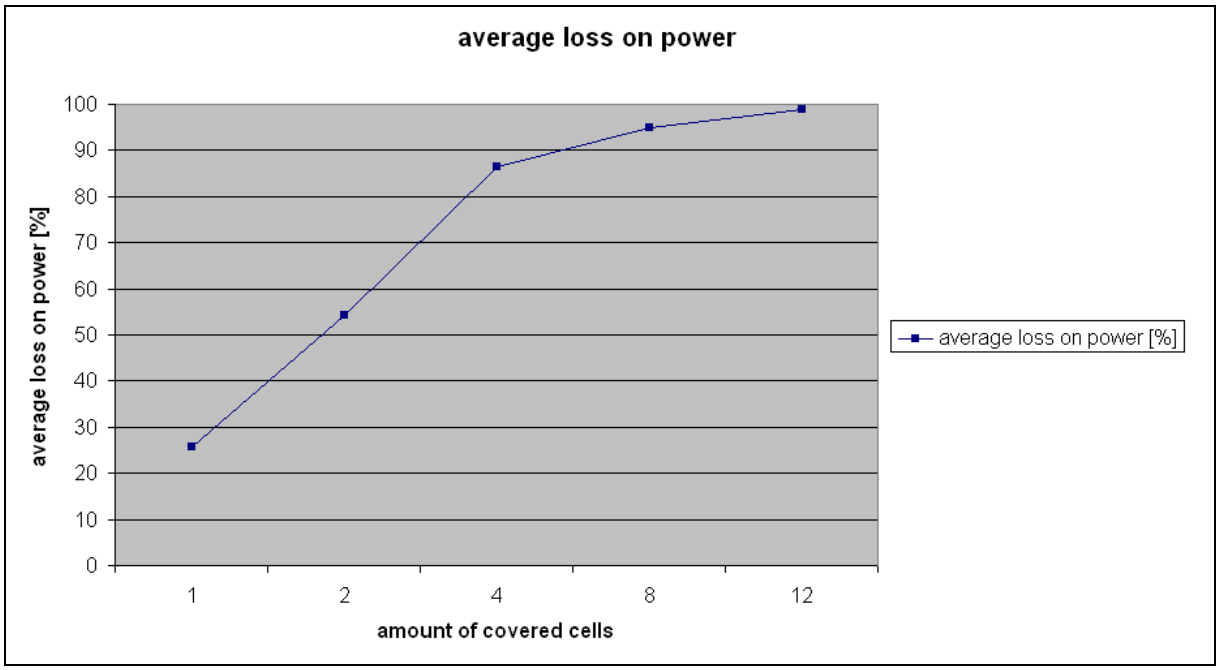

Figure 27: average loss on power in case of covered cells

The loss of power is significant and the covering of one cell results in a loss on average of 25% of power. With a covering of four cells nearly 90% is lost. It is unusual that only one cell is covered by shadow. Moreover it will be the case that the negative impact of shadowing will occur on more than one cell, for example on four cells. The measurement results show the possibility that the blower fan cannot be supplied if a small area of the solar panel is covered by shadow. This situation can be improved by the usage of maximum power point trackers.

2.5.6. Different kinds of loads on the solar panel

For all measurements, three resistors of the type RB50 from ATE which are suitable for a maximum power of 50W and four load resistances for a maximum power of 17W have been available. The value of the total real resistance was taken by measurement.

2.5.6.1. Variant 1 (total resistance R_{tot} = 15Ω, real total resistance $R_{tot,real}$ = 15.9Ω)

With additional load resistances of 10Ω and a maximal power of 17W the total resistance of the load can be reduced by a parallel connection of the additional load resistances with the previous ones.

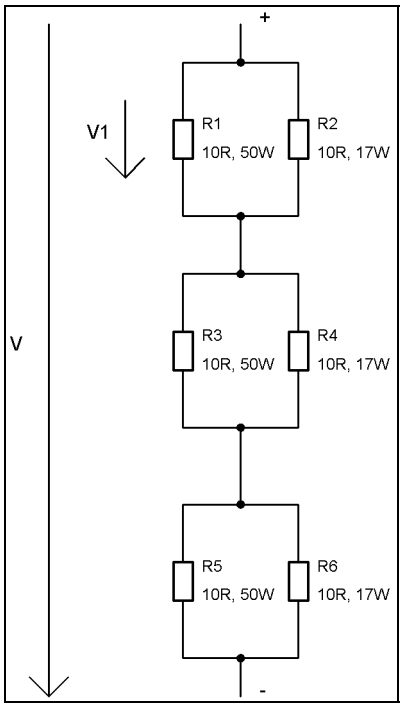

Figure 28: variant 1 load configuration

$$R_{12} = R_{34} = R_{56} = \frac{R_1 R_2}{R_1 + R_2} = \frac{R_3 R_4}{R_3 + R_4} = \frac{R_5 R_6}{R_5 + R_6} = \frac{10\Omega \times 10\Omega}{10\Omega + 10\Omega} = 5\Omega \rightarrow R_{tot} = 5\Omega + 5\Omega + 5\Omega = 15\Omega$$

$$V_{\max} = 18.18V; V_{\max,real} = 17.3V$$

$$P_{\max} = V_{\max} \times I_{\max} = V_{\max} \frac{V_{\max}}{R_{tot}} = \frac{(18.18V)^2}{15\Omega} = 22.03W$$

$$V_{1,real} = \frac{V_{\max,real}}{3} = 5.77V$$

$$R_{tot,real} = 15.9\Omega$$

$$V_{\max,real} = I_{\max,real} \times R_{tot,real} \rightarrow I_{\max,real} = \frac{V_{\max,real}}{R_{tot,real}} = \frac{17.3V}{15.9\Omega} = 1.09A$$

$$P_{\max,real} = V_{\max,real} \times I_{\max,real} = \frac{V_{\max,real}}{R_{ges,real}} V_{\max,real} = \frac{(17.3V)^2}{15.9\Omega} = 18.82W$$

With the given load of 15.9Ω a further measurement was made to gather information about the voltage, current and power stability over a certain period of time. If the solar panel is placed in full sunlight with the maximum amount on illumination which is possible for the location and the time of the year, a variety of characteristics of the solar panel can be calculated. This information can lead to a statement about the power output under normal working conditions as well as under nearly ideal working conditions. The basis for the calculation are 8268 measurement values which have been taken over a time period of about one hour (exactly one hour, nine minutes and 37 seconds) with the DataLogging measurement tool. Before the measurement was started, the solar panel was in operation for a certain time to ensure that it had reached its operating temperature.

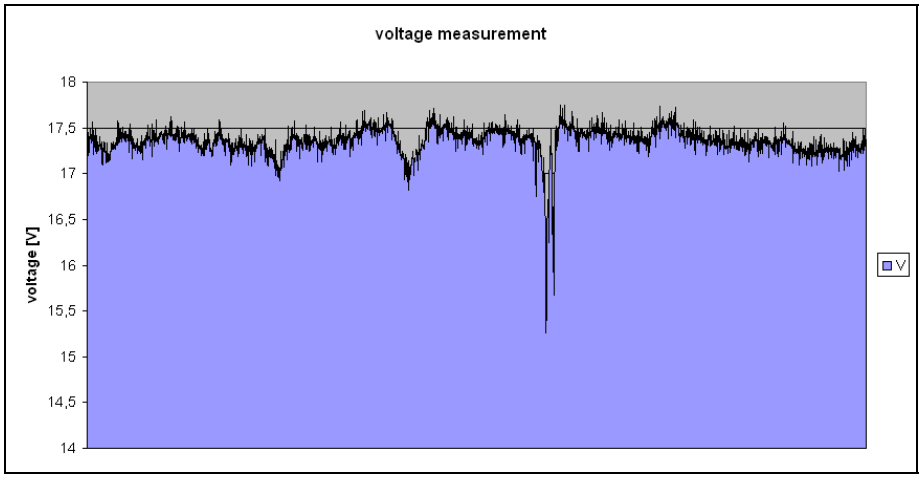

Figure 29: voltage level of the measurement of variant 1 (8268 values)

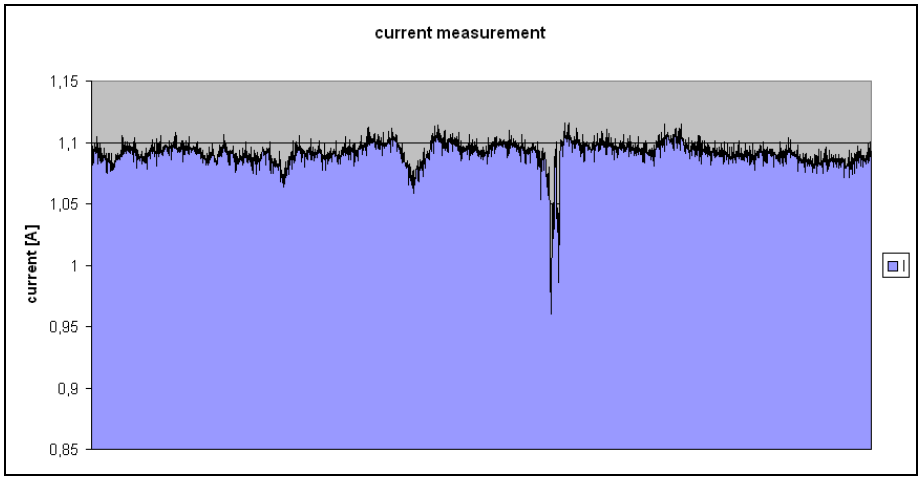

Figure 30: current level of the measurement of variant 1 (8268 values)

$$V_{\min} = 15.26V; V_{\max} = 17.74V; I_{\min} = 0.96A; I_{\max} = 1.12A$$

$$V_{average} = \frac{1}{8268}\sum_{i=1}^{8268} V_i = 17.36V$$

$$I_{average} = \frac{1}{8268}\sum_{i=1}^{8268} I_i = 1.09A$$

$$P_{\min} = V_{\min} \times I_{\min} = 15.26V \times 0.96A = 14.65W$$

$$P_{\max} = V_{\max} \times I_{\max} = 17.74V \times 1.12A = 19.87W$$

$$P_{average} = V_{average} \times I_{average} = 17.36V \times 1.09A = 18.92W$$

After a longer period of time and more measurement values, a more detailed statement can be made. The output voltage and current are usually close to the average output voltage and current under nearly ideal working conditions. Apart from a short exception, the output power is close to the possible maximum power derived by calculation.

2.5.6.2. Variant 2 (total resistance R_{tot} = 7.5Ω, real total resistance $R_{tot,real}$ = 7.9Ω)

If the connection is changed again in the following way, a reduction in the total resistance of the circuit can be reached. In comparison to variant 1 the total resistance is reduced by half.

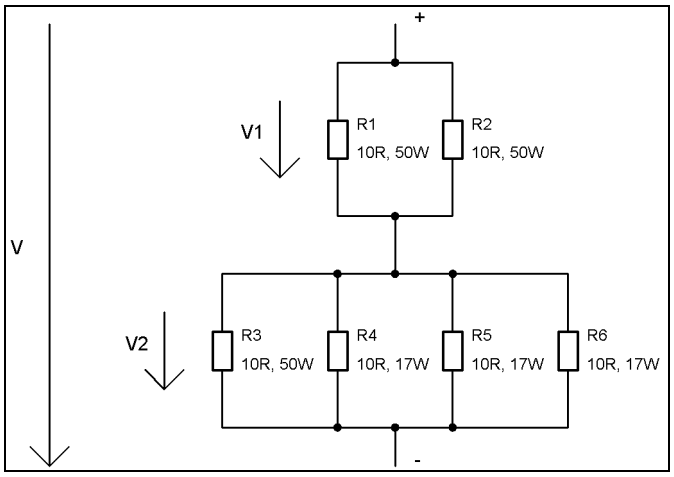

Figure 31: variant 2 load configuration

$$R_{12} = \frac{R_1 R_2}{R_1 + R_2} = \frac{10\Omega \times 10\Omega}{10\Omega + 10\Omega} = 5\Omega; R_{3456} = \frac{R_{34} R_{56}}{R_{34} + R_{56}} = \frac{5\Omega \times 5\Omega}{5\Omega + 5\Omega} = 2.5\Omega; R_{tot} = 5\Omega + 2.5\Omega = 7.5\Omega$$

$$V_{\max} = 18.18V; V_{\max,real} = 17.5V$$

$$P_{\max} = V_{\max} \times I_{\max} = V_{\max} \frac{V_{\max}}{R_{tot}} = \frac{(18.18V)^2}{7.5\Omega} = 44.07W$$

$$V_{1,real} = \frac{2}{3} V_{\max,real} = 11.67V; V_{2,real} = \frac{1}{3} V_{\max,real} = 5.83V$$

$$R_{tot,real} = 7.9\Omega$$

$$V_{\max,real} = I_{\max,real} \times R_{tot,real} \rightarrow I_{\max,real} = \frac{V_{\max,real}}{R_{tot,real}} = \frac{17.5V}{7.9\Omega} = 2.22A$$

$$P_{\max,real} = V_{\max,real} \times I_{\max,real} = \frac{V_{\max,real}}{R_{ges,real}} V_{\max,real} = \frac{(17.5V)^2}{7.9\Omega} = 38.77W$$

On variant 2 no measurements have been taken because of the better reduction in the total resistance in variant 3.

2.5.6.3. Variant 3 (total resistance R_{tot} = 6.6Ω, total real resistance $R_{tot,real}$ = 7.3Ω)

At this connection variant the value of the total resistance of the complete circuit is reduced again, which leads to a higher available power on the load. With this configuration, measurements over a short period of time have been made. Over about 20 minutes (exactly 20 minutes and five seconds) 2410 measurement values have been taken.

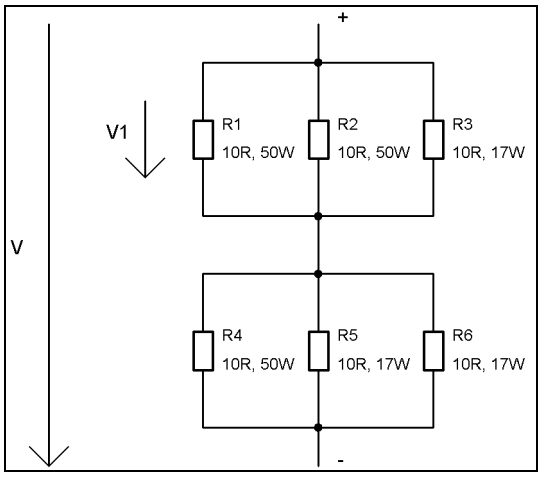

Figure 32: variant 3 load configuration

$$R_{123} = R_{456} = \frac{R_{12}R_3}{R_{12}+R_3} = \frac{R_{45}R_6}{R_{45}+R_6} = \frac{5\Omega \times 10\Omega}{5\Omega + 10\Omega} = 3.3\Omega; R_{tot} = 3.3\Omega + 3.3\Omega = 6.6\Omega$$

$$V_{\max} = 18.18V; V_{\max,real} = 15.7V$$

$$P_{\max} = V_{\max} \times I_{\max} = V_{\max}\frac{V_{\max}}{R_{tot}} = \frac{(18.18V)^2}{6.6\Omega} = 50.08W$$

$$V_{1,real} = \frac{V_{\max,real}}{2} = 7.85V$$

$$R_{tot,real} = 7.3\Omega$$

$$V_{\max,real} = I_{\max,real} \times R_{tot,real} \rightarrow I_{\max,real} = \frac{V_{\max,real}}{R_{tot,real}} = \frac{15.7V}{7.3\Omega} = 2.15A$$

$$P_{\max,real} = V_{\max,real} \times I_{\max,real} = \frac{V_{\max,real}}{R_{ges,real}} V_{\max,real} = \frac{(15.7V)^2}{7.3\Omega} = 33.77W$$

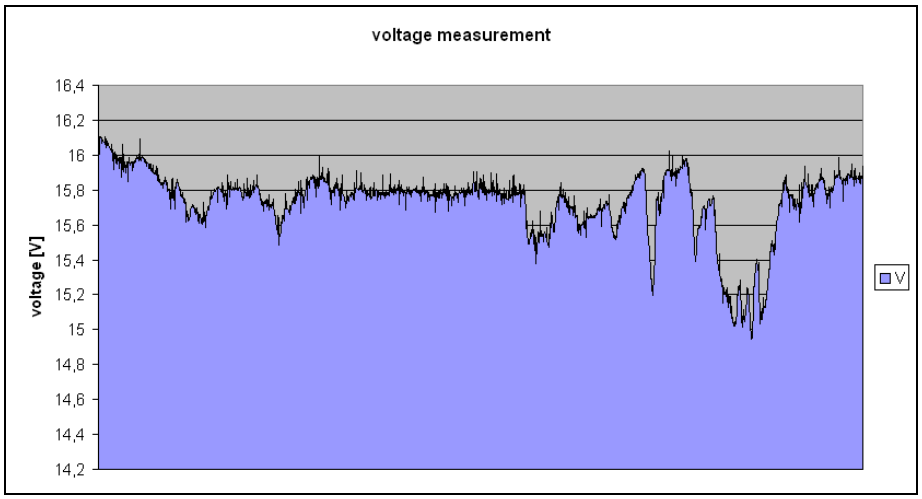

Figure 33: voltage level of the measurement of variant 3 (2410 values)

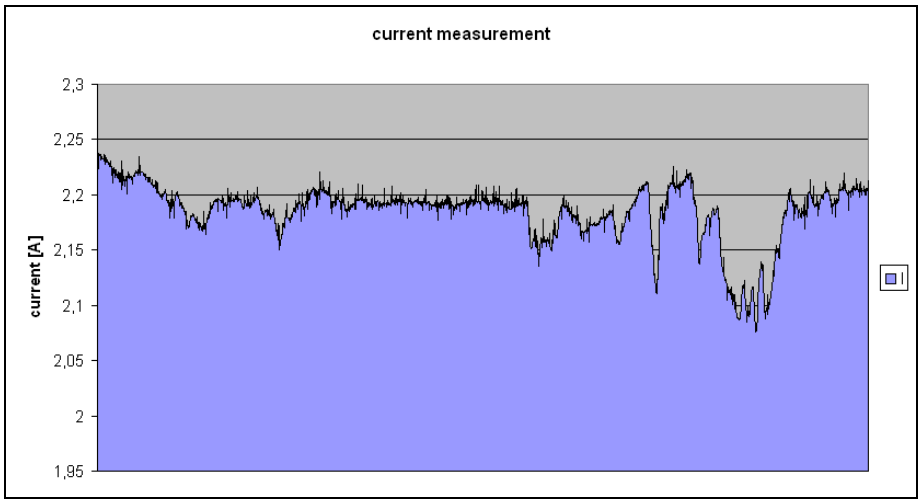

Figure 34: voltage level of the measurement of variant 3 (2410 values)

$$V_{\min} = 14.95V; V_{\max} = 16.12V; I_{\min} = 2.08A; I_{\max} = 2.24A$$

$$V_{average} = \frac{1}{2410}\sum_{i=1}^{8268} V_i = 15.73V$$

$$I_{average} = \frac{1}{2410}\sum_{i=1}^{8268} I_i = 2.18A$$

$$P_{\min} = V_{\min} \times I_{\min} = 14.95V \times 2.08A = 31.10W$$

$$P_{\max} = V_{\max} \times I_{\max} = 16.12V \times 2.24A = 36.11W$$

$$P_{average} = V_{average} \times I_{average} = 15.73V \times 2.18A = 34.30W$$

With variant 3 the situation yielded was that the voltage, current and power were more fluctuating than with variant 3. It can be stated that the solar panel was more sensitive to illumination even though the solar panel worked during the 20 minutes under nearly ideal conditions.

2.5.6.4. Variant 4 (total resistance R_{tot} = 6.6Ω, real total resistance $R_{tot,real}$ = 7.3Ω)

At this connection variant the value of the total resistance of the complete circuit is reduced again, which leads to a higher available power on the load. With the given equipment variant 4 was the maximum method to reduce the resistance of the load.

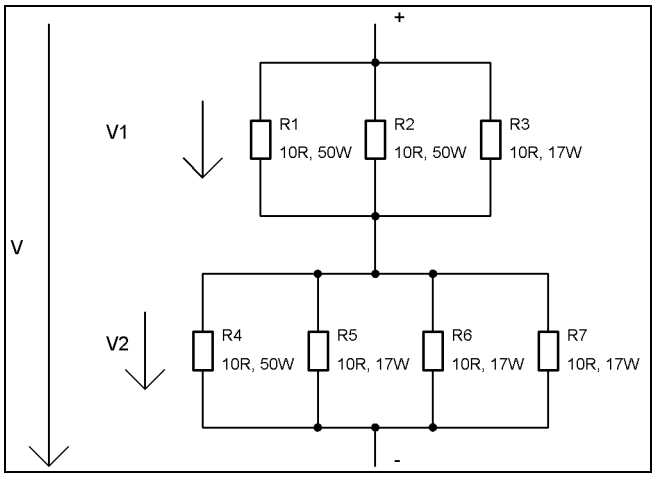

Figure 35: variant 4 load configuration

$$R_{123} = \frac{R_{12}R_3}{R_{12}+R_3} = \frac{5\Omega \times 10\Omega}{5\Omega + 10\Omega} = 3.3\Omega; R_{4567} = \frac{R_{45}R_{67}}{R_{45}+R_{67}} = \frac{5\Omega \times 5\Omega}{5\Omega + 5\Omega} = 2.5\Omega; R_{tot} = 3.3\Omega + 2.5\Omega = 5.8\Omega$$

$$V_{\max} = 18.18V; V_{\max,real} = 16.2V$$

$$P_{\max} = V_{\max} \times I_{\max} = V_{\max}\frac{V_{\max}}{R_{tot}} = \frac{(18.18V)^2}{5.8\Omega} = 56.98W$$

$$V_{\max,real} = V_1 + V_2 \rightarrow V_2 = V_{\max,real} - V_1$$

$$\frac{V_1}{V_2} = \frac{R_{123}}{R_{456}} = \frac{3.3\Omega}{2.5\Omega} \rightarrow V_1 = V_2 \times 1.32 = (V_{\max,real} - V_1) \times 1.32 = 9.22V$$

$$V_2 = V_{\max,real} - V_1 = 16.2V - 9.22V = 6.98V$$

$$R_{tot,real} = 6.5\Omega$$

$$V_{\max,real} = I_{\max,real} \times R_{tot,real} \rightarrow I_{\max,real} = \frac{V_{\max,real}}{R_{tot,real}} = \frac{16.2V}{6.5\Omega} = 2.49A$$

$$P_{\max,real} = V_{\max,real} \times I_{\max,real} = \frac{V_{\max,real}}{R_{ges,real}} V_{\max,real} = \frac{(16.2V)^2}{6.5\Omega} = 40.37W$$

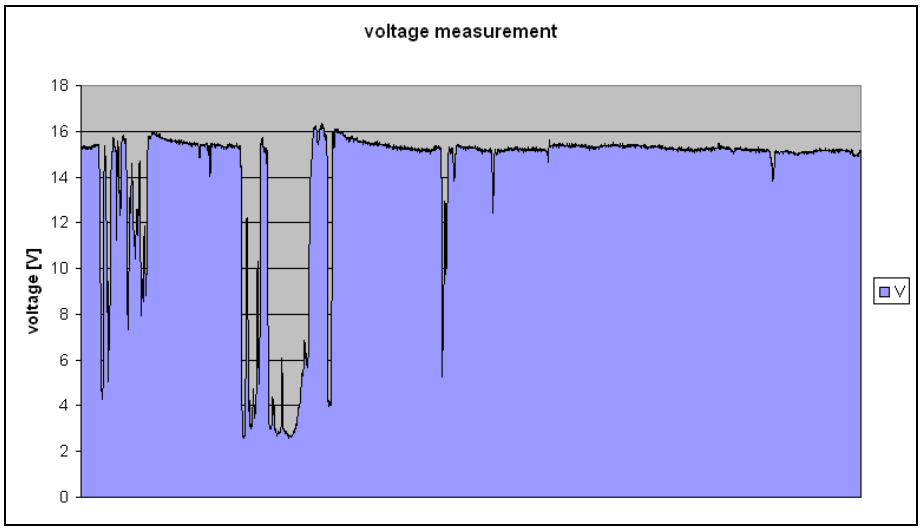

Figure 36: voltage level of the measurement of variant 4 (7530 values)

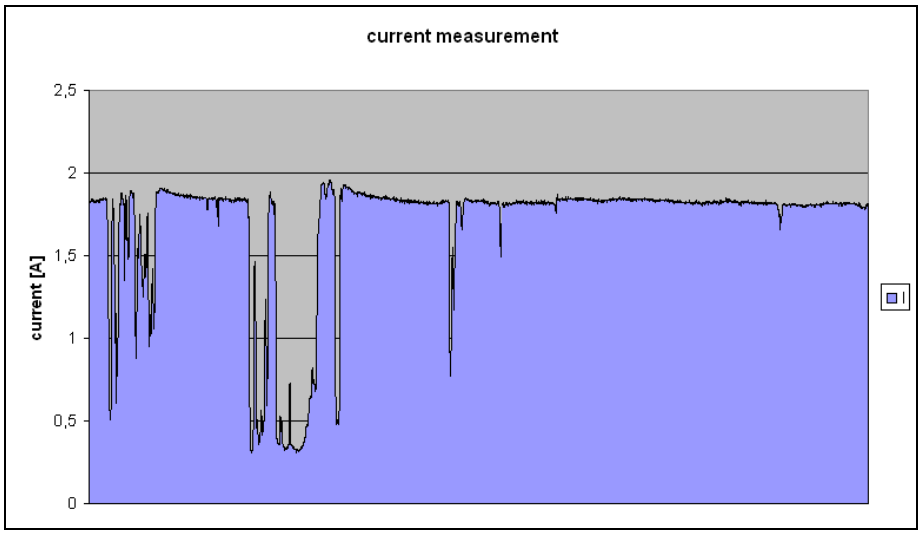

Figure 37: voltage level of the measurement of variant 4 (7530 values)

$$V_{\min} = 2.57V; V_{\max} = 16.35V; I_{\min} = 0.31A; I_{\max} = 1.96A$$

$$V_{average} = \frac{1}{7530}\sum_{i=1}^{8268} V_i = 14.12V$$

$$I_{average} = \frac{1}{7530}\sum_{i=1}^{8268} I_i = 1.69A$$

$$P_{\min} = V_{\min} \times I_{\min} = 2.57V \times 0.31A = 0.80W$$

$$P_{\max} = V_{\max} \times I_{\max} = 16.35V \times 1.96A = 32.05W$$

$$P_{average} = V_{average} \times I_{average} = 14.12V \times 1.69A = 23.86W$$

With variant 4 the mismatch between load and source is more than at variant 1 and variant 3. Even if the power on the load can be about 57W, in reality this value is not reached. This is not because of the illumination, but is the case because of the given mismatch. The maximum power value in the measurement time of one hour, two minutes and 45 seconds which leads to 7530 measurement values was about 32W. Furthermore it is the case that if the illumination is to less the voltage, current and power drop to a low value. During the measurement the output went down below 1W. To gather the maximum possible power at a certain given illumination from the solar panel, a match between the load and the solar panel as source is necessary in combination with a Maximum Power Point Tracker.
At the different variants the load was not changed during the measurement. The conditions of the car during driving can be changed. For example at a strong rise and a high speed, the necessary high amount of propulsion requires a lot of energy. In that case the load is higher than for example at a rapid decline where further energy can be gained by recuperation. It makes sense to provide the gathered energy from the solar panel directly for propulsion energy, to avoid converter losses by recharging the battery. A solar panel management system is necessary to decide in which sink the power needs to be supplied. The primary aspect is therefore the efficiency.

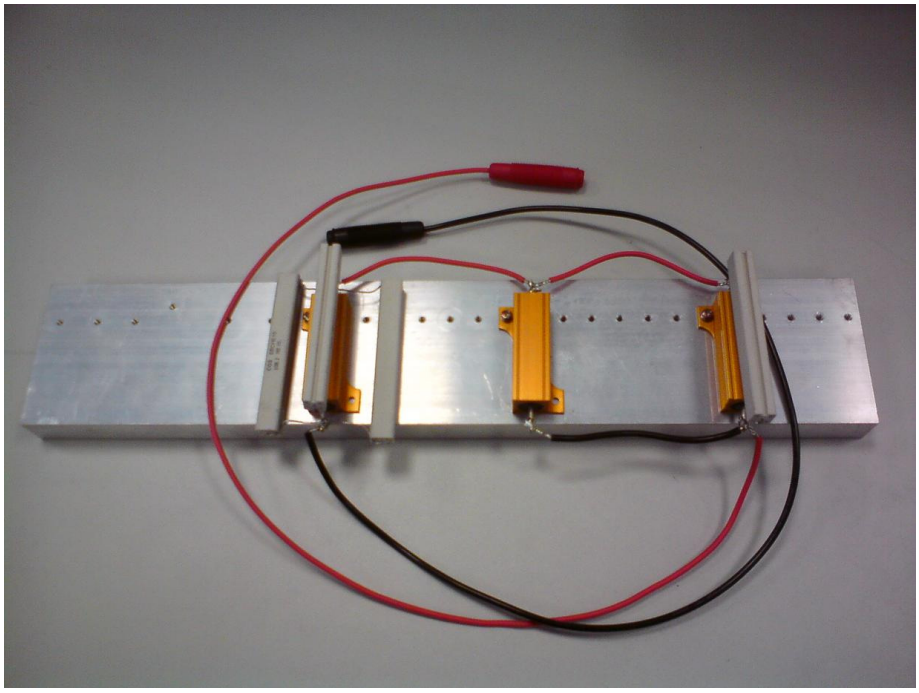

Figure 38: load variant 4 with passive cooler

2.5.6.5. Simulation of total load mismatch

For small electrical consumers, solar panels are designed according to the requirements of these consumers. This is done by defining a certain value of nominal maximum output power of the solar panel. In general the output power of the solar panel exceeds with a small value the required power of the load. A total load mismatch is given if a high energy consuming load is connected to a solar panel which is not designed to provide enough energy for that load even under ideal illumination conditions. The Enecom solar panel was connected in this experiment at first to one halogen lamp and afterwards to two halogen lamps by changing the connection.

Figure 39: halogen lamp box with two lamps

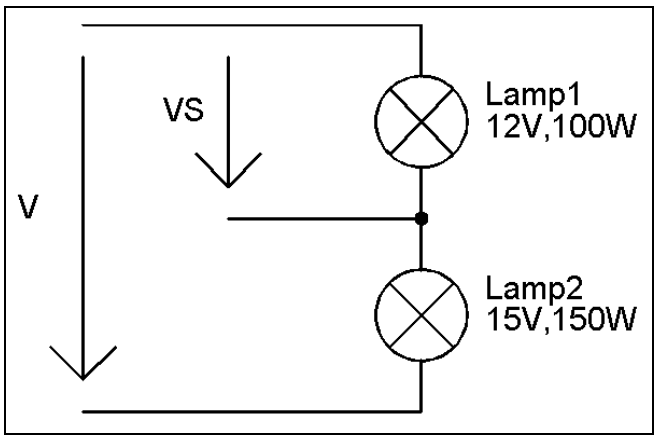

Figure 40: circuit of the lamp box

$$P_{Lamp1} = V_{Lamp1} \times I_{Lamp1} \rightarrow I_{Lamp1} = \frac{P_{Lamp1}}{V_{Lamp1}} = \frac{100W}{12V} = 8.33A$$

$$V_{Lamp1} = I_{Lamp1} \times R_{Lamp1} \rightarrow R_{Lamp1} = \frac{V_{Lamp1}}{I_{Lamp1}} = \frac{12V}{8.33A} = 1.44\Omega$$

$$P_{Lamp2} = V_{Lamp2} \times I_{Lamp2} \rightarrow I_{Lamp2} = \frac{P_{Lamp2}}{V_{Lamp2}} = \frac{150W}{15V} = 10A$$

$$V_{Lamp2} = I_{Lamp2} \times R_{Lamp2} \rightarrow R_{Lamp2} = \frac{V_{Lamp2}}{I_{Lamp2}} = \frac{15V}{10A} = 1.5\Omega$$

If the two halogen lamps are connected in serial a total voltage of 24V, a current up to 8A and a power 250W can be taken. Even under nearly ideal illumination conditions the voltage of the Enecom solar panel collapsed down to 2V. The same output voltage was available if one halogen lamp was connected. The output current was too small to power the lamp box.

2.5.7. Maximum Power Point

2.5.7.1. Principle

The maximum output power of a solar panel is determined by the product of voltage and current on the current-voltage curve under illumination. In this curve a direct connection between illumination and output current is shown. The point where the product of voltage and current is at maximum is named as Maximum Power Point (MPP). At that certain point the voltage is named V_{mp} (voltage at maximum power) and the current I_{mp} (current at maximum power). The theoretical maximum power of an ideal solar cell cannot overtake the product of open load voltage V_0 and short circuit current I_{SC}. For a typical silicon cell solar panel with a serial connection of 36 cells, the MPP is at about 17V.
In reality the MPP is related to illumination, temperature, exemplary scattering and aging. With the help of a Maximum Power Point Tracker (MPPT) which is an electronic system, the solar panel can operate in the MPP, a mode where the power is produced which they are capable of producing. With the rate of the current illumination and given temperature the electrical operating point of the module is varied to reach the state where the maximum available power is generated. The additional gathered power can be used as increased output current (Cullen R. A, 2004; Pastore R ., 2006; Schneider D., 2006; Schenke G., 2010).

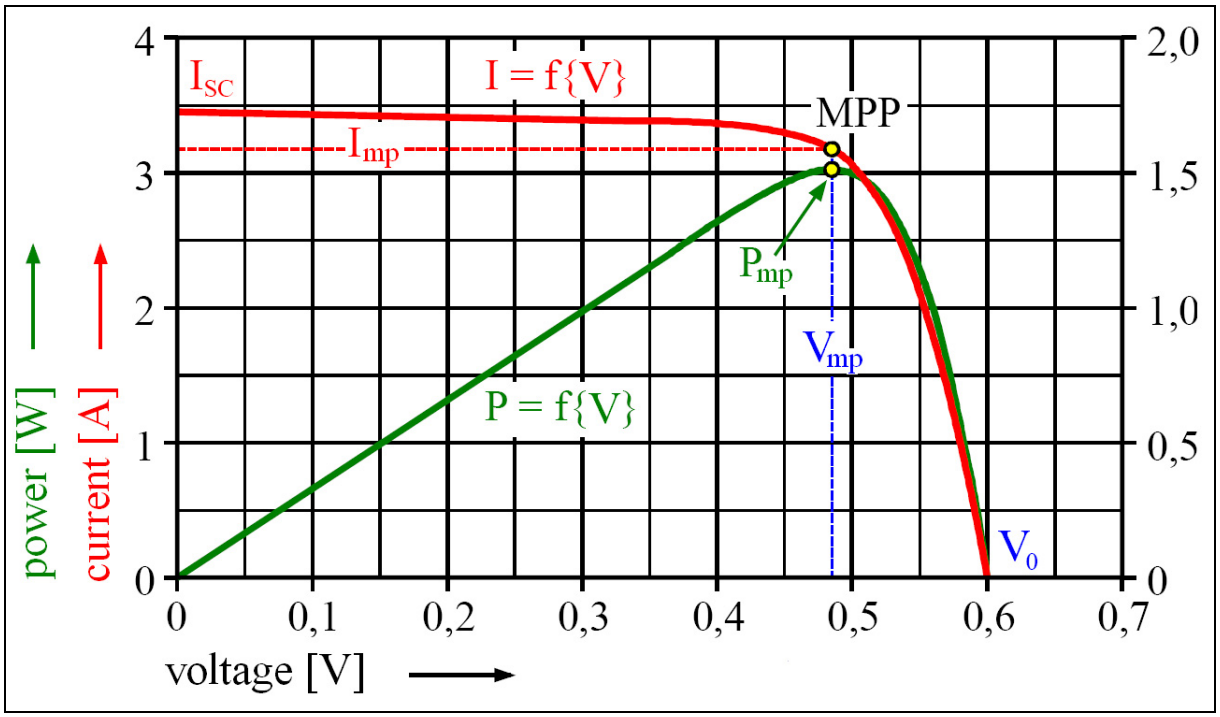

Figure 41: maximum power point diagram (Source: Schenke G.)

2.5.7.2. Implemented maximum power point tracking (MPPT) for the experimental vehicle

The realization mentioned for the experimental vehicle is oriented to work with about ten solar cells. In its first version, the maximum power point tracker is linked to a cell group of 15 or 18 cells. A prototype of this solar panel which will be mounted on the experimental vehicle is described later. The 10/15/18 cells are connected in serial to a small group. This variant of connection can be beneficial in cases where shadowing present or if the solar group is mounted on a curved surface. In the final version the maximum power point tracking units will be integrated into a back-contacted solar panel so that the solar panel works as a 'smart module'. The primary purpose of the MPPT is to power the 12V auxiliary net for extending the electrical driving range and for cooling the passenger cabin (FHJ, 2009).

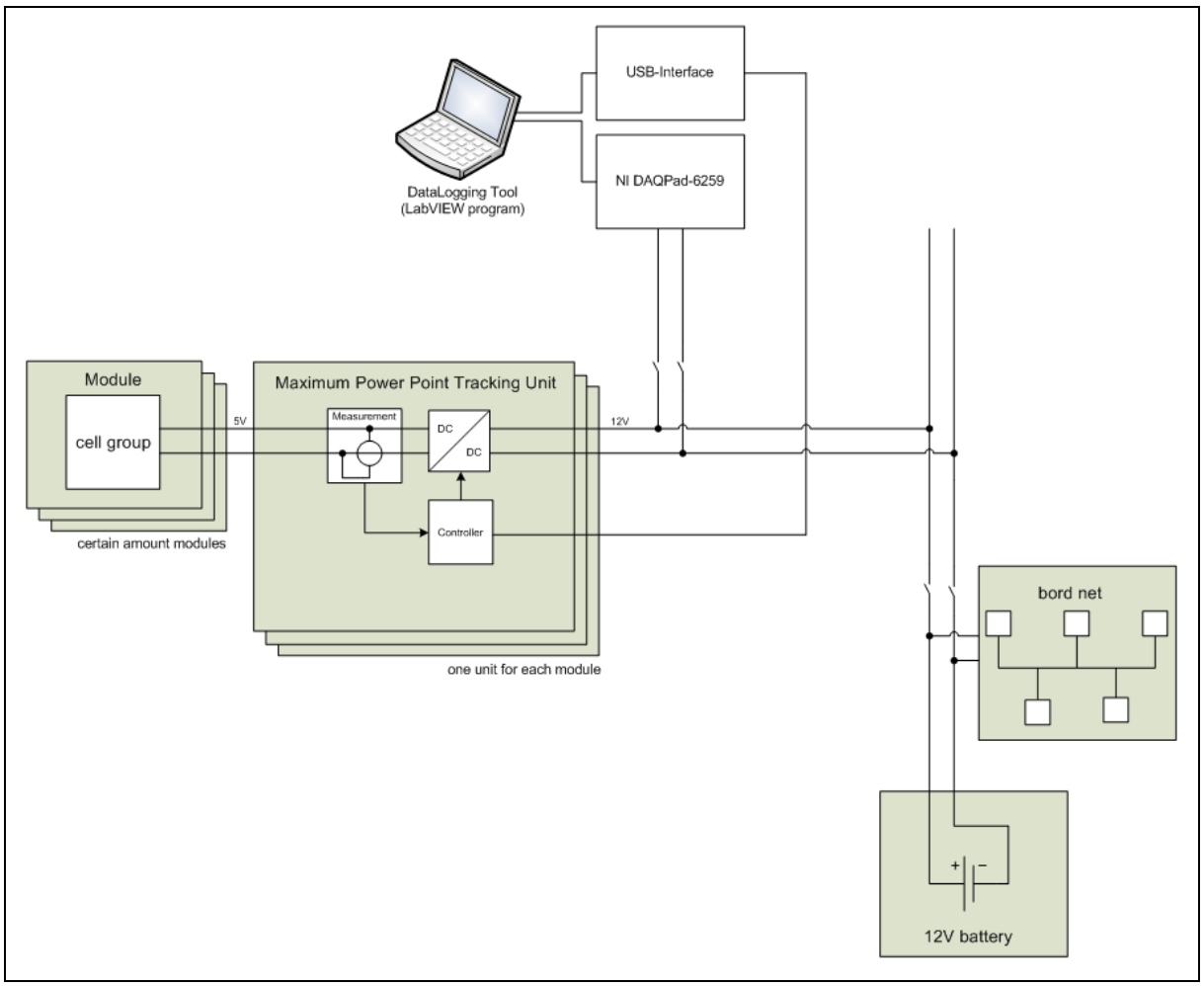

Figure 42: MPPT-unit and connection of the DataLogging Tool (Source: FHJ)

The maximum power point tracking unit is an active circuit which is supposed to replace the conventional Bypass-diode and work as middleware between the solar cells as power source and the 12V board net as power sink. In a solar panel suitable to provide a voltage of 12V 36 cells are used. In that kind of solar panel a Bypass-diode is located after 20 cells. By the usage of a conventional Bypass-diode the entire power which is produced by the 20 cells is lost. The MPPT offers the opportunity to avoid these losses and to secure a minimum amount of power which is still available by the for example shadowed solar cells.

With the maximum power point tracking the purpose of the DC/DC converters is to act as active circuit for intelligent impedance matching. A controller with an integrated MPPT algorithm is used in order to set the duty cycle of the DC/DC converters. Throughout the complete circuit each converter is acting as a power source with a voltage limit to draw the maximum available power out of the connected cell group.

2.5.7.3. Impedance matching theory and MPPT requirement

The solar panel is like a real power source with a resistance R_S. On this power source the load R_{load} ,as before in different variants, is connected. The calculation to be solved is the requiredproportional relationship of R_S and R_{load} for reaching the maximum power of the source. In this circuit the solar panel is the active component and the load the passive component. If this optimal proportional relationship is not solved, the degree of efficiency is reduced because the maximum available power of the solar panel is not taken or used (Fischer, 1991).

$$V = V_S - I \times R_S$$

$$P = V \times R_S = V_S \times I - I^2 \times R_S = \frac{V_S^2 \times R_{load}}{(R_S + R_{load})}$$

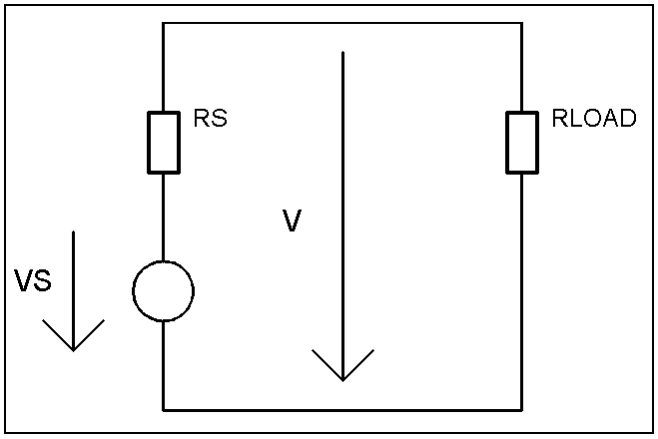

Figure 43: source and load connected (Source: Fischer)

For matching, R_{load} needs to be equal to R_i. If the proportion is made in that way on R_{load} the maximum possible power occurs (Fischer, 1991).

$$P_{\max} = \frac{V_S^2}{4 \times R_{load}} = \frac{V_S^2}{4 \times R_i}$$

$$P_S = V_S \times I = \frac{V_S^2}{R_S + R_{load}}$$

$$P_{S,\max} = \frac{V_S^2}{2 \times R_S} = \frac{V_S^2}{2 \times R_S}$$

$$\eta_{\max} = \frac{P_{\max}}{P_{S,\max}} \times 100\% = 50\%$$

The calculation leads to the statement that with an active source and a passive sink only a maximum degree of efficiency of 50% is possible. Because of this situation a Maximum Power Point Tracker is required.

2.5.8. Supplying the Toyota Prius with gained solar energy

The potentials to provide the gained power from the solar roof have to be analyzed. To supply the Toyota Prius, the most efficient possibility has to be found along with the highest degree of efficiency.

2.5.8.1. Hybrid Synergy Drive components and location

At first the structure of the hybrid technology needs to be analyzed. The Toyota Prius has a serial-parallel hybrid technology. This means that there are two electrical engines, one combustion engine and a high voltage (HV) battery available.

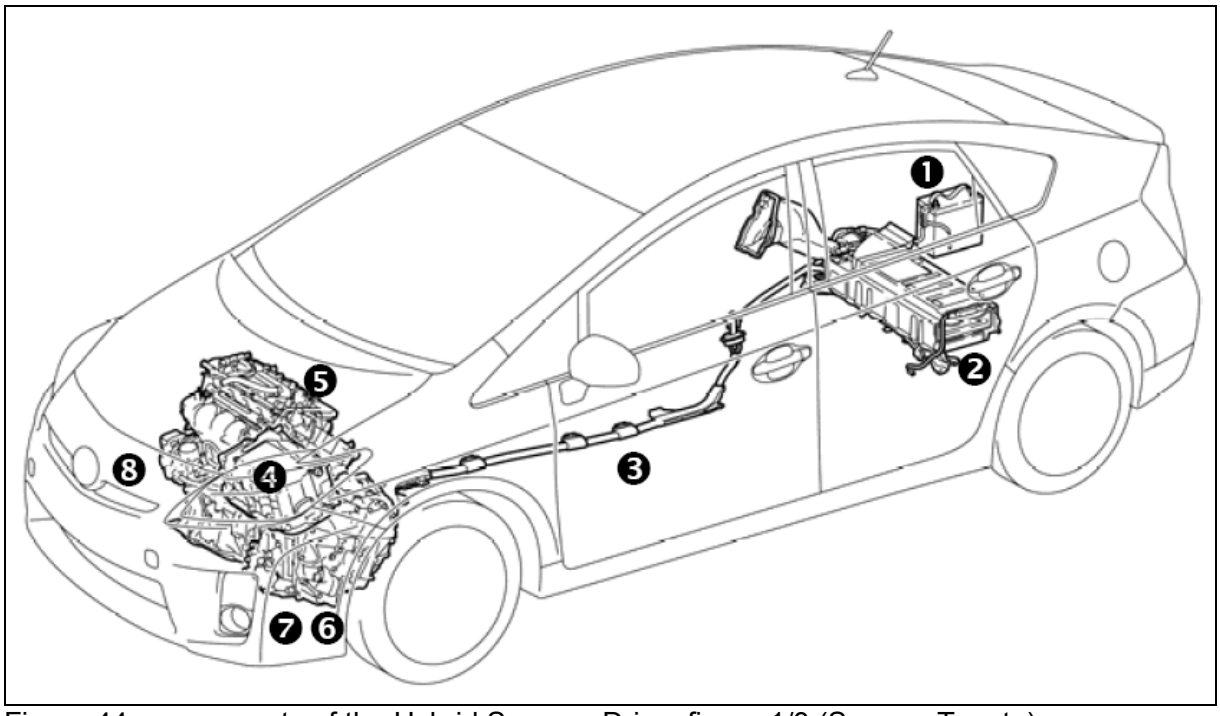

Figure 44: components of the Hybrid Synergy Drive, figure 1/3 (Source: Toyota)

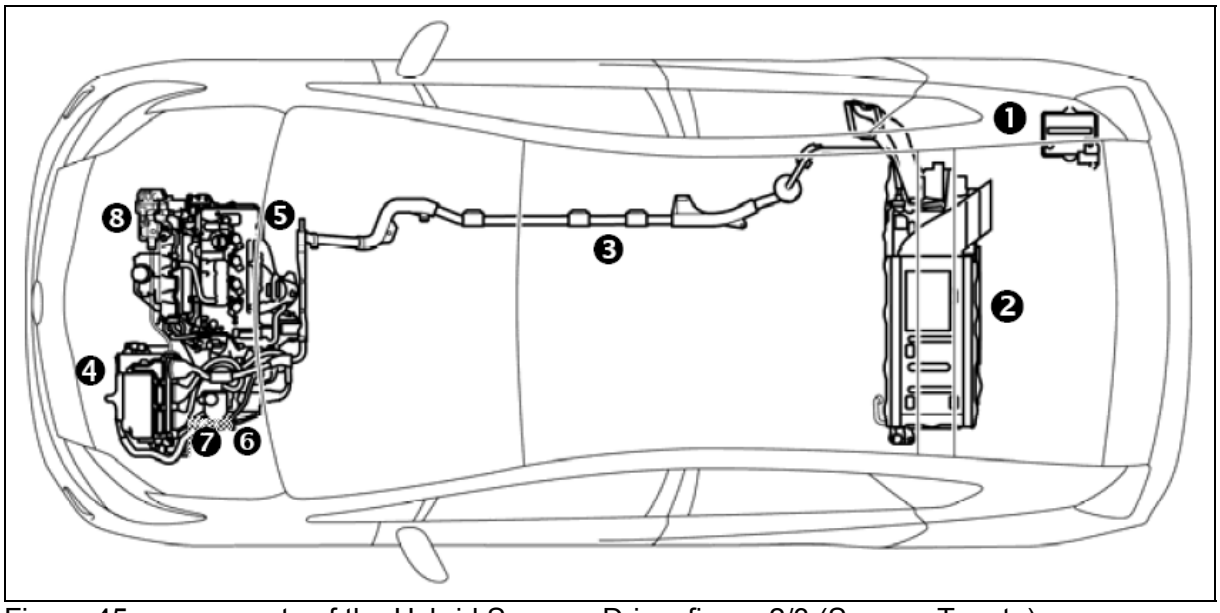

Figure 45: components of the Hybrid Synergy Drive, figure 2/3 (Source: Toyota)

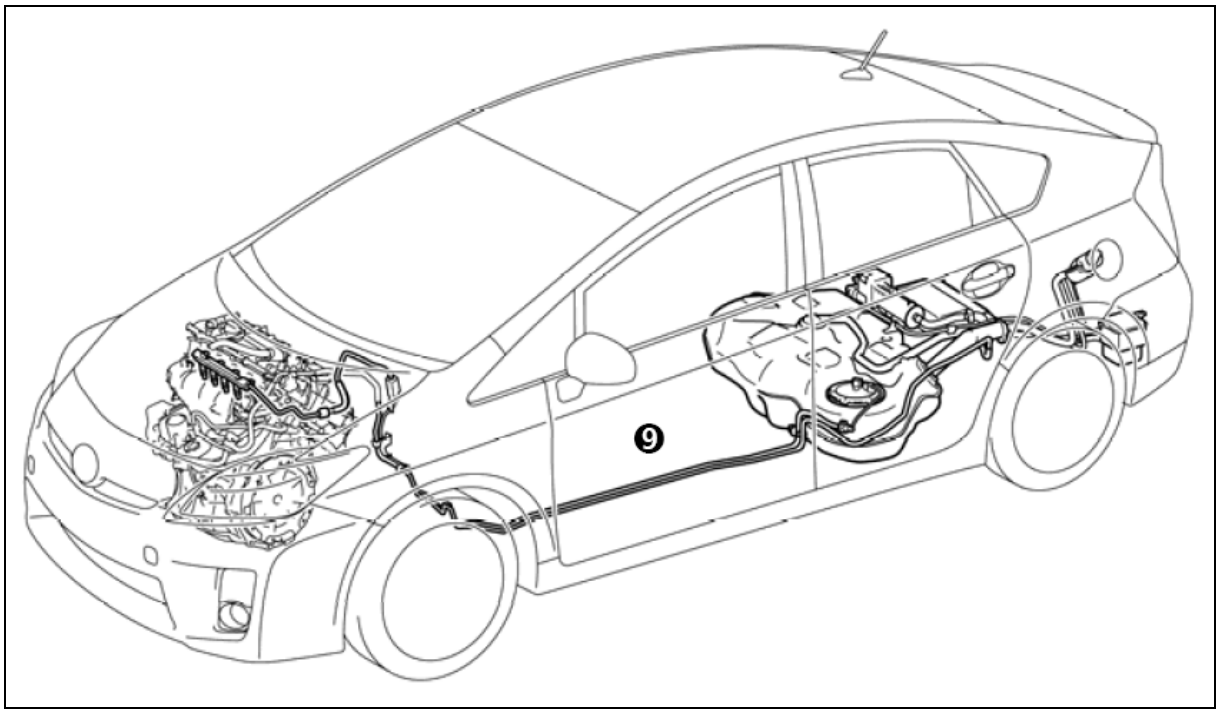

Figure 46: components of the Hybrid Synergy Drive, figure 3/3 (Source: Toyota)

number	component	location	description
1	12V auxiliary battery	on the right hand side of the cargo area	a conventional lead-acid that provides power to low voltage device on the board net
2	HV battery pack	cargo area behind the rear seat bench	201.6V Nickel Metal Hydride (NiMH) battery, 28 modules with 7.2V each module, 168 cells
3	power cables	undercarriage and engine compartment	these orange coloured cables with high voltage are the connection between the HV battery pack, inverter/converter, electric motor and electric generator
4	inverter/converter	engine compartment	For the electric motor and the electric generator. Boosts, inverts and converts DC to 3-phase AC in both directions
5	combustion engine	engine compartment	can deliver propulsion energy for the vehicle or power the electric generator
6	electric motor	engine compartment	is used for propulsion energy, nominal power is 50kW
7	electric generator	engine compartment	is used to recharge the HV battery pack, 10kW nominal power
8	A/C compressor (with inverter)	engine compartment	high voltage AC electrically driven motor compressor
9	fuel tank and fuel line	undercarriage and center	the fuel line is located in the rear end of the car with a capacity of about 50 litres (11.9 gallons)

Table 12: measurement results for other cell groups covered (Source: Toyota)

2.5.8.2. Possibilities for energy sinks

The Toyota Prius has a conventional 12V auxiliary battery which is not directly a component of the hybrid drive technology. The basic idea is to use the energy output of the solar panel to supply this battery. This opportunity is obvious because the output voltage of the DC/DC converters of the MPPT-unit is about 14V. By powering the 12V battery, normal consumers like the radio or the air conditioning system can be supplied. For example also the anti-theft device is connected to the 12V battery. If the vehicle is parked, the auxiliary battery can be overloaded, causing damage to the battery. If the vehicle is not used or the auxiliary has a high state of charge, energy can be supplied to the HV battery pack. This scenario requires an additional converter to power the high voltage battery. However, recharging the high voltage battery with external power is not recommended.
This is the case because the state of charge (SOC) has to be at a certain level to guarantee a long lifetime for the battery. Therefore a special electronic circuit unit (ECU) takes care of this matter. The role of this hybrid battery control system is to monitor the high voltage battery by calculating the SOC based on voltage, current and temperature. The ECU controls a blower fan to handle the temperature of the HV battery. The target is that the SOC can be constantly maintained at a median level. The charge amperage by the generator and the discharge amperage by powering the electric motor are estimated by the ECU. The target SOC is 60%. If the SOC drops below this value the ECU submits a request to recharge the HV battery pack. If the SOC is below 20% the electric motor will not be powered (Toyota, 2010).

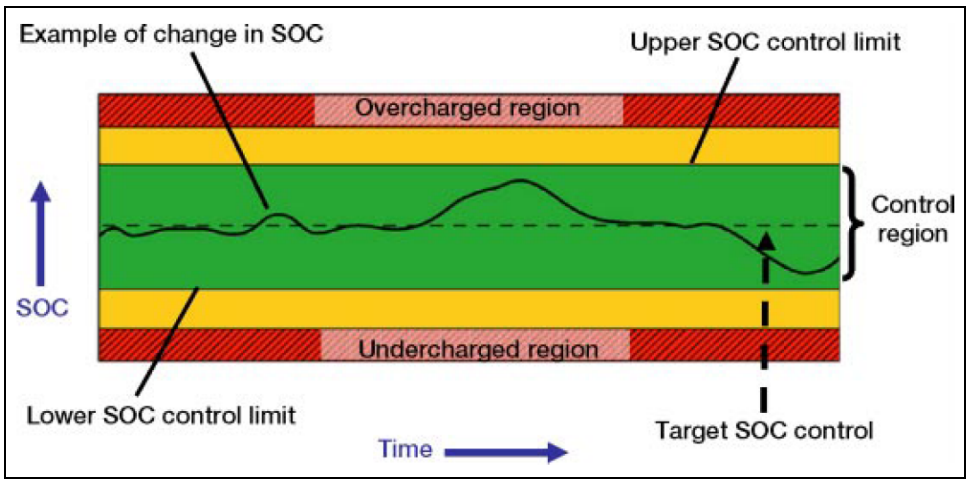

Figure 47: state of charge areas for the HV battery pack (Source: Toyota)

The high voltage battery is charged by the electric generator which either receives power from the combustion engine during driving or from recuperative braking. In case the HV battery pack needs to be charged otherwise, Toyota suggests using a special charger which comes from Japan and is not sold by dealers. The charger is used to charge the high voltage battery from a SOC below 15% to a SOC of 40-50% in about three hours (Toyota, 2010).

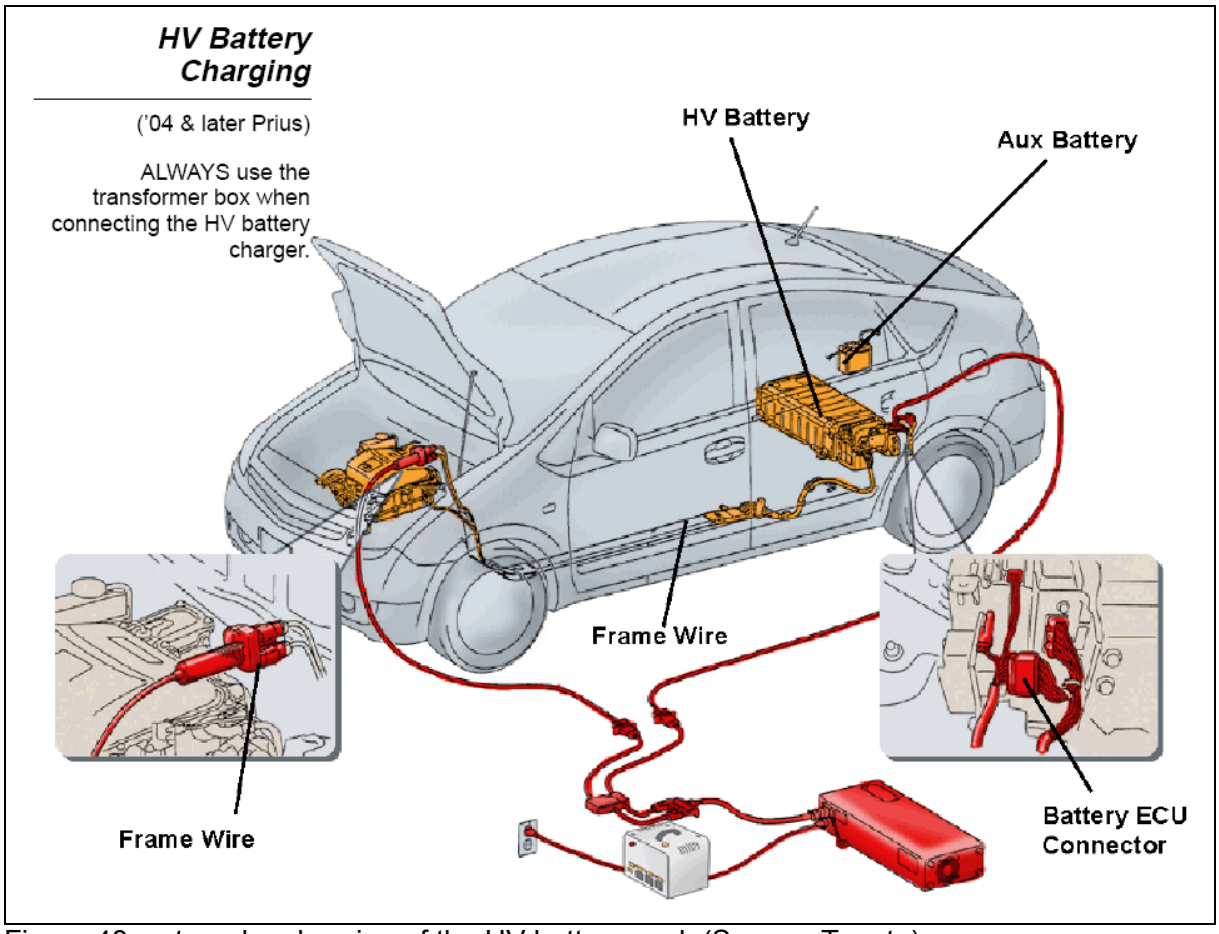

Figure 48: external recharging of the HV battery pack (Source: Toyota)

The process occurs to be extensive if energy from the solar panel is determined to power the high voltage battery. Even if the vehicle is parked, the ECU is not operating, which means that the blower fan to maintain the temperature of the HV battery is not in operation. The ECU needs to be integrated in to the charging process with the solar panel to avoid overcharge by the solar panel. Furthermore the ECU needs to know about the solar panel attendance to consider the output power of the solar panel in the estimations for the charge and discharge amperage.
For the normal auxiliary battery, different charging times can be estimated depending on the state of charge of this battery. By fast charging, a high current is used to recharge the battery in a short period of time. This method can shorten the battery's lifetime which leads to the necessity for a slow recharging. Furthermore the auxiliary battery provides a small amount of charge capacity which is between 28Ah to 34Ah. 12V batteries in conventional combustion vehicles have above 45Ah. If the total amount of charge capacity is lower, the self-discharge time is increased (Toyota, 2010; Schöllmann M., Hoff C., Schriek J., 2010).

reserve capacity rating	20h rating	5A	10A	20A	30A	40A
75min or less	50Ah or less	10h	5h	2.5h	2h	–
above 75min to 115min	above 50 to 75Ah	15h	7.5h	3.25h	2.5h	2h
above 115min to 1605min	above 75 to 100Ah	20h	10h	5h	3h	2.5h
above 160min to 245min	above 100 to 150Ah	30h	15h	7.5h	5h	3h

Table 13: typical charging rates for fully discharged batteries (Source: Toyota)

When recharging the 12V battery, the current needs to be regulated and the voltage needs to be checked according to a characteristic curve of the battery. The following points need to be considered to extend the battery's lifetime at slow charging:

- the maximum charging current needs to be less than 1/10th of the total battery capacity. For a battery capacity between of 28Ah to 34Ah the charge current is required to be at 2.8A up to 3.4A
- the voltage needs to be checked to provide the battery from emitting hydrogen gas. If the voltage is stable for more than one hour the battery is fully charged

The opportunity is given to provide the energy directly to the electric motor. In that case a communication via the CAN-bus is required because of the different possibilities of the energy flow. Several electronic circuit units need to be informed about the solar panel as an additional energy provider.

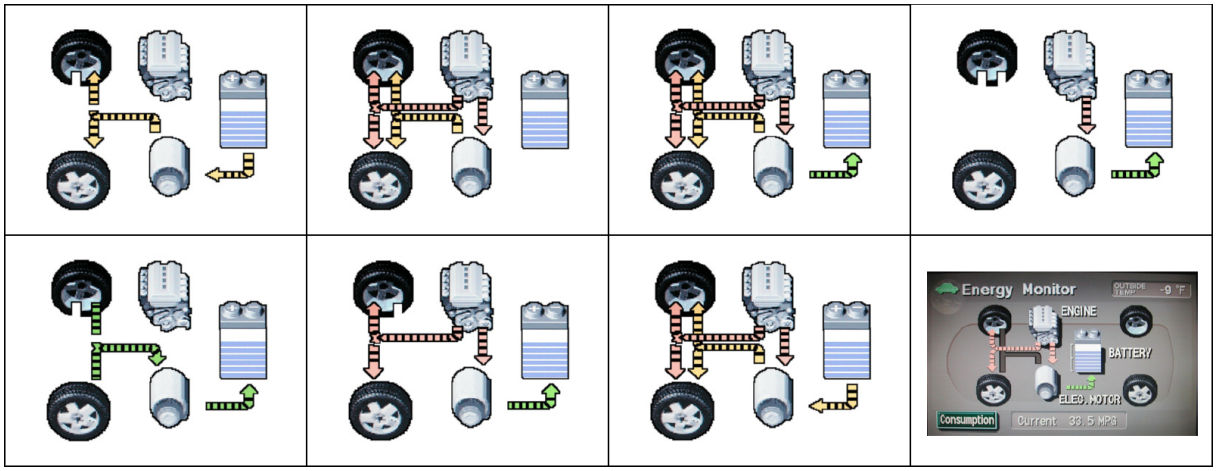

Figure 49: different energy flows of the Toyota Prius (Source: Toyota)

For the experimental vehicle there is an additional battery available. It is a lithium ion battery and it is installed in the spare tire well. The battery's function is a range extender to enhance the driving distance which can be taken electrically. With the additional battery the Toyota Prius uses the pure electric drive more often, which results in reducedfuel consumption. The lithium ion battery from A123Systems with a charge capacity of 5kWh can be recharged only by external electrical power. This leads to the necessity that the vehicle be parked for about 5 to 6 hours. The weight of the battery is 91kg or 200lbs. The charging voltage is 120V and the maximum charging current is 10A. This battery can also be used as an opportunity to store the gained power from the solar panel (A123Systems, 2008).

Figure 50: lithium ion battery in the Toyota Prius (Source: A123Systems)

3. Optical sensor unit

3.1. Prototype

The basic function of the optical sensor unit is to provide information about shadowing. Shadowing has a negative impact on the power output of the solar panel. The purpose of the sensor unit is either to deliver a reference signal to make sure that shadowing has taken place on the solar panel and to analyze the different shadowing activities.

The complete sensor unit consists of the following parts:

- 3V power supply for the sensor and the operation amplifier (supply 1, V_{BAT1})
- 3V power supply for the reference power supply (supply 2, V_{BAT2})
- Optical sensor with connections to pick up the measured signal
- Second optical sensor with connections to pick up the measured signal (optional)
- DIP-switch to enable and disable the hardware

The basic idea for the first test is to have one optical sensor unit at the front right hand side, and on the back left hand side. In general no prediction can be made as to whether there will be more shadowing at the left side or at the right side of the roof during driving. Shadowing itself influences the decision regarding how the cells are connected to the modules (Toshihisa S., 2001; Photon 2010).

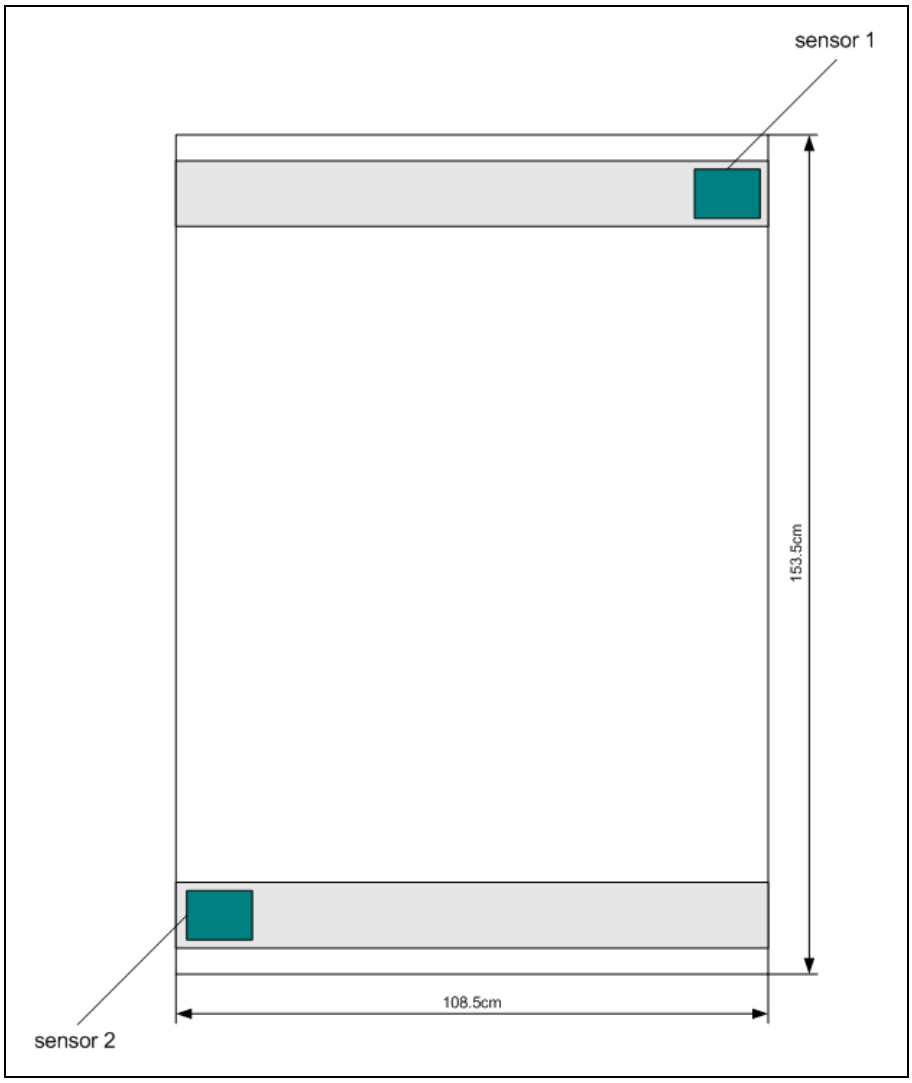

Figure 51: position of the optical sensor units

3.1.1. Description of the components

3.1.1.1. Normal power supply, optical sensors and operation amplifier

This power supply is needed to supply the optical sensor and the operation amplifier. For the prototype the optical sensor TSL250 and TSL250RD from TAOS are used. In general the TSL250 and TSL250RD are from the functional point of view equal; the difference is in the packaging. For the second board only the TSL250 is assembled.
The supply voltage for this light-to-voltage optical sensor is from 3V to 9V. The output voltage of the sensor is related to the light intensity (irradiance) on the photodiode which is used in combination with a transimpedance amplifier. An advantage of this sensor is the low power consumption which is required for the battery based power supply.

The output voltage of the optical sensor is related to the power supply of the sensor. In the datasheet the diagram shows only the range from 4V to 10V. A measurement leads to the result that a supply voltage of 3V produces an output voltage of about 2.1V (TAOS, 2010).

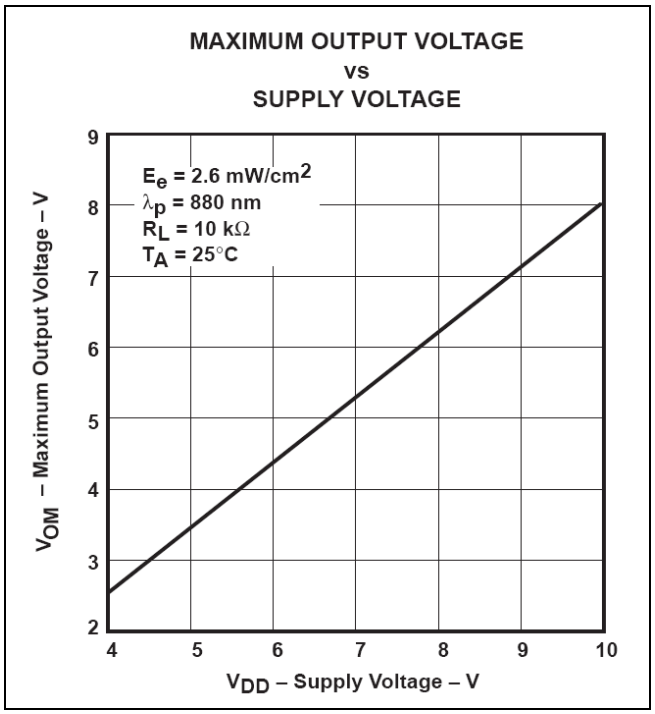

Figure 52: maximum output voltage related to the supply voltage (Source: TAOS)

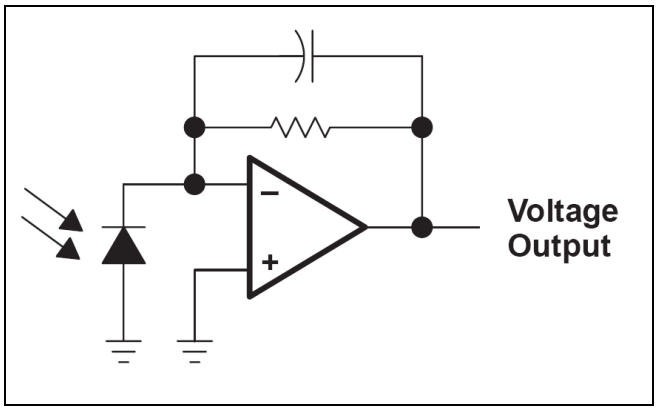

Figure 53: functional block diagram of the TSL250 and TSL250RD (Source: TAOS)

On the sensor unit the AD820AN is used. This low power FET-input operation amplifier is used as a differential amplifier and has a single supply capability from +3V to +36V which is needed because of the use of the battery supply. The used form of the differential amplifier has the advantage that the realisation of the circuit itself is possible by the use of only one operation amplifier. The basic function is that the differential voltage between the inverting input and the non-inverting input is amplified (Tietze U., Schenk Ch., 2002; Beuth K., Schmusch W, 1997).

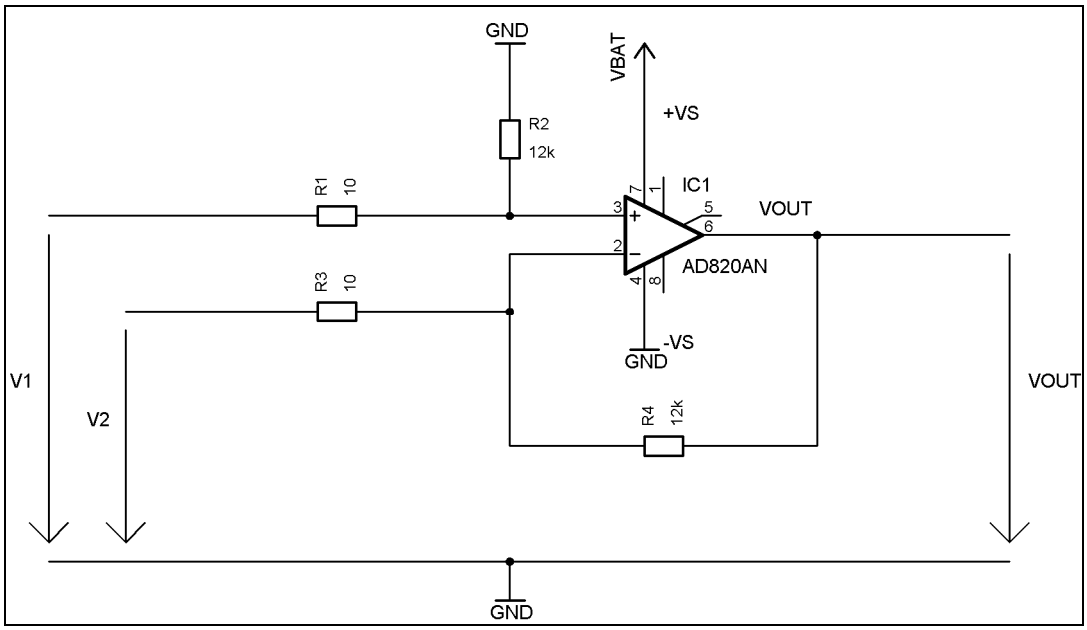

Figure 54: circuit of the differential amplifier (Source: Tietze U., Schenk Ch.).

The gain of this kind of amplifier can be calculated because of the circuit as follows:

In general:

$$U_a = \frac{(R_1 + R_2)R_3}{(R_3 + R_4)R_1}(U_2 - U_1)$$

With the choice of R_1=R_3=10Ω and R_2= R_4=12kΩ:

$$U_a = \frac{R_2}{R_1}(U_2 - U_1)$$

$$A_D = \frac{R_2}{R_1} = \frac{12k\Omega}{10\Omega} = 1200$$

At the prototype board a resistor with a value of 120Ω was initially used. After practical measurements it turned out that a higher gain is required, which led into the additional resistor of 10Ω in parallel to the 120Ω.

3.1.1.2. Reference power supply

The reference power supply provides a voltage which is used for a comparison. This comparison is performed with the operation amplifier (AD820AN). The concept of this kind of power supply is based on a divider with resistors. In general a divider with resistors is used to cut a voltage in half. Therefore both resistors have to be exactly the same value.
For the optical sensor unit a wider range to tune or adjust the voltage is necessary. This leads to different values of the resistors (Beuth K, Beuth O., 2003).

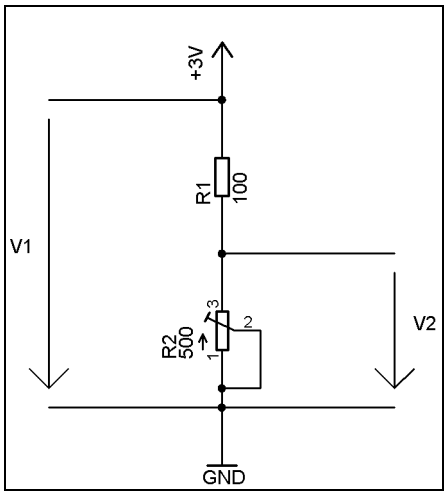

Figure 55: divider with resistors (Source: Beuth K, Beuth O.)

R_1 is a resistor with the value of 100Ω and R_2 is a potentiometer with 500Ω.

In general:

$$\frac{U_2}{U_1} = \frac{R_2}{R_1 + R_2}$$

Minimum reference voltage (R2 minimum at about 1Ω):

$$U_2 = U_1 \frac{R_2}{R_1 + R_2} = 3V \frac{1\Omega}{101\Omega} = 29{,}7mV$$

Maximum reference voltage (R2 minimum at about 500Ω):

$$U_2 = U_1 \frac{R_2}{R_1 + R_2} = 3V \frac{500\Omega}{600\Omega} = 2{,}5V$$

If higher voltages for a reference are needed, the value of R_2 can be changed. Therefore the value of the potentiometer needs to be increased.

3.1.1.3. DIP-switches

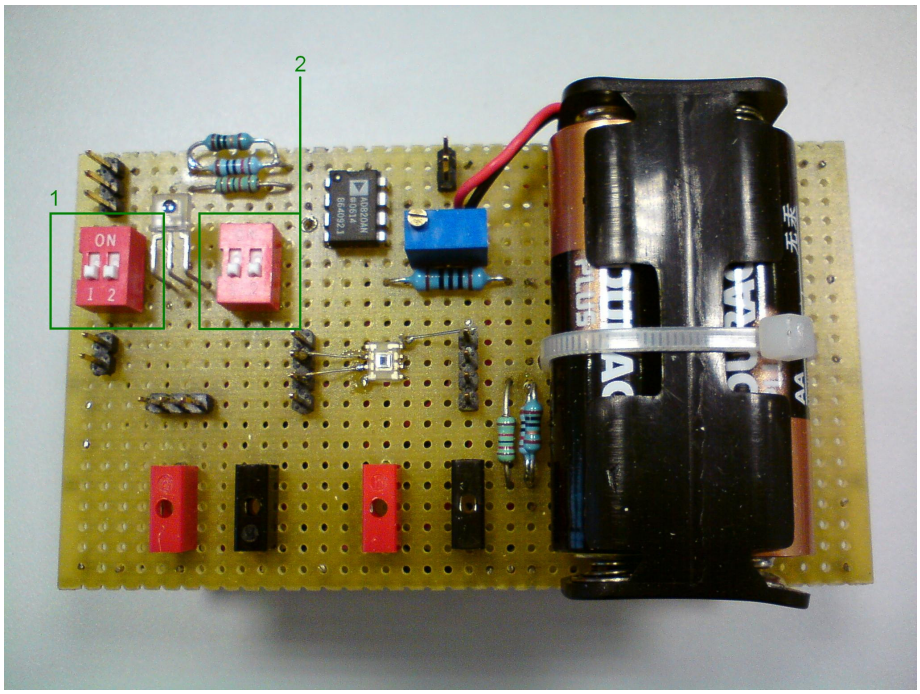

Figure 56: DIP-switches on the prototype

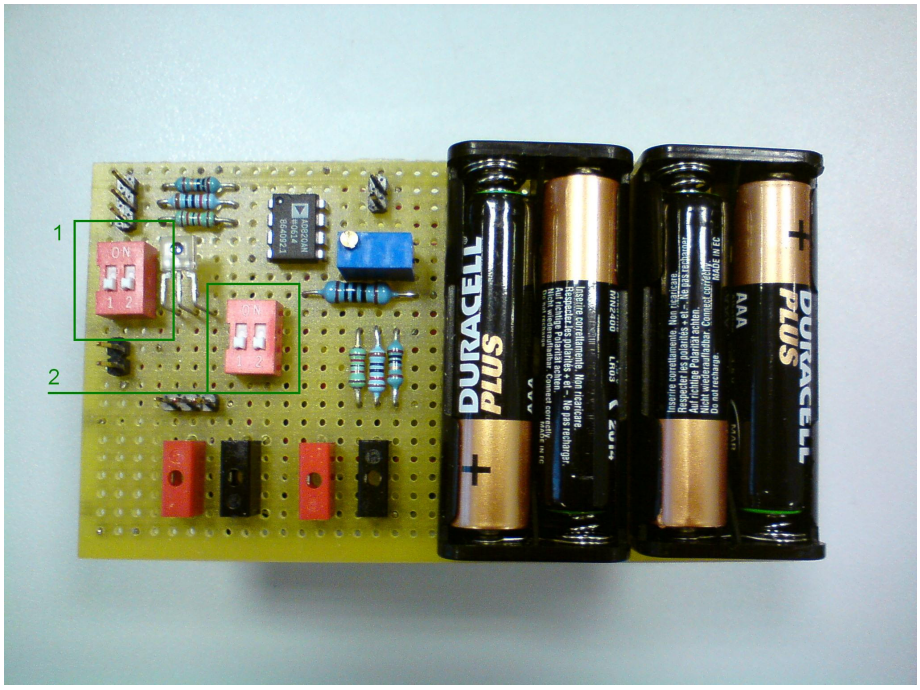

Figure 57: DIP-switches on the second board

position 1	supply for optical sensor(s) and operation amplifier
position 2	supply for reference power source

Table 14: connections on DIP-switch 1

position 1	supply for sensor 2 (optional) / reserved
position 2	supply for sensor 1

Table 15: connections on DIP-switch 2

3.1.1.4. Connection possibilities and parts of the optical sensor unit

On the prototype of the optical sensor unit, the position (7) is additionally available. All the other connection opportunities are similar. The connection option (5) on the second board is available even though it is unconnected.

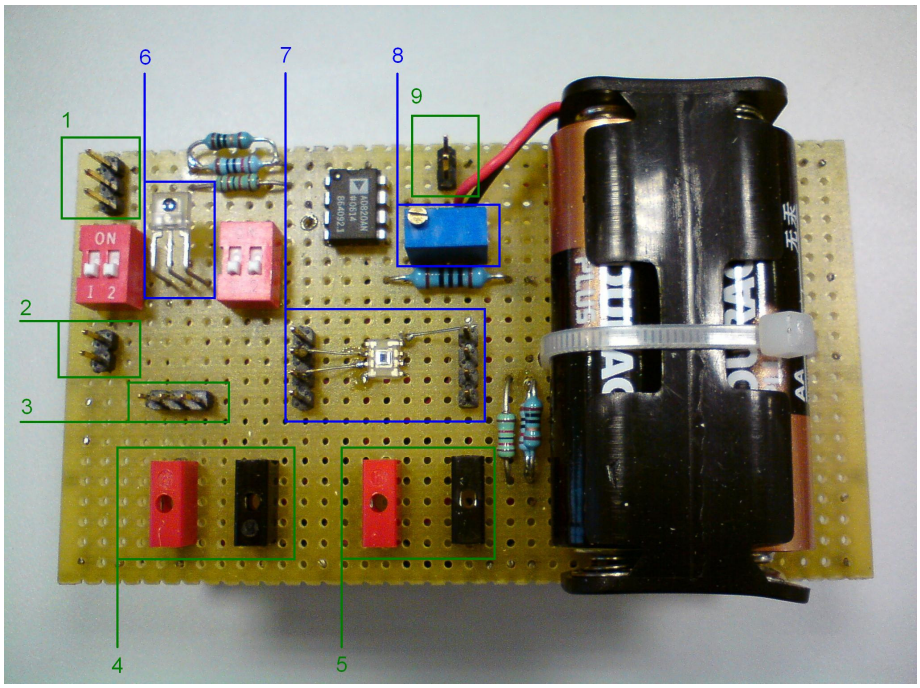

Figure 58: connection possibilities on the optical sensor unit

1	V_{OUT}, Output voltage for the software of the sensor unit
2	GND, connection for the measurement cable
3	measurement of sensor 1 with the same pin layout
4	sensor 1 output
5	sensor 2 output (optional)
6	sensor 1, TSL250
7	sensor 2, TSL250RD (optional)
8	Potentiometer for the configuration of the reference source
9	reference source voltage

Table 16: description of the connections of the optical sensor unit

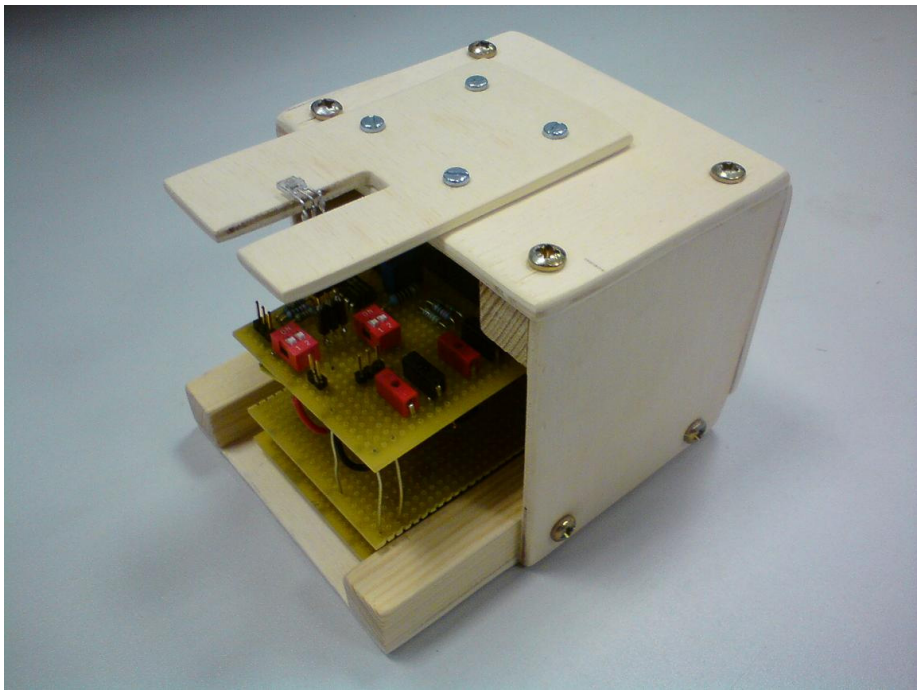

Figure 59: sensor unit including wooden case

To protect the electronics, the operation amplifier and the batteries, from direct sunlight and possible influence of thereby increased temperatures, a small wooden case was designed. The sensor is raised so that the electronic circuit is below and can be covered from the sun by the wood. A wooden case has the advantage, compared to a metal case, of offering better heat protection. A metal case can offer the opportunity to run higher speeds because of higher stability.

3.1.1.5. Output signal of the optical sensor unit

The output signal of the optical sensor unit is measured with the help of a computer. In the development of the prototype the decision was made to use the light-to-voltage optical sensor for a basic decision between shadow and sun. This decision is derived by computer with the program LabVIEW.
Basically, the difference of the output voltage is low according to the low supply voltage of 3V. The reference source is adjusted close to the output voltage of the sensor when shadow occurs. With the differential amplifier this difference is amplified to enhance the sensibility of the optical sensor unit itself. For the measurements, the configuration was set up that 0.4V are equal to shadow, and 0.4V plus a security distance voltage up to 0.8V are detected as sun. The security distance can easily be set with the software on the computer. Furthermore the optical sensor unit can be adjusted along a decreasing power supply voltage because of the usage of batteries.

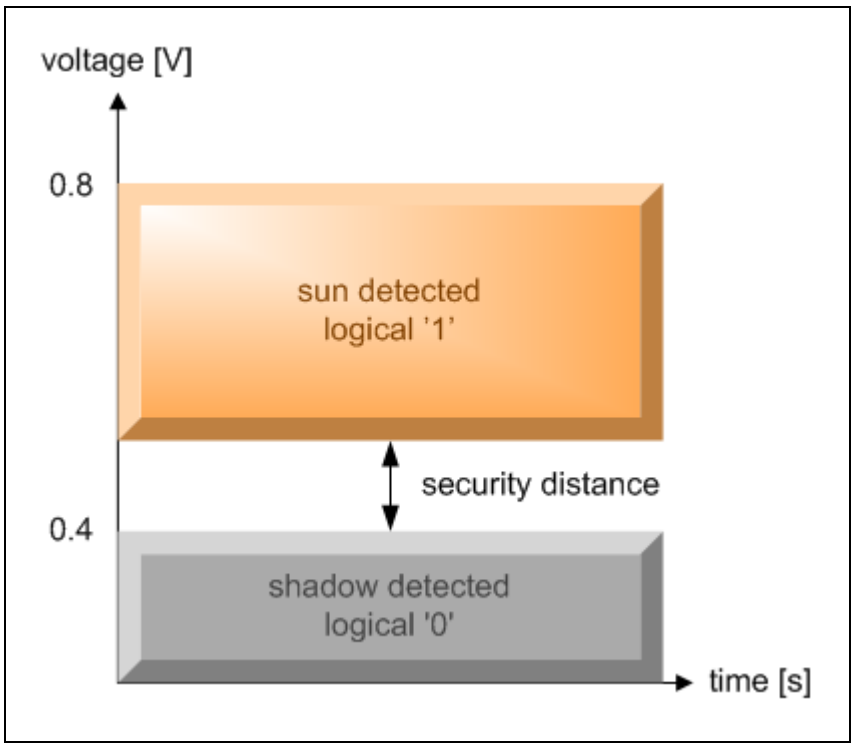

Figure 60: graphical representation of the output signal of the optical sensor unit

3.1.2. Description of the measurement

3.1.2.1. Basic objective

During driving in urban areas, different impacts can occur on the mounted solar panel on the roof of the vehicle, resulting in a totally different situation from that of a parked vehicle. The shadowing effects depend for example on:

- direction
- speed
- time of day (kind of month)
- location
- traffic conditions
- weather conditions

However, generalized data cannot be used to make statements about the efficiency of the solar panel with movement in urban areas. The output characteristic is strongly connected to individual factors which appear during the driving. For example it can be the situation that one traffic-lane of the street is totally in shadow while the other one is fully in the sun. When the driving direction is changed, for example by turning left or right at a junction, the level of efficiency can turn from very high to very low.

Figure 61: example picture for shadowing in urban areas

The example picture for shadowing in urban areas, taken on the 2nd of August at 2 o'clock p.m. in the 2nd urban district in the centre of Graz, shows an interesting aspect for movement in urban areas. The height of the buildings and also of the trees along the street has also an effect according to the daytime and the month on the shadowing of the road. If the street is driven in the morning or in the afternoon, the energy output will be not the same. The length of the street is not that long but the situation is similar in other streets. If measurements are made the results cannot be simply summed up to lead to a result for the whole year. Thus the efficiency and a statement about how much energy can be generated with the solar panel on the roof of the vehicle are strongly connected to the use of the car, and any estimation for the entire year bears an undefined uncertainty.
Even if the vehicle is parked, it does not need to be the case that energy is generated over the whole day. If the parking place is for example in the centre of the city, as shown on the example picture above, it depends on the daytime and the location nearby. In the morning it can be in shadow, whereas the battery will be charged in the afternoon. If the vehicle is needed in the afternoon the possible good charging option is not given. Furthermore many people do not have a fixed parking place in urban areas where the recharging possibilities are similar. This is the case because of the high amount of apartments which are for rent. For example the person who lives in the 2nd urban district of Graz can have a parking place in a certain area called zone 7. This leads to the fact that the parking possibilities and the recharging possibilities are restricted and different for every vehicle owner. With higher density of traffic, it can happen that a stop occurs in the sunlight or in the shadow. Furthermore the weather itself is a key component to the possible energy output.

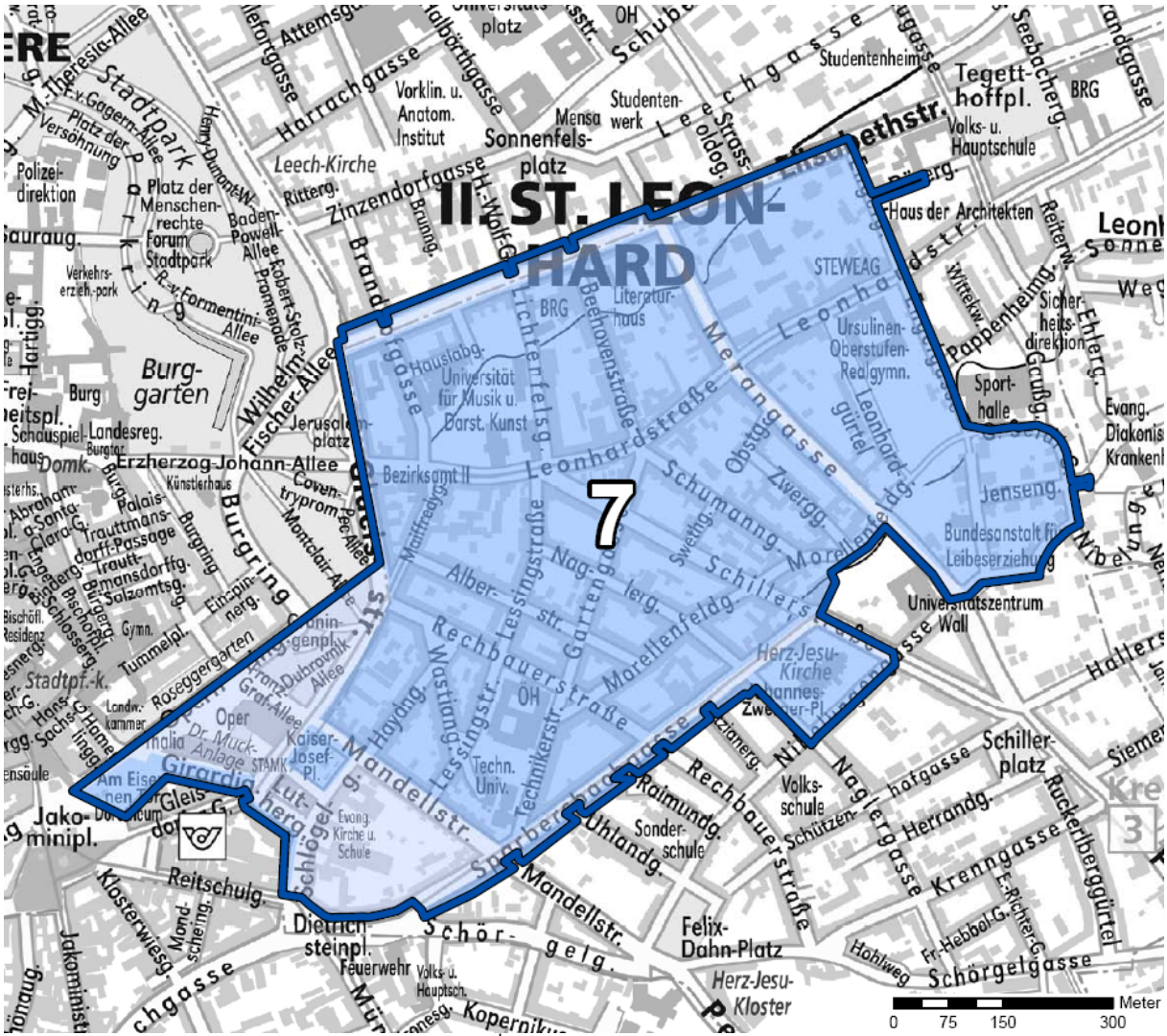

Figure 62: parking possibilities in the 2nd urban district of Graz (Source: City of Graz)

3.1.2.2. Measurement preparation

The two optical sensor units are mounted on the roof as described at the beginning of the chapter. This arrangement of the sensors on the roof leads to the largest possible distance between the two sensors.

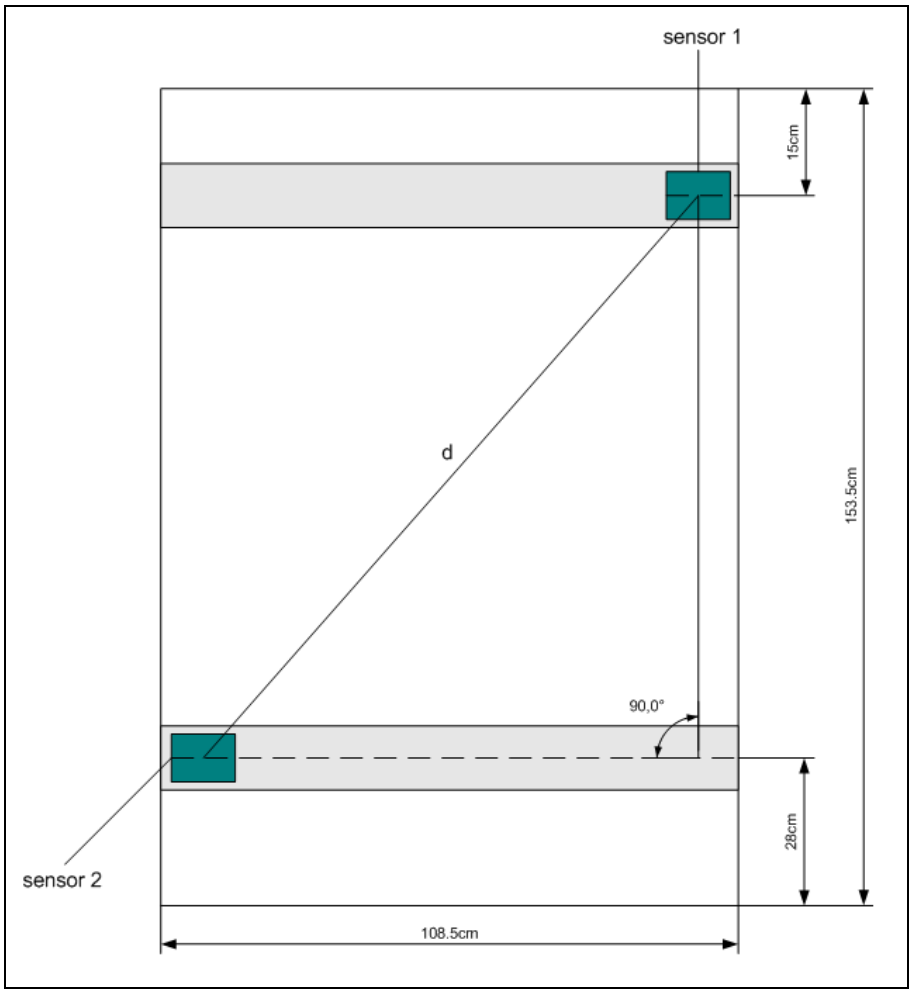

Figure 63: distance between the optical sensor units

The distance can be calculated simply as follows:

$$a = 153.5cm - 28cm - 15cm = 110.5cm$$

$$b = 100cm$$

$$d^2 = a^2 + b^2$$

$$d = \sqrt{(110.5cm)^2 (100cm)^2} = 149.03cm$$

If the optical sensor unit is directly integrated in the roof, the possible distance will be increased. For the mounting of the optical sensor units a thin 4mm wooden plate is used. The length of the plate is for the front side 120cm and for the rear end of the roof 116cm. The advantage of it is the flexibility that it lies close on the roof and has a good stability with lashing straps, offering the opportunity to run speeds up to 80km/h or 50mph with the vehicle.

Figure 64: experimental vehicle with mounted optical sensor units in the urban area

The picture above illustrates a further scenario. It is also the case that on a parked vehicle shadowing can appear. This effect can be analyzed as well with the optical sensor units. In general the configuration of the measurement looks like the following illustration.

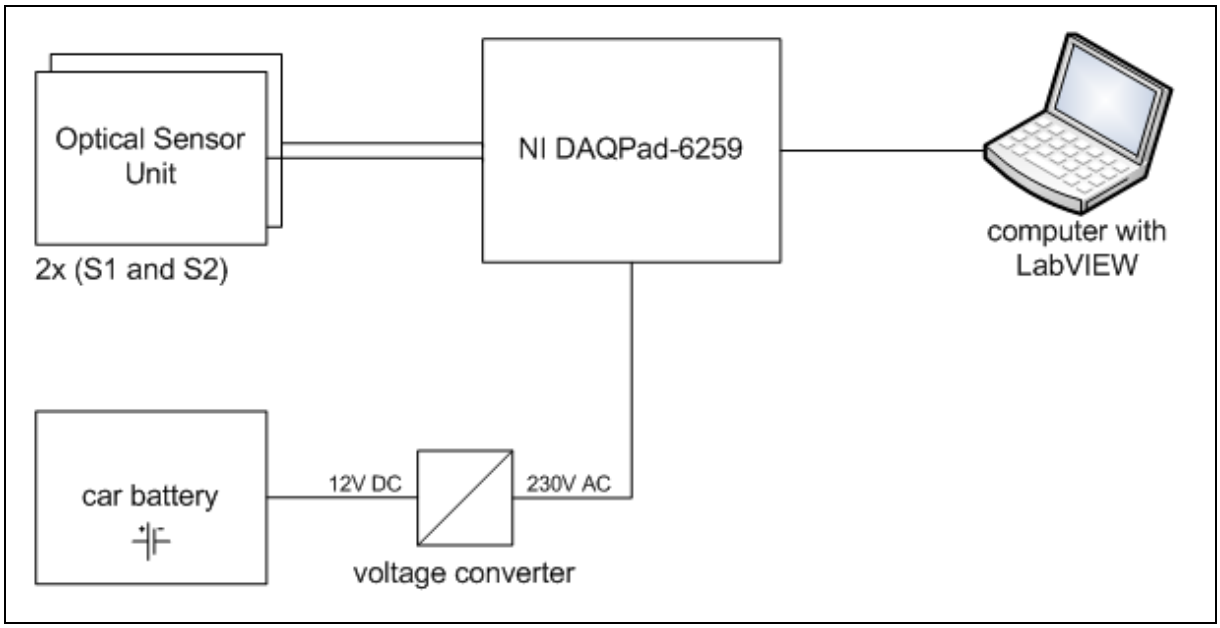

Figure 65: experimental vehicle with mounted optical sensor units in the urban area

3.1.2.3. Example measurement

The following picture illustrates a typical situation which can be found in the urban area during a normal sunny day, as already shown in the example picture at the beginning of the chapter. The following measurement results are similar to other results from other measurements which have been made on streets with similar conditions. The measurement has been made on the 2nd of August at 3 p.m in the 'Naglergasse' in the 2nd urban district in the city centre of Graz. The outside temperature was 26°C or about 80°F.

Figure 66: view into the 'Naglergasse' from the measurement starting point

The street has a length of approximately 300 metres. Each 500ms the software made a caption from the actual value of both sensor units. The car was driven with a constant speed of 25km/h or about 15mph. In total 48 measurement values were recorded , and these are listed in the following table.
At the starting point of the measurement it is the case that one optical sensor unit is in the sun, in the picture it is sensor 1 (S1) on the right hand side at the front of the roof of the vehicle, and the other optical sensor unit, in the figure sensor 2 (S2), is in the shadow. A visual check of the shadow behaviour in the street gives the impression that it will be several times the case that the optical sensor modules will deliver different values according to different shadowing effects on the roof where the solar panel is mounted. As a proof of this impression the measurement data needs to be analyzed.

Nr.	Time	S1	S2	sensors equal
1	14:57:02	1	0	no
2	14:57:02	1	0	no
3	14:57:03	1	0	no
4	14:57:03	1	0	no
5	14:57:04	1	0	no
6	14:57:04	1	0	no
7	14:57:05	1	0	no
8	14:57:05	1	0	no
9	14:57:06	0	1	no
10	14:57:06	0	0	yes
11	14:57:07	1	0	no
12	14:57:07	1	0	no
13	14:57:08	1	1	yes
14	14:57:08	1	1	yes
15	14:57:09	1	1	yes
16	14:57:09	1	1	yes
17	14:57:10	1	1	yes
18	14:57:10	0	0	yes
19	14:57:11	0	0	yes
20	14:57:11	1	0	no
21	14:57:12	1	1	yes
22	14:57:12	1	1	yes
23	14:57:13	1	1	yes
24	14:57:13	1	1	yes
25	14:57:14	1	1	yes
26	14:57:14	1	1	yes
27	14:57:15	1	0	no
28	14:57:15	0	0	yes
29	14:57:16	1	0	no
30	14:57:16	1	1	yes
31	14:57:17	1	1	yes
32	14:57:17	1	1	yes
33	14:57:18	1	1	yes
34	14:57:18	1	1	yes
35	14:57:19	1	1	yes
36	14:57:19	1	1	yes
37	14:57:20	1	1	yes
38	14:57:20	1	1	yes
39	14:57:21	1	1	yes
40	14:57:21	1	1	yes
41	14:57:22	1	1	yes
42	14:57:22	1	1	yes
43	14:57:23	1	1	yes
44	14:57:23	1	1	yes
45	14:57:24	1	1	yes
46	14:57:24	1	1	yes
47	14:57:25	1	1	yes
48	14:57:25	1	1	yes

Table 17: Measurement data from the example measurement

A comparison from the picture taken with the camera and the collected measurement data with the computer shows a connection. The shadowing effect is seen in two ways in the picture. If a small band of shadow appears from the front, sensor 1 can be ‘0’ while sensor 2 can be ‘1’ or later on sensor 1 can be ‘1’ while sensor 2 can be ‘0’. The band of shadow can also be long enough to cover the complete roof. In this case both sensor units will signal ‘0’.

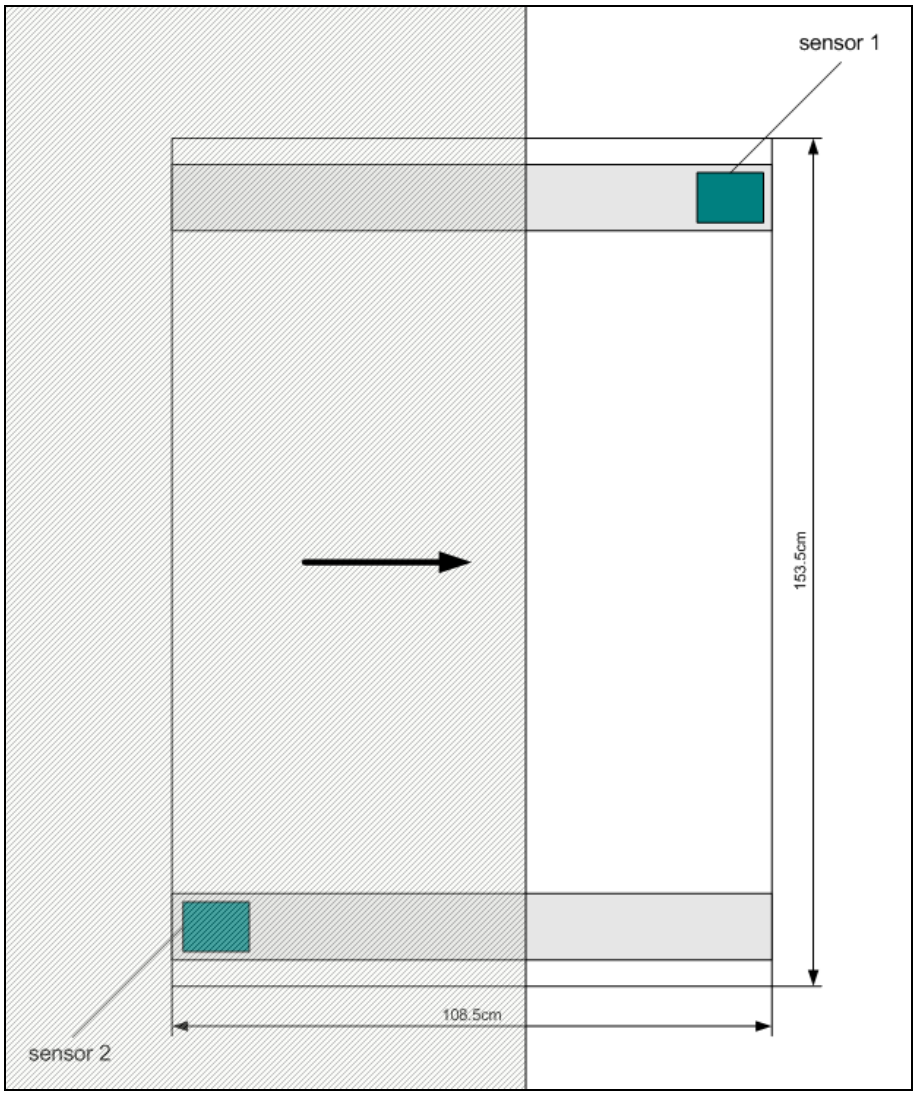

Figure 67: shadow appears from the front

In the same way the shadow can appear more on one the side as it is the case in the beginning of the measurement. In this case sensor 1 signals ‘1’ and sensor 2 signals ‘0’. The same case can be the other way around. Sensor 1 can signal ‘0’ while sensor 2 can signal ‘1’. The optical sensor units can be moved along the mounted wooden plate. This leads to additional other cases which can be tested with the two units. They can be for example:

- sensor 1 on the left hand side, sensor 2 on the right hand side
- sensor 1 on the left hand side, sensor 2 on the left hand side
- sensor 1 on the right hand side, sensor 2 on the right hand side
- sensor 1 in the middle of the roof, sensor 2 in the middle of the roof

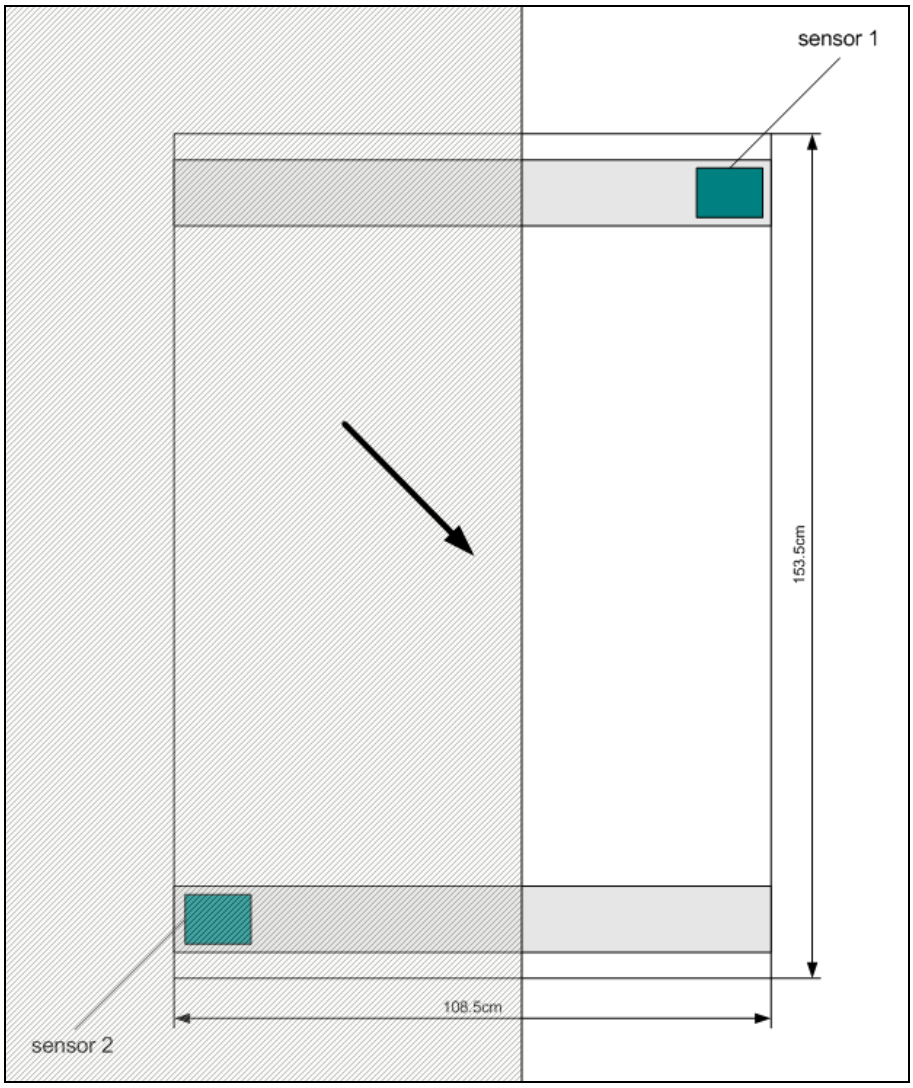

Figure 68: shadow appears on one side of the roof

Figure 69: experimental vehicle half in the sun and half in the shadow

For a more detailed statement or a better analysis, more sensors are needed. Even for the information how huge the shadowing area is on roof. If the measurement is performed in more detail, which requires more sensor units, a better statement can be given regarding how the cells should be connected in groups. The efficiency and the output power of the solar panel are related to the interconnection of the cells and the placement of the modules on the roof. With the usage of more optical sensor units, the software features have to be adapted so that the measurement of more sensor units at the same time is supported.
In general there are plenty of possibilities to interconnect the cells in groups. To generate a suitable output voltage for the DC/DC-converter for the maximum power point tracking, at least nine cells should be connected in serial. In the following figure a few examples are given. There is the opportunity to connect nine cells in serial if the dimensions are a little bit extended:

- as a three times three block (46.8cm x 46.8cm)
- as one times nine block (15.6cm x 156cm)
- as a block of three and a block of six (46.8cm x 15.6cm plus 93.6cm x 15.6cm)

With the different placing possibilities up to 54 cells or 6 modules can be mounted on the roof of the experimental vehicle.

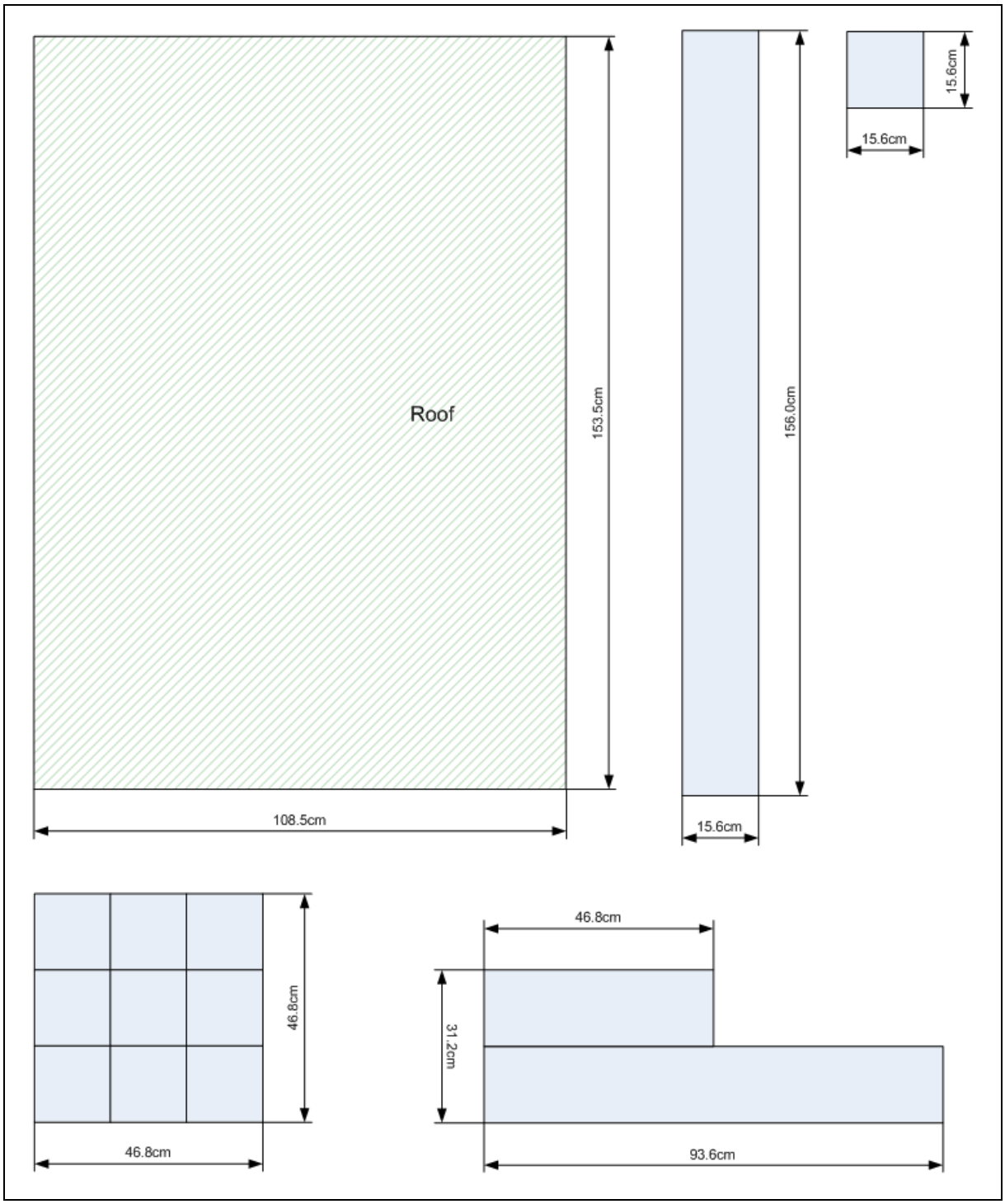

Figure 70: possibilities to connect the cells to modules with dimensions

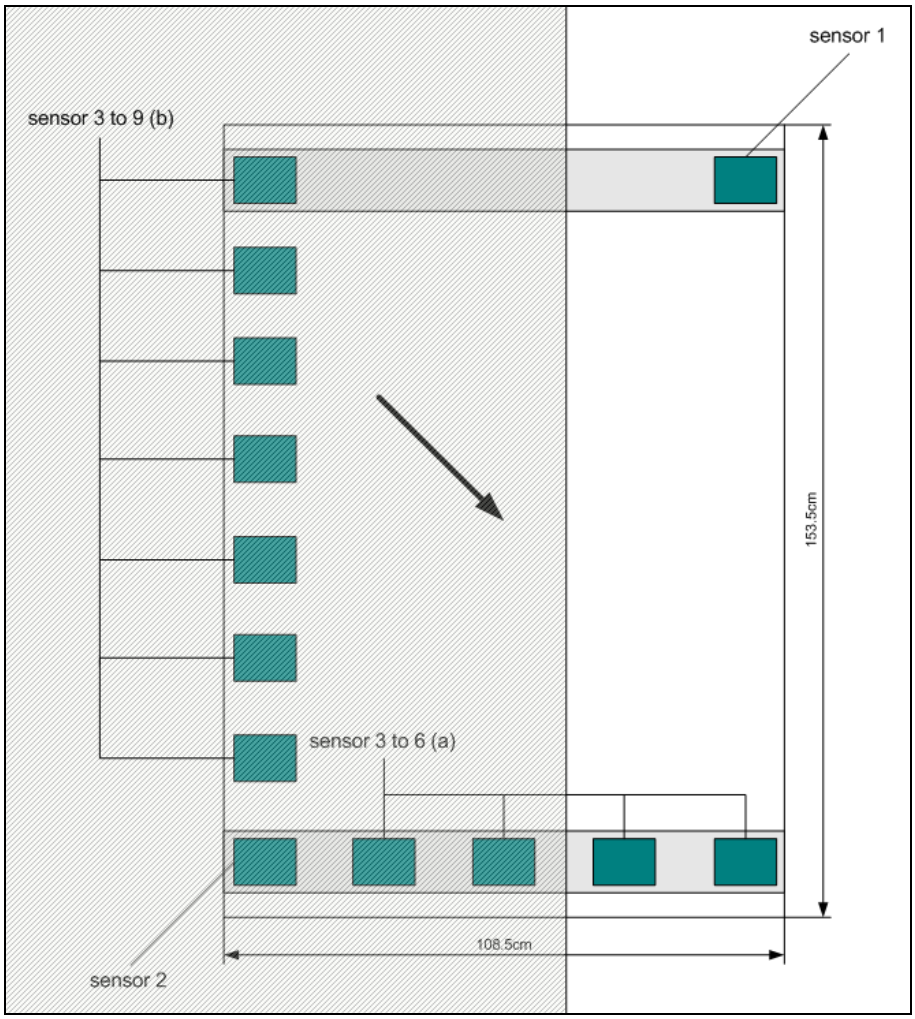

Figure 71: experimental vehicle half in the sun and half in the shadow

For conventional use it does not make sense to mount so many sensors on the roof of the vehicle, but it helps to generate statistics with the experimental vehicle. With the help of a long period of measurement at different daytimes and over a couple of months, a better decision can be made for the interconnection of the cells to the groups.
A method could be to place several sensor units along the roof, for example sensor 3 to 6 as option (a) in the figure above. This method can produce information about how much of the total area of the roof is covered by shadow from the side. Another possibility is to place sensor units along the roof, for example sensor 3 to 9 as option (b) in the figure above. This method generates information about how long the roof is covered by shadow. Even at a stop in an area with a mixture of sun and shadow, for example at a traffic light where a waiting time can be about 30 seconds, the situation can be better analyzed with more sensors.

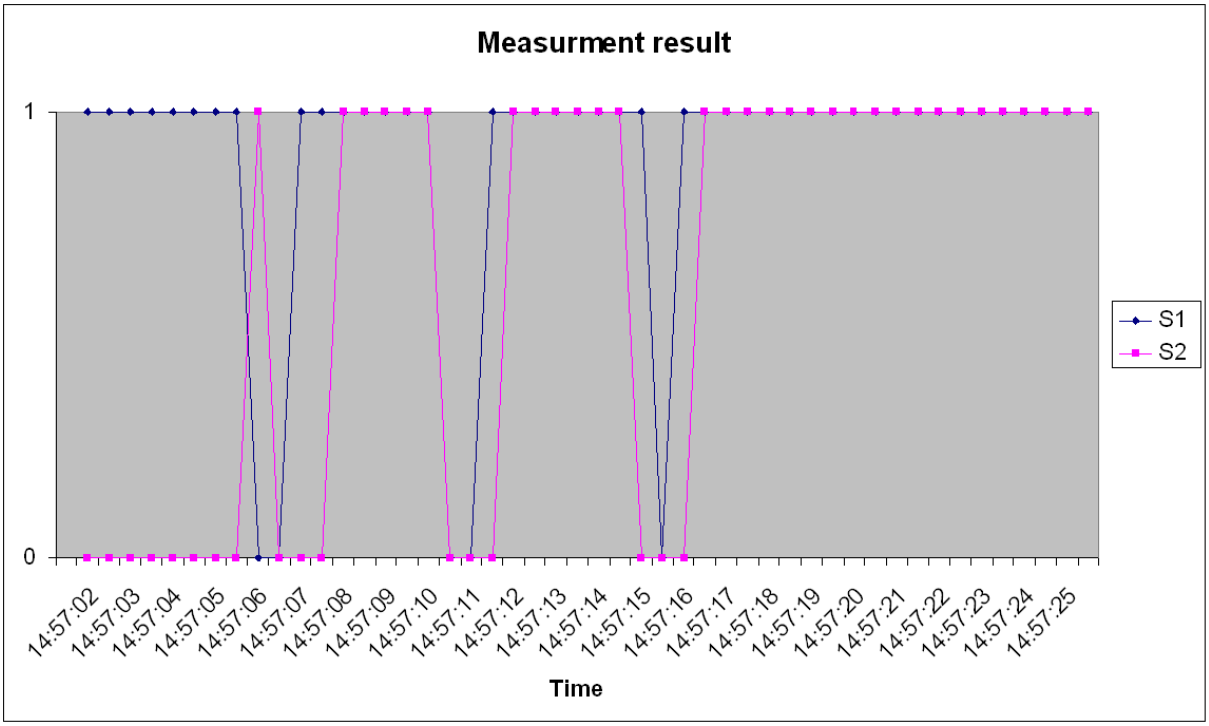

Figure 72: graphical representation of the measurement result

times	description	in percent
48	totally collected measurement values	100%
14	different values between S1 and S2	29.17%
43	sun on S1 detected	89.58%
31	sun on S2 detected	64.58%

Table 18: analyzed measurement data from the example measurement

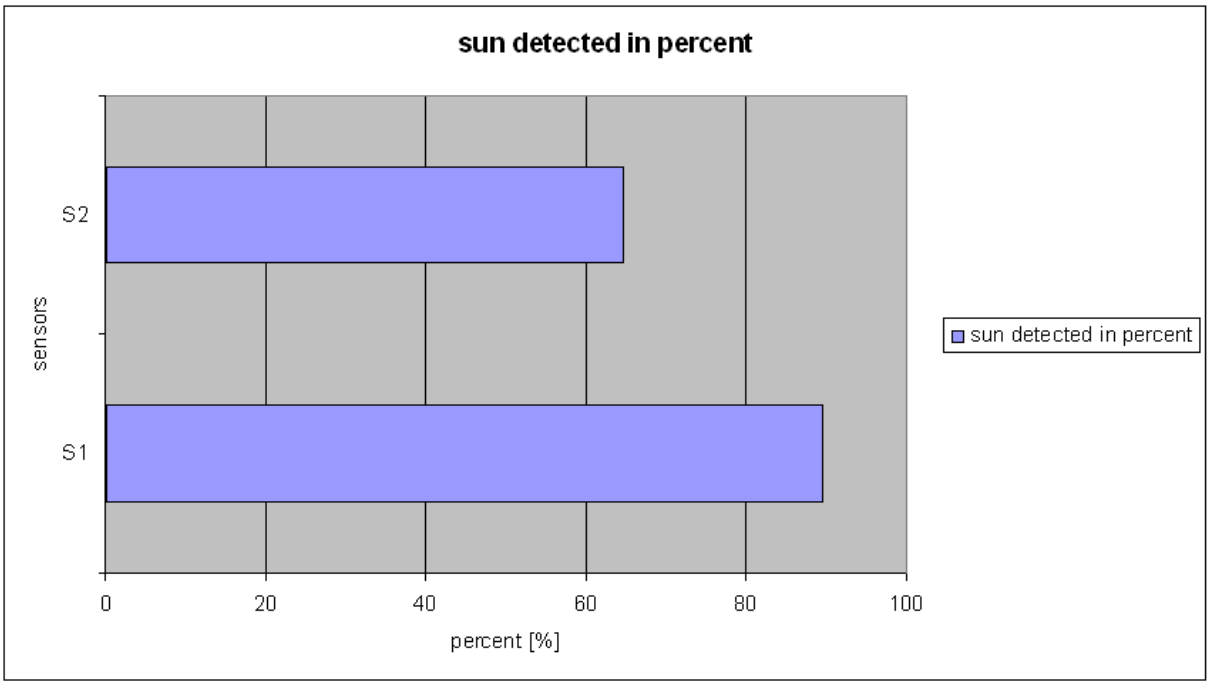

Figure 73: sun detection as percentages of sensor 1 and sensor 2

However, the result of the example measurement shows that there is a difference which has to be taken into account and shows that the topic of how the cells are connected with each other is not redundant. The optical sensor unit is suitable to perform measurements to generate statistical data. Furthermore it can be used as a reference source to support the energy management of the vehicle with data about the current amount of shadowing on the roof. For a better performance and an integration into the roof of the vehicle some improvements can be made which are discussed in the following chapter.

Figure 74: sun situation in urban areas

3.2. Improvement of the optical sensor unit

The experimental vehicle provides an area at the maximum of about 1.5m² (153,5cm x 108,5cm). A larger area would be given by the mounting on a hybrid bus used for public transport. If a solar panel is mounted on the roof on that kind of bus the negative impact of shadowing is much more because in this case the vehicle spends so much time in movement. Of course a normal bus can also be parked in the sun to avoid shadowing. But for a bus used for public transport in an urban area the situation is different.

3.2.1. Volvo 7700 Hybrid

The Volvo 7700 Hybrid would be such a bus. The propulsion is provided by a diesel engine and electric power. Within the parallel hybrid system the electric engine can work as a motor or generator. Under normal circumstances the electric motor is suitable to accelerate from a standstill to a speed of about 20 km/h or about 12,5 mph. This action promotes considerable fuel savings. If higher speeds are reached the diesel engine takes care of propulsion. When the diesel engine is operating the electric engine is used as a generator to recharge the batteries. This hybrid solution is ideal for urban operations and that kind of combination results in fuel savings up to 30% (Volvo, 2008; Volvo, 2009).

Figure 75: Volvo 7700 Hybrid bus (Source: Volvo)

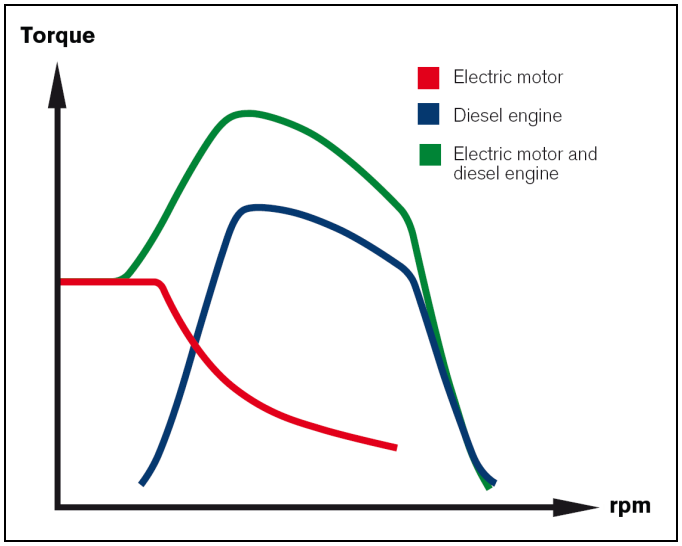

Figure 76: Volvo 7700 Hybrid torque (Source: Volvo)

With the saving of fuel by efficient propulsion, also the operating costs are reduced. A further reduction is achieved in the caused emissions. The benefit of the hybrid system appears if the bus pauses for example at a bus stop or a traffic light. The bus produces in this case no emissions because the diesel engine is switched off and the electric engine takes care of the necessities. This leads to a reduction of CO_2 as well of NO_x and other emissions of about 40 to 50%. A further benefit shows up with the overall noise reduction by 4 db(A). It can be said that the Volvo 7700 Hybrid bus provides a good amount of capacity combined with low emissions (Volvo, 2008; Volvo, 2009).

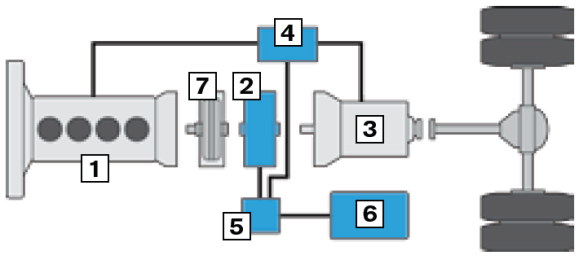

The main components of the Volvo hybrid system
1. Diesel engine **2.** Electric motor/generator
3. Transmission **4.** Powertrain Management Unit (PMU)
5. Energy converter DC/DC 600V/24V **6.** Batteries
7. Clutch

Figure 77: Volvo 7700 Hybrid main components (Source: Volvo)

It is the case that the electrical energy can only be produced by the diesel engine. However, for recharging the batteries, emissions have to be taken into account. If more pauses need to be made for example because of a traffic jam or close bus stops, the diesel engine needs to be switched on to prevent the battery being discharged. An external recharge possibility cannot help to improve this situation because of the given movement of the bus. With the implementation of a solar panel a possibility is established in which the batteries are recharged during the drive.
The advantage of a bus is the large area available where solar cells can be mounted. A calculation can be made for the area for solar modules which can be implemented on the surface of the roof of the Volvo 7700 Hybrid. Flexible solar cells can help to avoid problems caused by the rising of the roof at the front and at the rear end of the bus.

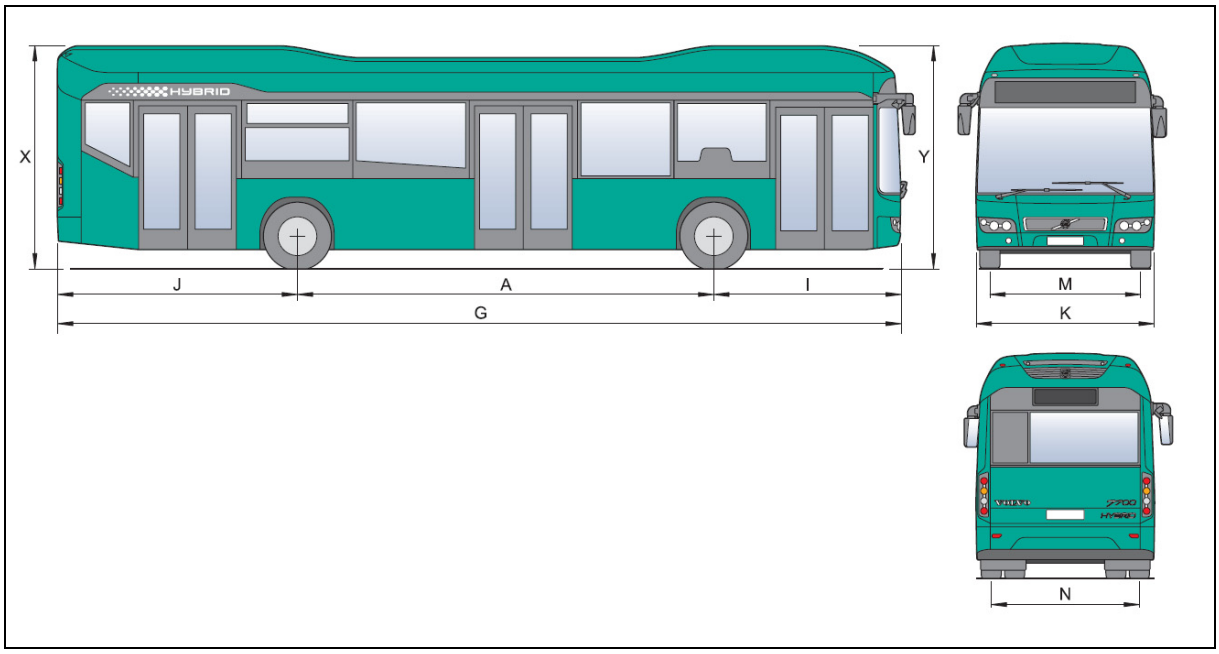

Figure 78: Volvo 7700 Hybrid Bus Dimensions (Source: Volvo)

Part	Description	Length [mm]
G	Overall length	12074
Y	Height at battery cover	3216
X	Height at radiator cover	3207
K	Overall width	2520
A	Wheelbase	5945
I	Front overhang	2694
J	Rear overhang	3435
M	Track, front	2107
N	Track, rear	1885

Table 19: Volvo 7700 Hybrid Bus Dimensions (Source: Volvo)

$$A_{roof} = 11050\text{mm} \times 2000\text{mm} = 22100000 mm^2 = 22.1 m^2$$

The Toyota Prius offers as a comparison an area to mount solar cells of about 1.5m². The first implemented version of the solar panel on the roof of the experimental vehicle does not require the entire available area. There is 15 times more space on the Volvo 7700 Hybrid in comparison to the Toyota Prius.
If there is the opportunity to mount more solar cells, the situation changes in different ways in a conventional vehicle compared to a large public transport vehicle. With the higher number of solar cells the energy output will increase. This situation leads to the necessity of additional implementations.

3.2.2. Additional implementation requirements

The prototype version of the optical sensor is designed to generate measurement data for a statement about shadowing on a roof of a vehicle during driving in urban areas. If the amount of energy output is higher, which is the case on larger roofs as for example on public transport vehicles, then further expects show up, which leads to an improvement of the optical sensor unit and a fix implementation to the solar cells on the roof.

3.2.2.1. Differential amplifier

To enhance the gain performance of the optical sensor unit an instrumentation amplifier can be used instead of the current different amplifier. For the realisation, three instead of one AD820AN are required. The most noteworthy benefit is the adjustable gain (over the resistor R_{gain}); other additional characteristics are the very low DC offset, low drift, low noise, a very high common mode rejection ratio and very high input impedances. In general instrumentation amplifiers are used for operations where great accuracy and stability is required, both for short-term solutions as well as for long-term solutions (Tietze U., Schenk Ch., 2002).

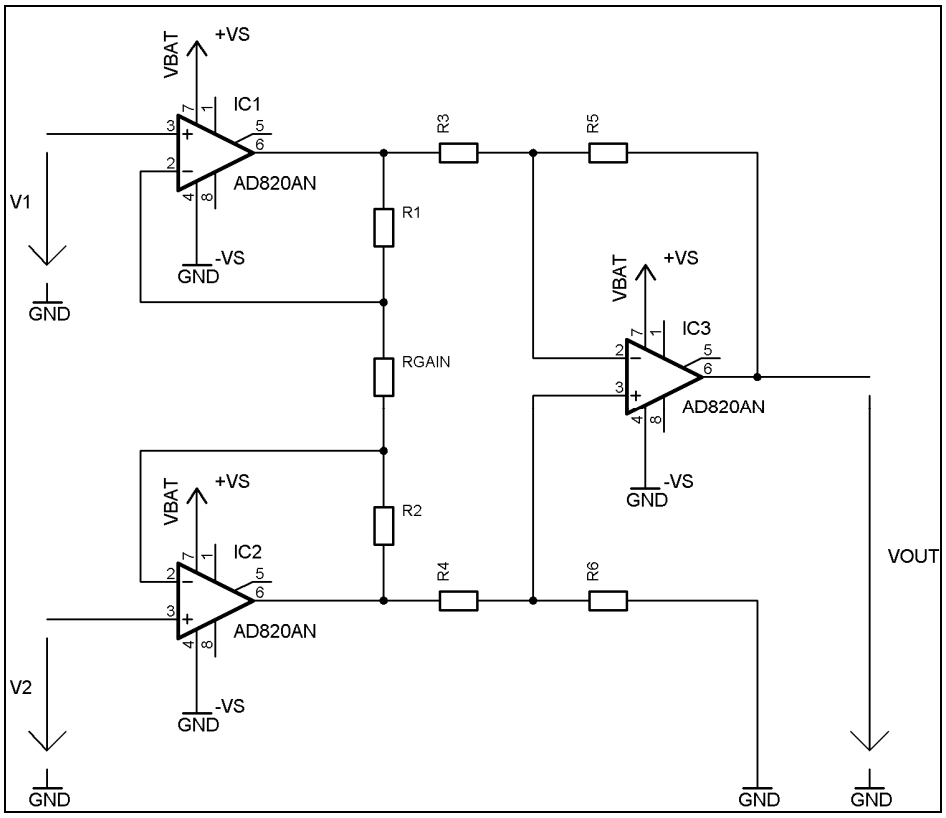

Figure 79: instrumentation amplifier (Source: Tietze U., Schenk Ch.)

For the dimensioning the following settings can be choosen:
$R_a = R_1 = R_2$
$R_b = R_3 = R_4$
$R_c = R_5 = R_6$

$$A = \frac{V_{out}}{V_2 - V_1} = (1 + \frac{2R_a}{R_{gain}}) \frac{R_c}{R_b}$$

3.2.2.2. Power supply for the optical power unit

To support the optical sensor unit with power for a longer period of time, a converter from 12V, which for example a USB interface offers, can be integrated into the optical sensor unit. The AS1341 is a Step-Down Converter which offers the opportunity to provide this voltage. The AS1341 itself has an efficiency of up to 96%. To operate more sensitively with the optical sensor unit there is the possibility to establish a real light-to-voltage measurement and not to decide only between shadow and light detection. Therefore a higher supply voltage for the used optical sensor from TOAS is recommended. The AS1341 can also be designed to provide higher output voltages if the input voltage is for example 12V.

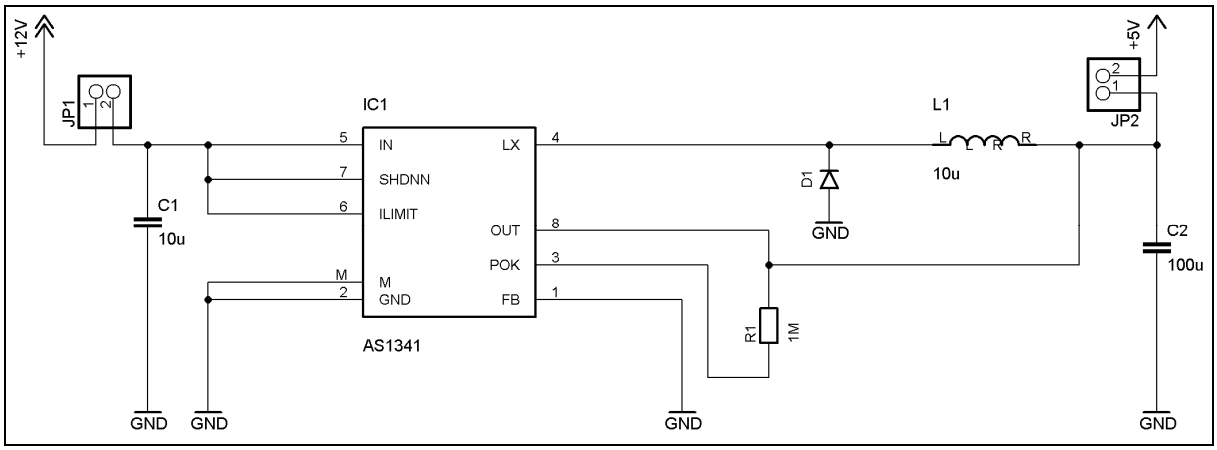

Figure 80: AS1341 Step-Down Converter from 12V to 5V (Source: austriamicrosystems)

3.2.2.3. Direct supply of the energy and LIN bus communication

If the energy output of the solar panel is high enough, for example if the solar panel is mounted on a bus, further steps can be performed. If solar modules with equivalent solar cells of the Toyota Prius are mounted on the Volvo Hybrid 7700, a solar energy output of about 3.2kW can be generated. In general to extend the lifetime of the high voltage battery the energy can be provided directly to the electric motor. At the Volvo Hybrid 7700 this can be done with the I-Shift transmission. In the case of the Toyota Prius the energy produced by the electric generator can be directly supplied to the electric motor without charging and discharging the HV battery pack.
The optical sensor unit can provide the different electronic circuit units with information about the sun illumination on the roof of the vehicle, and provides in that way data for an estimation of how much energy can be gained from the solar panel. For the ECU, which controls the charge and discharge of the high voltage battery, this information can be useful and necessary. Therefore a certain amount of communication is required. A LIN bus with a gateway to a CAN communication offers the opportunity for the expected amount of information traffic (Volvo, 2008; Volvo 2009; Bosch, 2007).

4. DataLogging tool and software implementation

4.1. Approach

The measurement software is implemented in LabVIEW in its version 8.0 from National Instruments. The basic function of the software is to collect measurement data from solar panels or solar modules, which can be used for statistical evaluation to gain information and knowledge about the level of efficiency. To establish freedom for the measurements, options need to be implemented to allow the operator different kind of settings according to need. The DataLogging tool in the version 2.0 at the moment of the creation of this diploma thesis offers the opportunity to use the multifunction data acquisition (DAQ) module mentioned in an earlier chapter or to communicate with the FPGA via USB to receive the measurement values.

4.2. Opportunities

At the beginning the operator has to check several settings and to provide some input information before the measurement itself can be started. These settings can be made on the second page ‘configuration’ and on the first page as well. However, the measurement can be stopped at any time and the configurations can be changed. In case of necessity, the configurations can be set without stopping the measurement. If the path where the data is stored is changed, the program needs to be restarted. Furthermore there is no specified order in which the settings have to be done . If the DataLogging tool is started the operator gets to the main page.

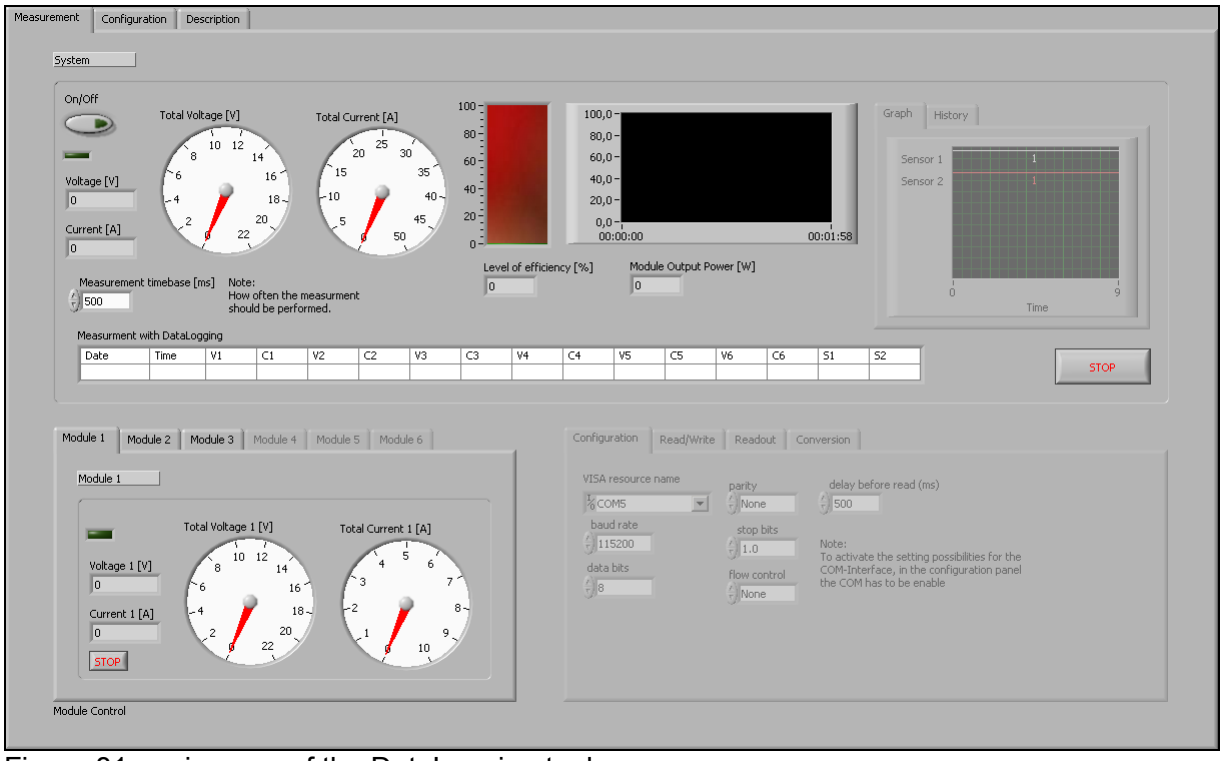

Figure 81: main page of the DataLogging tool

4.2.1. Basic software flow

The DataLogging tool is realized on a basis following the settings.

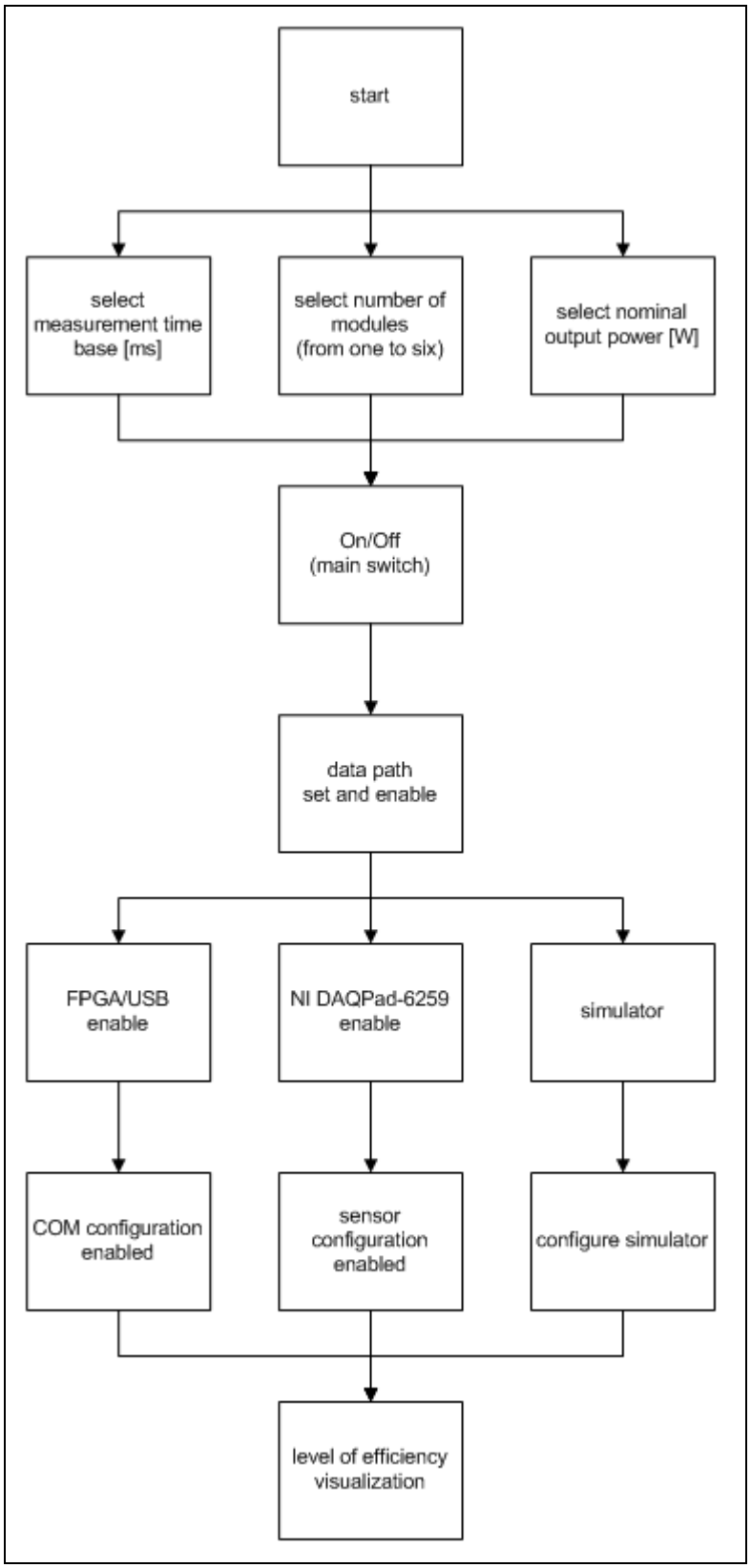

Figure 82: data flow of the DataLogging tool

At the beginning the operator can, but does not need to, set:

- the measurement time base [ms] – the default value is 500ms. For this setting there is no minimum or maximum value given
- the amount of modules which are measured – the default is three modules
- the nominal output power [W] of the panel or module which is measured – the default value is 80W

If the On/Off switch is pressed the measurement tool is activated. Afterwards the option can be selected that the data is stored into a text-file. Measurement is also possible without saving the captured data. In case of necessity, the storage of the data can be started at any time.

The next step is to select the source from which the measurement data is taken. Only one of the three possible sources can be chosen at the same time:

- the communication with the FPGA via USB
- the multifunction data acquisition (DAQ) module
- the integrated simulator

4.2.2. Main page elements

The order of the elements and components on the main page is presented to offer the operator a clear view of the measurement tool possibilities and functions.

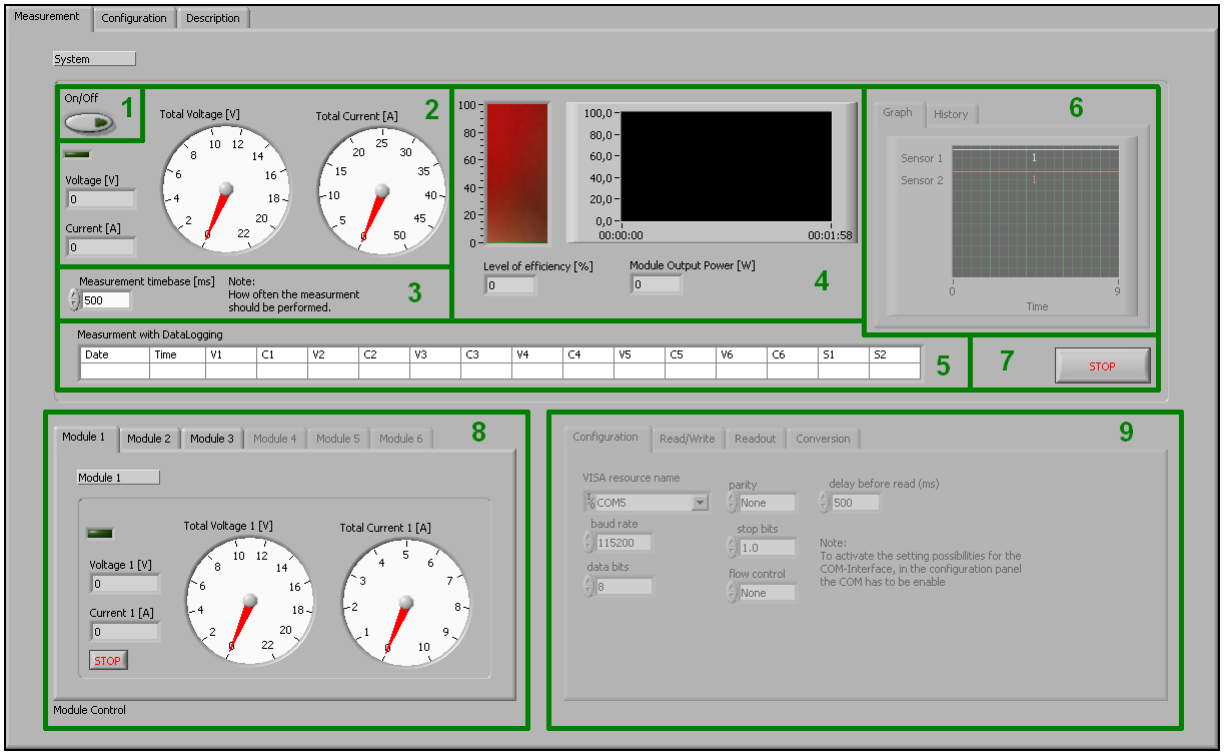

Figure 83: elements of the main page of the DataLogging tool

element	name	description
1	Main On/Off switch	by pressing this swich the DataLogging tool is activated
2	Main voltage and current gauge	depending on the number of modules the total current and voltage is displayed
3	time base selection	this value defines how often a recall is made to get measurement data – there is no restriction given for the setting of this value
4	level of efficiency visualization	the current and several past values of the level of efficiency is displayed here. The value is displayed as an absolute percentage value in comparison to the possible or nominal maximum output power of the module(s)
5	DataLogging values	if the data is mentioned to be stored in this table all the values are displayed
6	optical sensor unit visualization	if the multifunction data acquisition (DAQ) module is used the optical sensor unit can be connected and will be visualized on the main page
7	Main Stop switch	to switch off the tool at any time
8	Module Control	each voltage and current values can be watched separately
9	COM configuration	if the communication via USB is used this control panel will be activated for the settings

Table 20: elements of the main page description

4.2.3. Settings at the configuration panel

4.2.3.1. Module Measurement Control

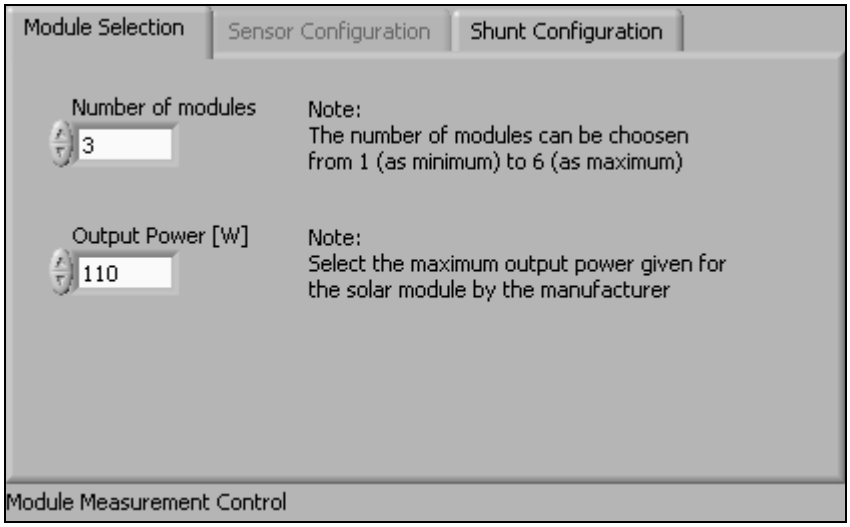

Figure 84: Module Measurement Control, figure 1/2

The Module Measurement Control is located at the configuration panel. Here the amount of modules can be set for the measurement. Depending on the activated number of modules at the front panel, more or less modules are displayed. The DataLogging tool is capable of measuring six modules at the same time and store the data into a text file. At least one module needs to be enabled.

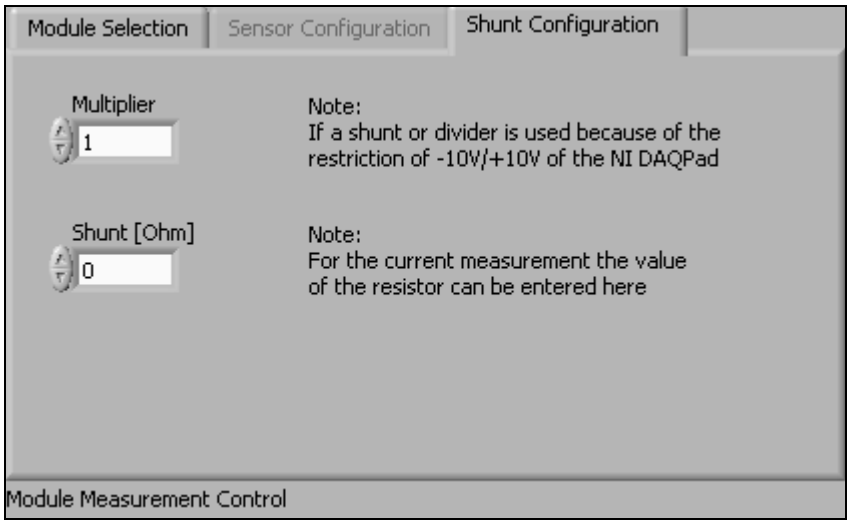

Figure 85: Module Measurement Control, figure 2/2

If the multifunction data acquisition (DAQ) module from National Instruments is used, a shunt can be used for the current measurement. Furthermore a multiplier can be chosen for the voltage measurement if the total voltage exceeds 10V. With a voltage higher than 10V the measurement with the DAQ module does not work correctly. Therefore it is useful to have this multiplier function in the case where a serial circuit with a certain amount and kind of loads is measured. For example if two equal resistors are connected in serial to each other, half of the voltage will be at each resistor. By a multiplier of two the total voltage can be calculated and will be correctly visualized.

4.2.3.2. Measurement Tool Selection Control

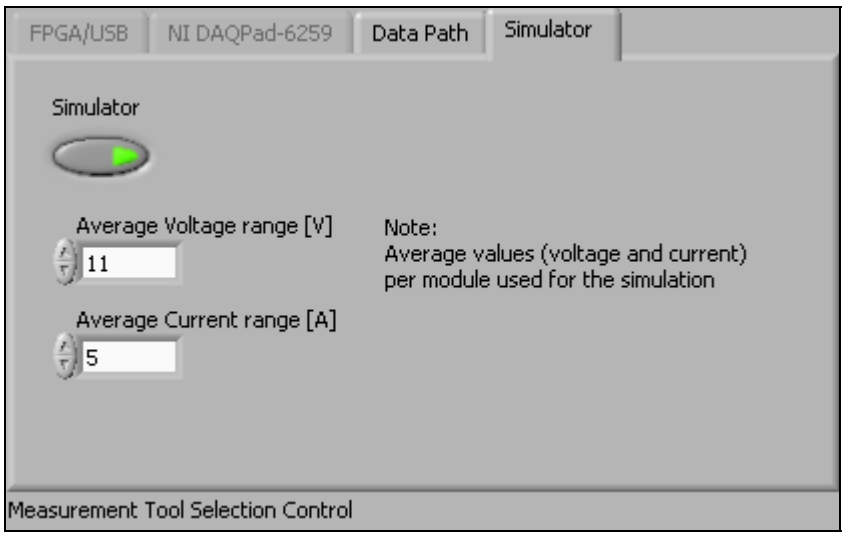

Figure 86: Measurement Tool Selection Control, figure 1/3

At the Module Selection Control also located on the configuration panel the source can be chosen from where the measurement data is gained. To get to know the DataLogging tool it is possible to use the simulator instead of the measurement with the DAQ module or the communication via USB with the FPGA. The simulator will generate for the amount of selected modules random voltage and current values. The values will be different for each module and are located around a definable voltage value with a difference of -0.23V up to +1.2V and around a definable current value with a difference of -0.47A up to +1.2A.

Also the data from the simulator can be stored into a text file as the measurement data taken by the DAQ module or from the FPGA.

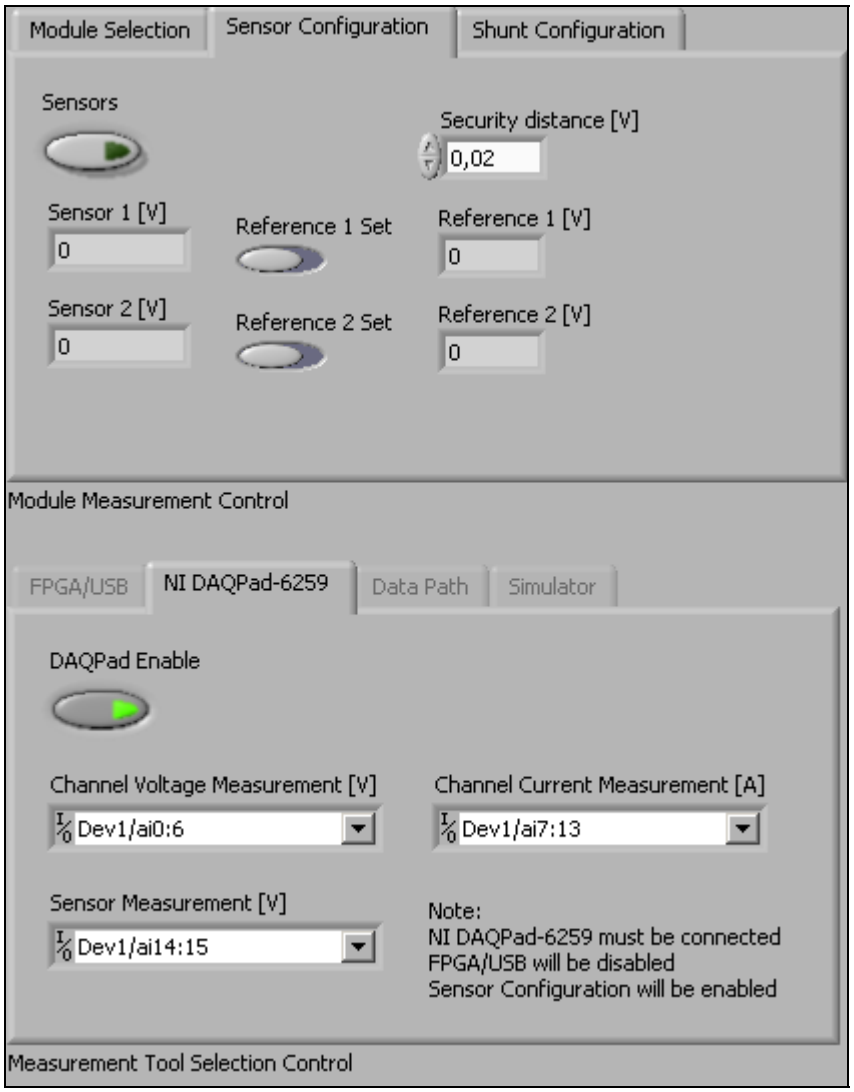

Figure 87: Measurement Tool Selection Control, figure 2/3

If the DAQ module is selected, the measurement channels can be selected according to the table on the DAQ module. However, some recommend default channels are already set. At the time of activating the option to measure with the DAQ module, the opportunity to take measurement data by the communication with the FPGA or to run the simulator to produce data will be disabled, for as long the DAQ module option is enabled. If the DAQ module is chosen the second page of the Module Measurement Control will be enabled.
At the configuration page called Sensor Configuration, a visualization of the values received from the sensors is available if required. If the DataLogging function is enabled, the data from the optical sensor units is both displayed on the main page and stored in the text file. The sensors can be configured by pulling the slide switch. The actual sensor voltage value and a security distance are used to define the logical ‘0’ and the logical ‘1’ as described in the earlier chapter 3. Furthermore the security distance can also be adjusted here. If the sensor measurement is enabled, the detection of shadow or sun is displayed in a diagram on the main page in the upper right corner.

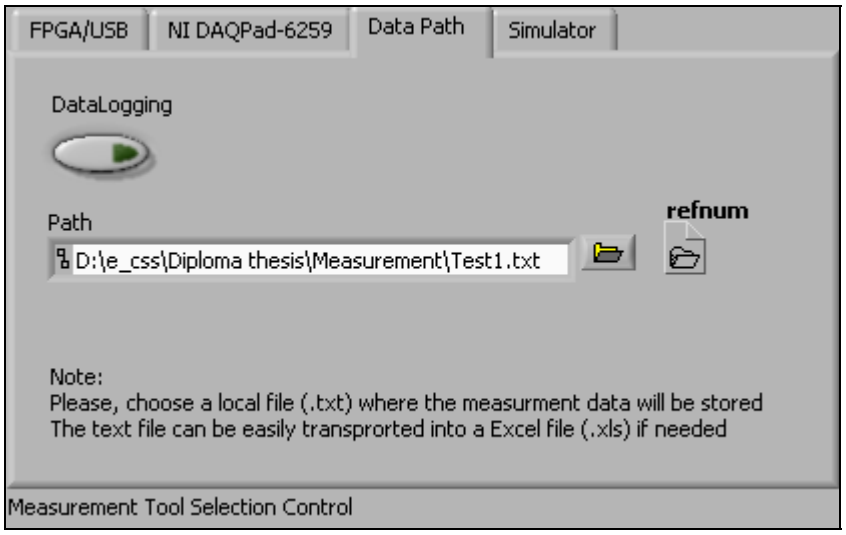

Figure 88: Measurement Tool Selection Control, figure 3/3

The measurement data can be stored into a text file by pressing the switch on the third frame of the Measurement Tool Selection Control. For statistical evaluation of the measurement data the content of the text file can easily be transported into an Excel file. This was done also in the earlier chapters for example to generate diagrams for the Enecom solar panel.

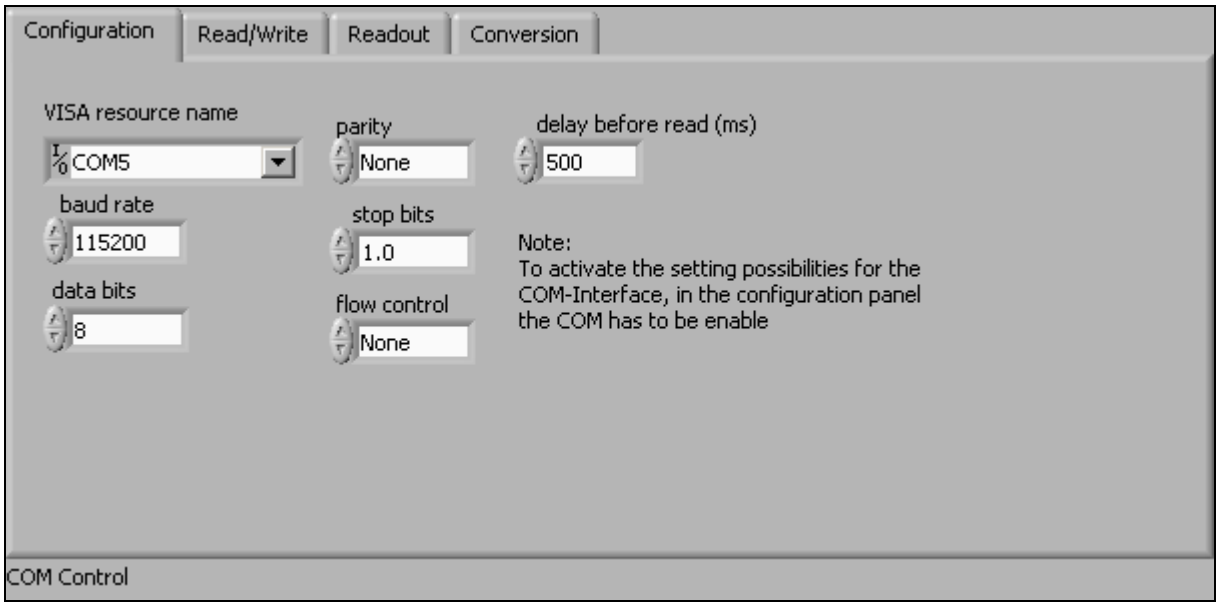

Figure 89: COM Control panel on the main page

If the communication via USB with the FPGA is chosen the COM control panel on the main page is activated and available. The settings by default are recommended but can be changed if necessary. The LabVIEW program sends a command to the FPGA via USB and receives a data string from a register of the FPGA. A parser is implemented in LabVIEW which analyzes and converts the received data to measurement data. This measurement data can be stored in a text file.

The following figure shows the DataLogging tool in mode of operation. The measurement data is generated by the integrated simulator. The sensors are not simulated along the integrated simulator. Furthermore the data is stored into a text file and in the table on the main page the last saved values are displayed. The last values which have been taken during the last two minutes are shown in a diagram. The level of efficiency is not stored into the data file because the purpose is only a visualization of the current energy output of the measured solar module.

Figure 90: main page with activated simulator

5. Analysis

5.1. For comparison: energy of oil

One barrel of oil is equivalent to approximately 6.1GJ or 1,700kWh. In one barrel there are 158.987295 litres of oil. With a level of efficiency it can be said that with 1litre benzene, diesel or heating oil generates about 10kWh. Thus for 1kWh, approximately 0.1l fuel is necessary. The same value can be used in calculation of the possibility to save 95 to 120l on heating oil with an illumination of 975 to 1,275kWh/m². The available area to mount solar cells on the roof is, for the Toyota Prius, 1.5m². With 45 solar cells with a dimension of 156mm by 156mm an area of about 1.1m² are taken. The nominal maximum output power is 180W and with the flat and curved surface and the non-ideal angle to the sun, the possible output power is 156.6W to 171W (DFS, 2002).

5.2. Estimation of the output and possible benefit

5.2.1. Replacement of benzene

For estimations to generate output data, some simplifications need to be made. This leads to a possible prediction regarding approximately how many kilometres the car needs to go until the solar panel will be a benefit from the point of view of the costs of the solar panel. This point is called break even point in the economics and finance sector (Wöhe, 2008; Grohmann-Steiger C., Schneider W., Eberhartinger E., 2008; Bundesministerium für Finanzen, 2010).

- the effective area is the energy output of 1m² solar cells or 165W of nominal output power
- with a certain amount on illumination the possible output is calculated to be between 900kWh/m² and 1,200kWh/m² for the whole year
- because of certain impacts for example because of shadowing during driving, the possible output is reduced to 800kWh/m² to 1,100kWh/m²
- over the entire year from 800kWh up to 1,100kWh can be gained
- the solar panel itself will cost €1,200 without government support. To integrate the solar panel into the roof of the car a cost of €400 is assumed in addition to €400 for further electronics, cables and configurations of the board net. leading to total costs of €2,000
- the solar panel is capable of surviving the of 15-year lifetime of the vehicle and will not reduce its power output over this period of time. This can be expressed as average costs of €133.33 for each year
- the fuel used for the vehicle is benzene with a price per litre for January 2010 of €1.10. With a rising of the price on average of 8% each year a price for January 2015 is approximately €1.50 and for January 2020 €2.20

This leads to the following equations:

$$800kWh/m^2 = 800 \times 0.1l = 80l$$

$$1{,}100kWh/m^2 = 1{,}100 \times 0.1l = 110l$$

$$2010: 80l \times €1.1 = €88; 2011: 80l \times (€1.1 \times 1.08) = €95.04$$

After performing all calculations a table can be made with the values which are required for the diagram.

year	800kWh/m²	1,100kWh/m²
2010	€88.00	€121.00
2011	€95.04	€130.68
2012	€102.64	€141.13
2013	€110.86	€152.43
2014	€119.72	€164.62
2015	€129.30	€177.79
2016	€139.65	€192.01
2017	€150.82	€207.37
2018	€162.88	€223.96
2019	€175.91	€241.88
2020	€189.99	€261.23
2021	€205.18	€282.13
2022	€221.60	€304.70
2023	€239.33	€329.07
2024	€258.47	€355.40

Table 21: savings on fuel over the years of the entire lifetime

The total savings on money are between €2,389.39 for 800kWh/m² and €3,285.4 for 1,100kWh/m².

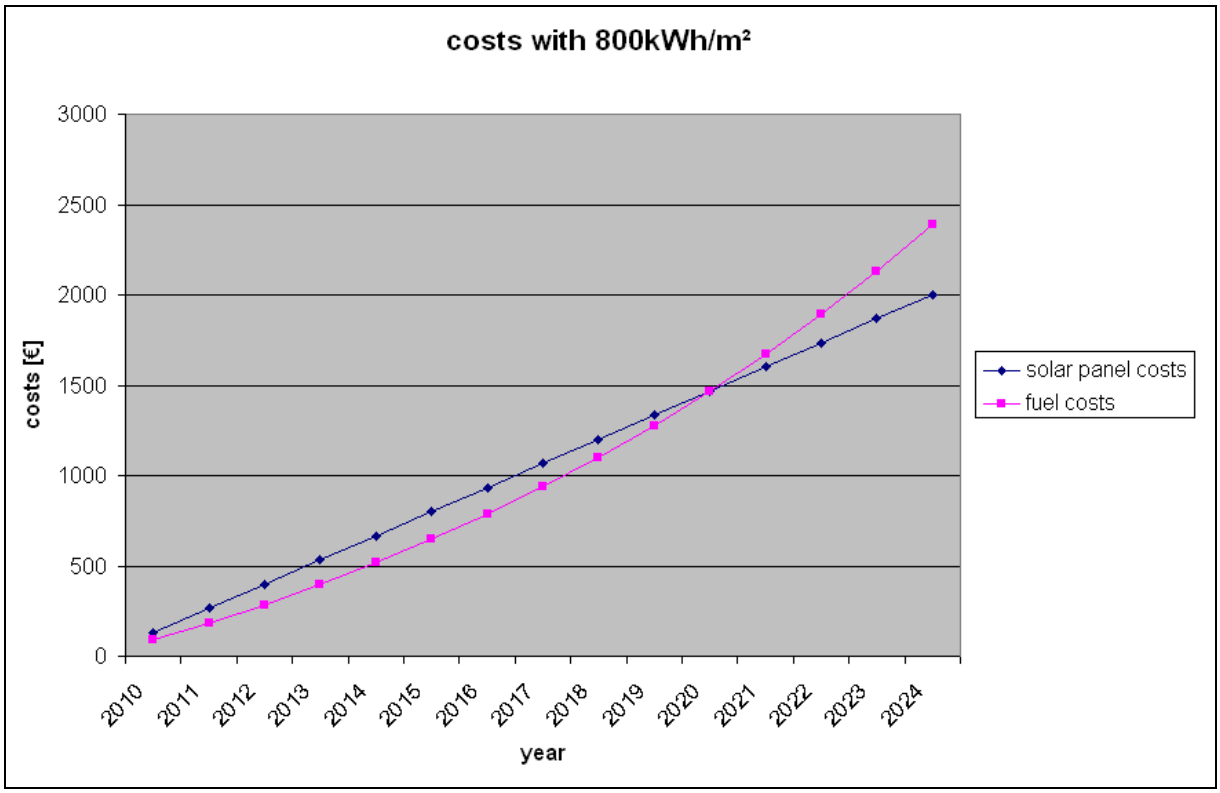

Figure 91: costs with 800kWh/m² and replacement of benzene

Figure 92: costs with 1,100kWh/m² and replacement of benzene

5.2.2. Replacement of electrical energy

A plug-in vehicle can also be recharged with external energy. If it is the case that only 100% renewable energy is used for recharging the vehicle's battery the same amount can be saved on external energy as on fuel. The basic conditions are the same as on the fuel saving calculations. The change is according to the prices of the used energy resource.

- 1kWh 100% renewable energy costs €0.215 by day and €0.155 at night. For the calculation, an average value of €0.185 is taken
- the prices are increasing by 8% each year. The price in the year 2010 is €0.185

This leads to the following equations:

$$800kWh/m^2 = 800 \times €0.185 = €148$$

$$1{,}100kWh/m^2 = 1{,}100 \times €0.185 = €203.5$$

$$2010 : €148$$

$$2011 : 800 \times (€0.185 \times 1.08) = €159.84$$

After performing all calculations again a table with the values can be made which are required for the diagram.

year	800kWh/m²	1,100kWh/m²
2010	€148.00	€203.50
2011	€159.84	€219.78
2012	€172.63	€237.36
2013	€186.44	€256.35
2014	€201.35	€276.86
2015	€217.46	€299.00
2016	€234.86	€322.93
2017	€253.65	€348.63
2018	€273.94	€376.66
2019	€295.85	€406.80
2020	€319.52	€439.34
2021	€345.08	€474.49
2022	€372.69	€512.48
2023	€402.50	€553.44
2024	€437.70	€597.72

Table 22: savings on energy over the years of the entire lifetime

The total savings on money are between €4,021.51.39 for 800kWh/m² and €5,525.34 for 1,100kWh/m².

Figure 93: costs with 800kWh/m² and replacement of electrical energy

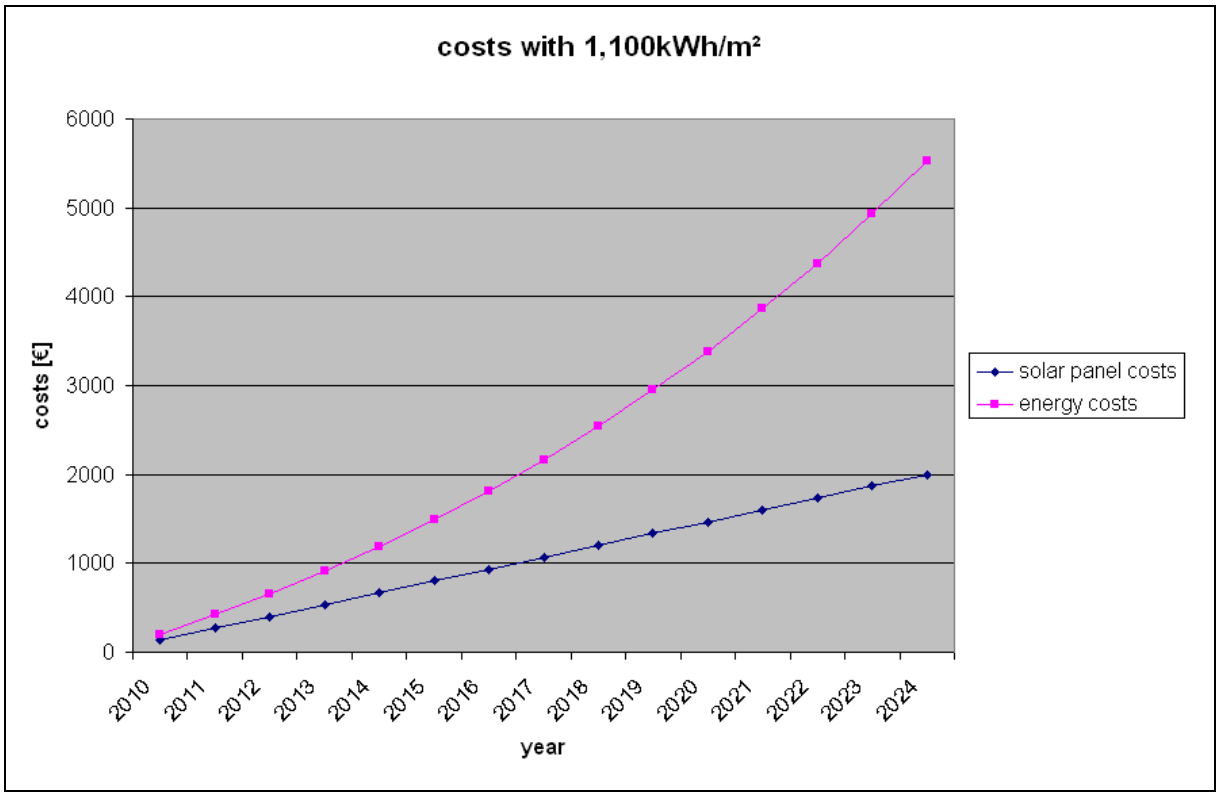

Figure 94: costs with 1,100kWh/m² and replacement of electrical energy

6. Conclusion

The performed research shows that different benefits will occur if a solar panel is used to extend the electrical driving range of either a hybrid vehicle or a pure electrical vehicle. Firstly, it can be said that the fuel amount can be reduced in case of a hybrid car by an annualamount of up to 120litres. This leads to a reduction of emissions like CO_2. Each kilometre which can be taken electrically is a benefit for the environment and society because of the usage of solar energy as a 100% renewable energy resource. A first analysis of profitability shows that the investment in a solar panel pays for itself. The costs which need to be met in the beginning change into a profit over the lifetime of the vehicle. The level of efficiency of use of solar energy is increasing, which offers the opportunity to see the car as a small power plant if the energy is not used for driving.
The area on the roof of a vehicle is restricted. Analyses carried out in this diploma thesis point to the necessity of using this amount carefully in order to establish a high level of efficiency and to maximize on available output power. The DataLogging tool is suitable to gain information and knowledge regarding how cells can be connected in groups on the roof. As a reference source the optical sensor unit is a suggestion. By the usage of the maximum power point tracking unit a further step is taken in the right direction to establish a high level of efficiency. The situation can vary depending on the vehicle where a solar panel can be integrated. The battery management and the participating electronic circuit units need to be provided with information. Communication between the different distributed components can be a key in saving energy without a negative impact on driving conditions.
The solar panel is a very lightweight construction. The solar panel from Enecom has a weight of less than 2kg. An introduction of solar energy as a power resource for a vehicle does not lead to a higher amount of fuel consumption. In comparison the lithium battery has a capacity of 5kWh and a weight of about 100kg, which can cause a slightly higher amount of fuel consumption. With further research, the solar panel is capable of completely substituting for the normal roof of a car. The substitution of fuel with 100% renewable energy in hybrid vehicles is the correct way to establish a transition to the electric car until the costs of the electric car are reduced and the electrical car becomes more attractive. Solar energy can already help today to lower the battery capacity and so also the total costs of a vehicle, even if money needs to be spent on the solar panel. Therefore the opportunity is available.

7. Literature Index

[1] AS1341 Step-Down Converter datasheet (2007, revision 1.0). austriamicrosystems AG

[2] Beuth K., Beuth O. (2003). Elementare Elektronik. Vogel Verlag, Würzburg

[3] Beuth K., Schmusch W. (1997). Grundschaltungen. Vogel Verlag, Würzburg

[4] BLUEMAG – Peugeot magazine (2010, nr. 14). Peugeot, p. 2,11-15,25

[5] Blume P. A. (2007). The LabVIEW Style Book. Pearson Education, Inc.

[6] Bosch R. GmbH (publisher). (2007). Autoelektrik, Autoelektronik. Friedr. Vieweg & Sohn Verlag/GWV Fachverlage GmbH.

[7] Bundesministerium für Finanzen (2010). Steuergesetze 2010 – Kodex des Österreichischen Rechts. Linde Verlag, Wien

[8] Datasheet AD820 (1999, Rev. B). Analog Devices, p. 1-16

[9] Datasheet TSL250, TSL251, TSL252 (1995, SOES004C). TAOS – Texas Advanced Optoelectronic Solutions, p. 1-6

[10] Datasheet TSL250RD, TSL251RD, TSL260RD, TSL261RD (2005, TAOS050C). TAOS – Texas Advanced Optoelectronic Solutions, p. 1-10

[11] Demonstrator Description for Supply Chain 6 & 17 – Deliverable 2.1 of the E³Car-Project (2009-04-02). Lead partner FHJ, University of Applied Science Joanneum

[12] Discover the new Volvo 7700 Hybrid – information folder (2009, RSP83880). Volvo Bus Corporation, p. 1-2

[13] Einmal Volttanken (2010-06.01). VIS!ON, p. 4-13

[14] Wöhe G. (2008) Einführung in die Allgemeine Betriebswirtschaftslehre. Verlag Franz Vahlen GmbH, München

[15] Einführung in die Photovoltaik (2006-01-02). Schneider D., Universität Kassel

[16] Enecom brochure (2009-12-03). Enecom Italia s.r.l., p. 4-5

[17] Enecom factsheet for different solar panels (2009-12-03). Enecom Italia s.r.l., p. 1-2

[18] European SmartGrids Technology Platform – Vision and Strategy for Europe's Electricity Networks of future (2006). European Commission – Community Research

[19] Factsheet of Volvo 7700 Hybrid (2008-09-01, BED00353). Volvo Bus Corporation, p. 1-2

[20] Fischer O. (1991). Elektrotechnische Grundlagen. R. Oldenbourg Verlag, Wien

[21] Fixed power wirewound resistor, datasheet (2007-10-10). ATE, p. 3-4

[22] Generation Control Circuit for Photovoltaic Modules (2001-05-03). Toshihisa S.

[23] Gipfelstürmer unter Strom (2010-05-01). Kleine Zeitung, p. 34-35

[24] Grohmann-Steiger C., Schneider W., Eberhartinger E. (2008). Einführung in die Buchhaltung im Selbststudium, Band I Informationsteil. Facultas Verlags- und Buchhandlungs AG, Wien

[25] Grohmann-Steiger C., Schneider W., Eberhartinger E. (2008). Einführung in die Buchhaltung im Selbststudium, Band II Übungsteil. Facultas Verlags- und Buchhandlungs AG, Wien

[26] Helmers E. (2009). Bitte wenden Sie jetzt, Das Auto der Zukunft. WILEY-VCH Verlag GmbH & Co. KGaA, Weinheim

[27] High-Speed M Series Multifunction DAQ for USB (2009-04-15). National Instruments, p.1-4,6,8-29

[28] Hymotoin L5 Plug-In Conversion Module PCM – Owner's Manual (2008, Release 03). A123 Systems, Inc.

[29] I-Shift Transmission (2008-12-03, BED00345). Volvo Bus Corporation, p. 1-2

[30] Infofolder (2008-11-03). oekostrom Vertriebs GmbH

[31] LabVIEW Basics I Introduction – Course Manual (May 2006 Edition). National Instruments Cooperation, p. 1-476

[32] LabVIEW Basics II Development – Course Manual (May 2006 Edition). National Instruments Cooperation, p. 1-207

[33] Maximum Power Point Tracker – The principles of optimizing photovoltaic cell power output (2006). Pastore R.

[34] Parking districts of Graz, map – new (2010-03-19). City of Graz

[35] Parking districts of Graz, map – old (2007-06-04). City of Graz

[36] Parking districts of the 2nd urban district of Graz, map – new (2010-05-10). City of Graz

[37] Parking districts of the 2nd urban district of Graz, map – old (2010-06-04). City of Graz

[38] Photon – Das Solarstrom-Magazin (2/2010, February 2010). Photon Europe GmbH

[39] Photon – Das Solarstrom-Magazin (7/2010, July 2010). Photon Europe GmbH

[40] Photon Profi – Photovoltaik-Fachwissen für die Praxis (8/2010, August 2010). Photon Europe GmbH

[41] Photovoltaik und Solartechnik (2010). Schenke G., p. 18-29

[42] Photovoltaic Solar Energy: present and future (2009-04-21). Nijs J., p. 1-103

[43] Schöllmann M., Hoff C., Schriek, J. (publisher) (2010). Energiemanagement und Bordnetze III. expert verlag.

[44] Solarwärme – Die Zukunft heute beginnen (2002-07-11). Deutscher Fachverband Solarenergie e.V. (DFS)

[45] Solarzelle Blue Chip (2010-02-01) Blue Chip Energy GmbH Austria

[46] Sonnenenergie als Hauptenergiequelle (2010-01-29). Benkler C., ETH Zürich

[47] Specification of optimised solar cell topology together with module and photovoltaic IC specification – Deliverable D1.11 of the E³Car-Project (2009-12-31). Lead partner FHJ, University of Applied Science Joanneum

[48] The Smart Grid: An Introduction (2008). U.S. Department of Energy (Litos Strategic Communication)

[49] Time for a change – information folder for ThinkCity (2010). Think, p. 1-12

[50] Tietze U., Schenk Ch. (2002). Halbleiter-Schaltungstechnik. Springer-Verlag Berlin Heidelberg

[51] Toyota Hybrid System – Section 3 High-Voltage Battery (2010, course 071). Toyota

[52] Toyota Hybrid System – Section 4 Hybrid Vehicle Control System (2010, course 072). Toyota

[53] Toyota Hybrid System – Section 5 HV Battery Control Systems (2010, course 072). Toyota, p. 1-9,13

[54] Toyota Prius – Emergency response guide (2009-09-21). Toyota, p. 1-38

[55] Toyota Prius – Prices and facts (2010-07-26, M10057a). Toyota, p. 16-17,22,24

[56] Toyota Technical Training – Electrical Circuit Diagnostics, Section 3 (2010, course 623). Toyota p. 25-26

[57] Volvo 7700 Hybrid Bus Dimension Sheet (2009). Volvo Bus Corporation, p. 1-2

[58] Volvo 7700 Models (2009, RSP83817). Volvo Bus Corporation, p. 1-18

[59] Was Ihr Auto wirklich kostet (2010-04-23). Format, p. 66-71

[60] What is Maximum Power Point Tracking (MPPT) and how does it work? (2004). Blue Sky Energy Inc., Cullen R. A.

[61] Zellspezifikationen (2010-03-01). Blue Chip Energy GmbH Austria, p.1-4

[62] Zero Emissions, Zero Noise – information folder for Citroën C-Zero (2010-03-01). Citroën, p. 1-4

8. Figure Index

9. Appendix

9.1. Schematic plan of the optical sensor unit prototype

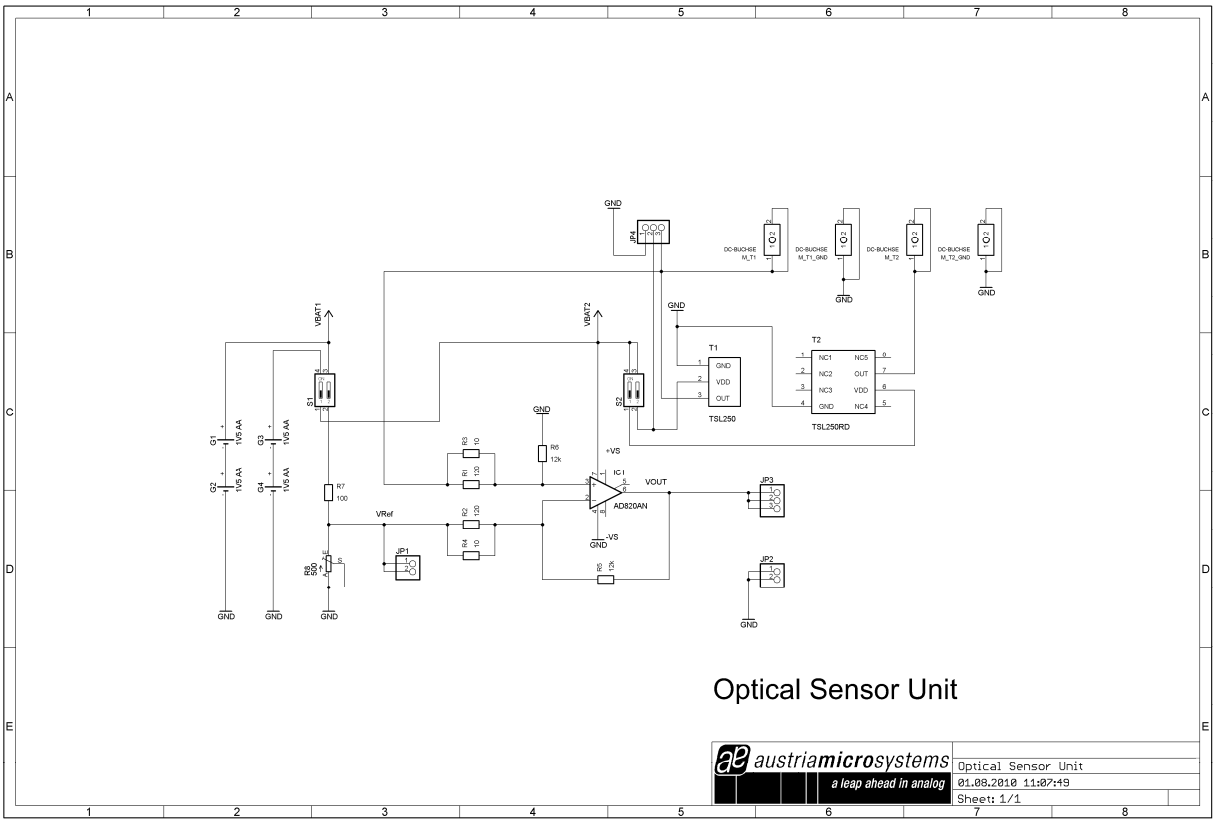

Figure 95: schematic plan of the optical sensor unit

9.2. Final measurements and outlook

At the final days of working on this diploma thesis final measurements have been made in cooperation with the University of Applied Science Joanneum. The following figures show the measurement and give an idea of the following steps which will be the evaluation of the performance of the Maximum Power Point Tracker (MPPT). The basic idea has been to justify the correct communication between the DataLogging tool and the FPGA board via USB to secure the opportunity for further tests. Furthermore a prototype of a solar module has been constructed which allows different configurations on the connection of solar cells and which is equivalent to the solar module which will be integrated in the experimental vehicle.

Figure 96: prototype of the solar module

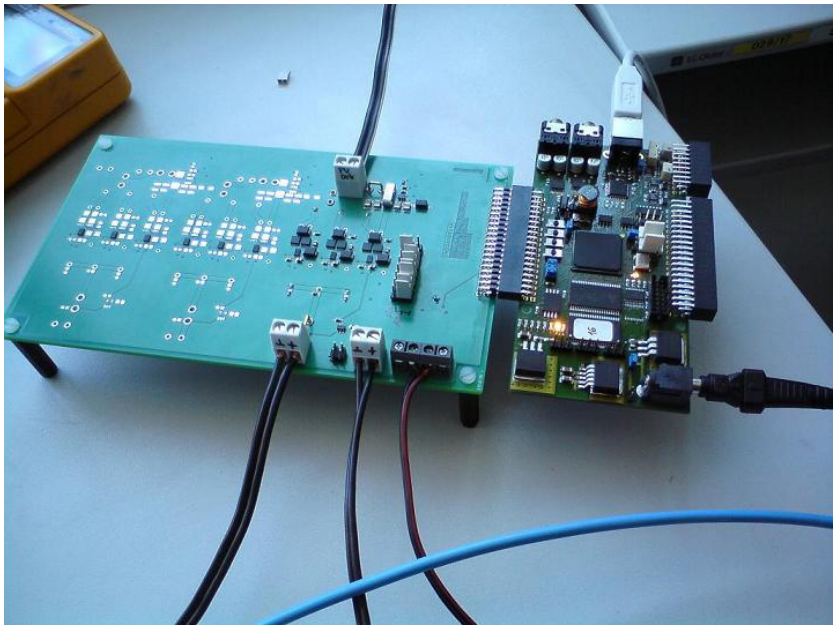

Figure 97: converter with attached FPGA board

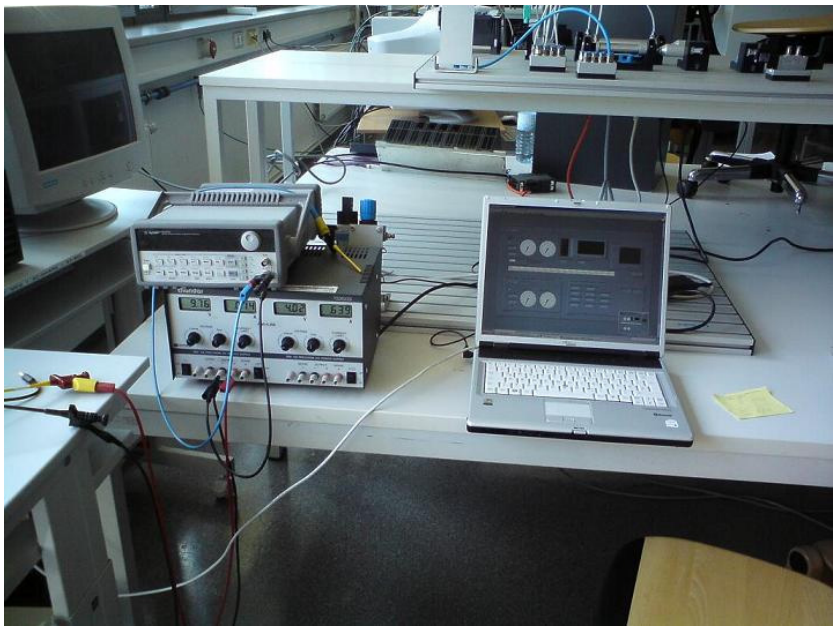

Figure 98: power supply and computer with DataLogging tool

Figure 99: measurement with effects of shadowing